X-923-77-210
PREPRINT

TMX-71382

LAND USE/LAND COVER MAPPING (1:25,000) OF TAIWAN, REPUBLIC OF CHINA BY AUTOMATED MULTISPECTRAL INTERPRETATIONS OF LANDSAT IMAGERY

QUO-CHENG SUNG
LEE D. MILLER

AUGUST 1977

GSFC — GODDARD SPACE FLIGHT CENTER —
GREENBELT, MARYLAND

For information concerning availability
of this document contact:

Technical Information & Administrative Support Division
Code 250
Goddard Space Flight Center
Greenbelt, Maryland 20771

(Telephone 301–982–4488)

Land Use/Land Cover Mapping (1:25,000) of Taiwan, Republic of China by Automated Multispectral Interpretations of LANDSAT Imagery

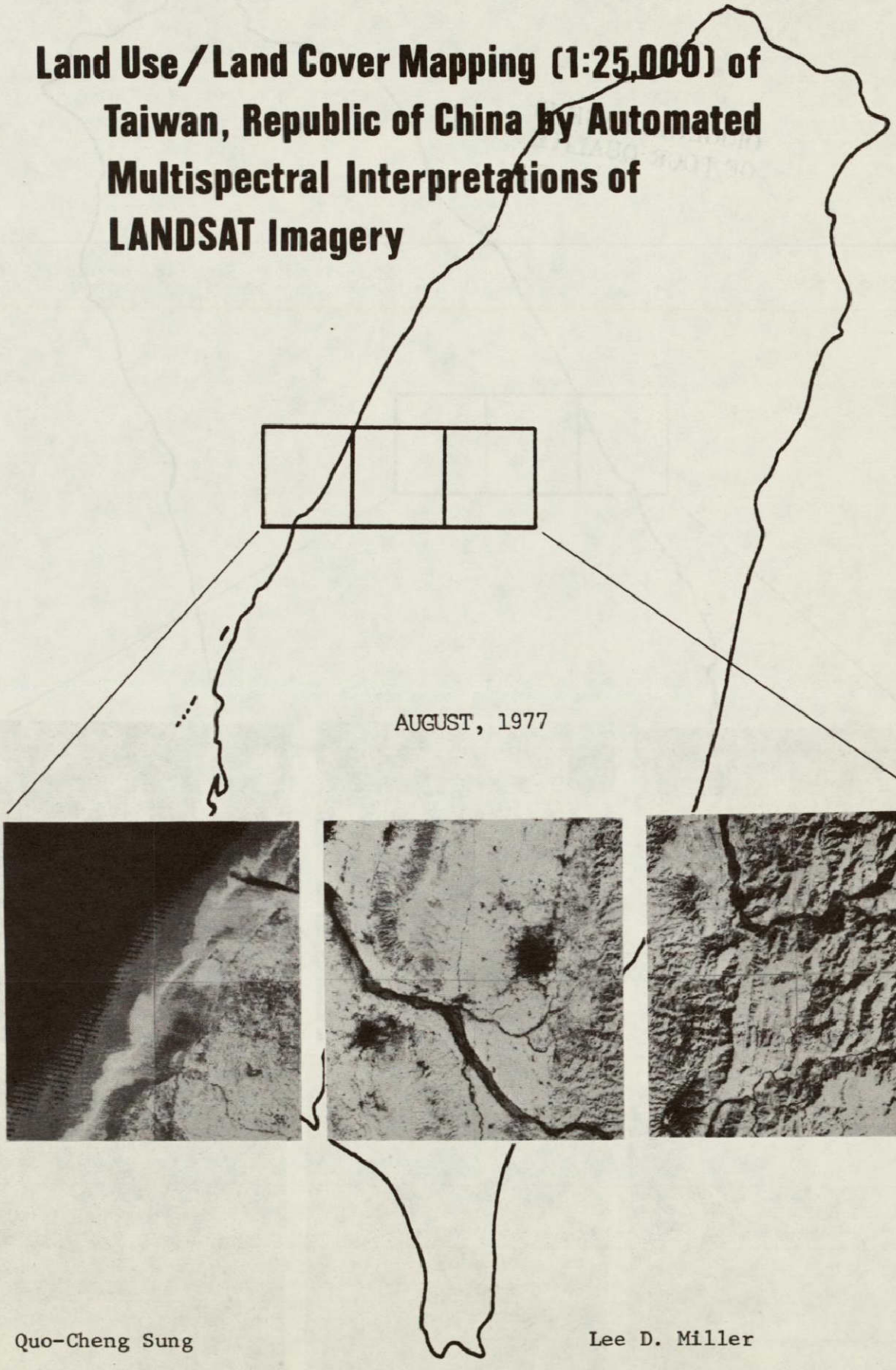

Quo-Cheng Sung

Lee D. Miller

Backpiece

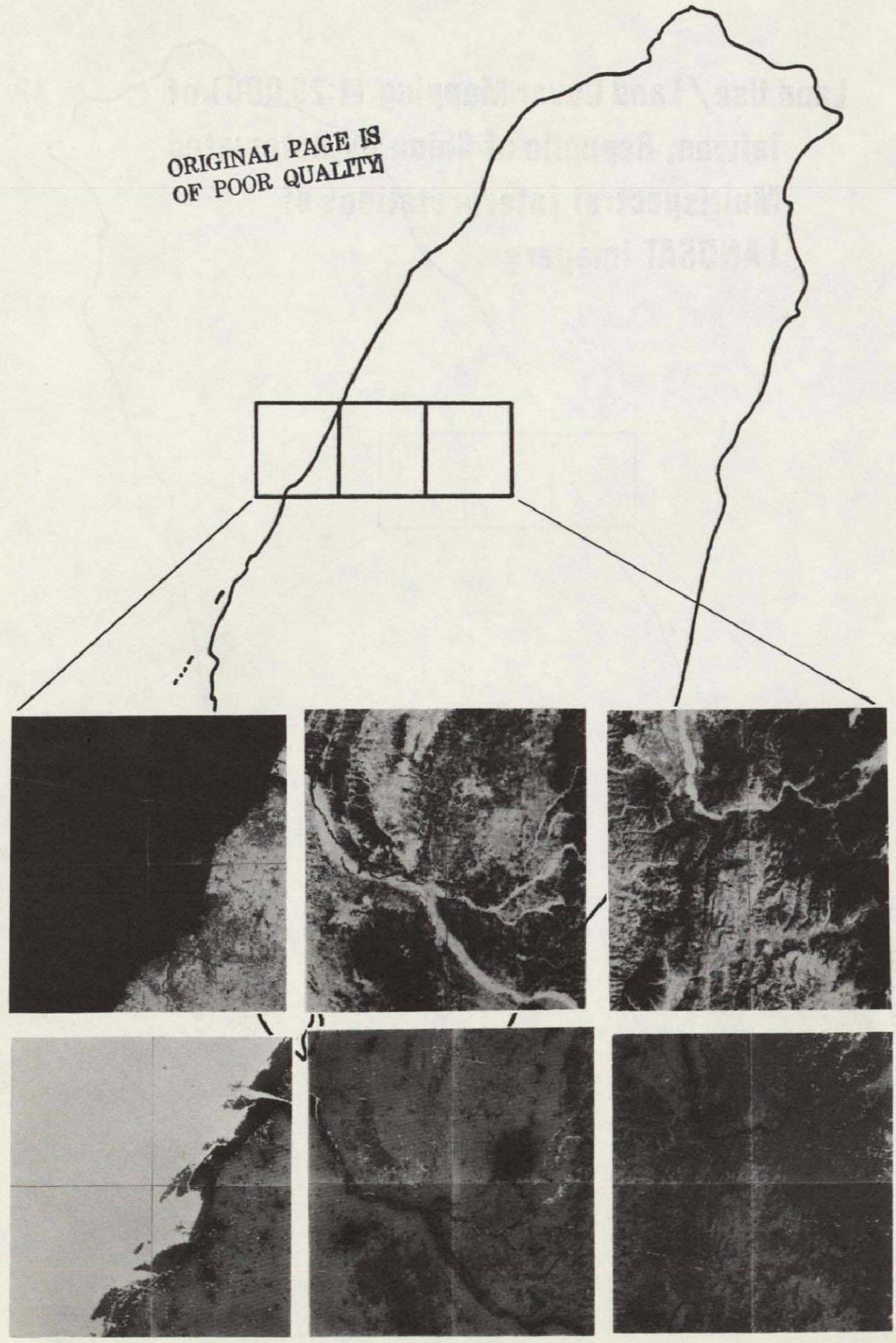

ABSTRACT

LAND USE/LAND COVER MAPPING (1:25,000) OF TAIWAN, REPUBLIC OF CHINA BY AUTOMATED MULTISPECTRAL INTERPRETATIONS OF LANDSAT IMAGERY

The applicability of digital computer-aided analysis techniques of LANDSAT images to identify and classify major land cover types of Taiwan was tested with a minimal amount of ground control data extracted from black and white airphotos by photointerpretation. A limited study area was selected to represent the wide spectrum of land covers present in Taiwan. A land use/land cover classification scheme was evolved in a step by step fashion for use with airphotos and LANDSAT imagery. The single date LANDSAT image taken on Nov. 1, 1972 was analyzed using supervised computer image processing techniques.

Three methods were tested for collection of the training sets needed to establish the "spectral signatures" of the land uses/land covers sought due to the difficulties of retrospective collection of representative ground control data. Computer preprocessing techniques applied to the digital images to improve the final classification results were geometric corrections, spectral band or image ratioing and statistical cleaning of the representative training sets. The geometric corrections provided a map base at 1:25,000 with position errors only slightly more than 50 feet. The statistical cleaning of

the representative training sets did not improve the training set accuracy. However, a final evaluation of the value of statistical cleaning must await a future test of its impact upon map verification accuracy. A stepwise discriminant analysis was applied to evaluate the training set accuracy for 17 land uses/land covers. Ratios of MSS bands contributed little to the final accuracy achieved. MSS band 5 and 7 achieved an overall training set accuracy of 79% which is comparable to that obtained by 10 MSS bands/ratios.

A minimal level of statistical verification was made based upon the comparisons between the airphoto estimates and the classification results. The verifications provided a further support to the selection of MSS band 5 and 7. It also indicated that the maximum likelihood ratioing technique can achieve more agreeable classification results with the airphoto estimates than the stepwise discriminant analysis.

Subsequently, final land use/land cover classification maps were produced at a scale of 1:25,000 with the cost of N. T $0.16/ hectare (U.S. $0.004/hectare) for computer time only. A further verification of the classification maps needs to be done in the field. An application of land use/land cover mapping over the entire island is strongly recommended by the author. However, the validity of signature extension over the entire island should be further investigated.

ACKNOWLEDGMENTS

Various portions of the work reported upon here have been supported at various institutions as shown:

Joint Commission on Rural Reconstruction, Taipei, Taiwan, Republic of China (approximately $12,000 student support).

Mining Research and Service Organization, Taipei, Taiwan, Republic of China (approximately $5,000 student and computer support).

Colorado State University, Department of Civil Engineering, Ft. Collins, Colo. (approximately $2,000 computer support plus senior staff time).

Professional staff contributing directly to the effort reported were:

Dr. L. D. Miller, Senior Resident Research Associate, NASA/ Goddard Space Flight Center, Greenbelt, Md. 20771

T. P. Chang, Dept. of Civil Engineering, Colorado State University, Ft. Collins, Colo. 80523

Q. C. Sung, C. L. Huang, T. T. Feng, W. T. Cheng, and S. P. Li, Mining Research and Service Organization, Taipei, Taiwan, Republic of China

W. C. Hu, S. W. Lee, C. C. Koh, Joint Commission on Rural Reconstruction, Taipei, Taiwan, Republic of China

Dr. S. Wang, Associate Professor, Dept. of Geography, National Taiwan University, Taipei, Taiwan, Republic of China

TABLE OF CONTENTS

LIST OF TABLES

LIST OF FIGURES

I. INTRODUCTION

1.1 Background

It becomes increasingly important to manage Taiwan's natural resources more efficiently as pressure upon them increases due to a growing population with expectations of ever rising standards of living. The task requires that accurate inventories of the spatial distribution of natural resources be periodically completed in a timely fashion. Until as recently as a generation ago such inventories were made almost entirely on the ground for Taiwan. Geologists traveled widely in exploring for minerals; foresters and agronomists examined trees and crops at close hand in order to assess their condition; surveyors walked the countryside in the course of preparing the necessary large scale topographic maps. The advent of the collection of aerial photography in Taiwan represented a big step forward. However, the airphotos have not gained wide use for natural resource management as they are sensitive material and are classified.

Remote sensing methodology, of which the use of aerial photography is a subset, uses images collected singlely or simultaneously in spectral ranges distributed over the electromagnetic spectrum. The technique employs images taken throughout the spectrum

from the very short wavelengths at which gamma rays are emitted to the comparatively long wavelengths at which RADAR operates. These images can potentially secure far more information about the nature and condition of an area's resources than can be obtained with conventional aerial photography which is restricted approximately to the sensitivity range of human vision and little beyond into the photo infrared. Remote sensing images are obtained from aircraft or spacecraft, including unmanned satellites. This technique employs both cameras and a large number of other more recent sensing devices. Remote sensing techniques are currently being extended so that the image obtained by the sensing devices can be processed and interpreted automatically and a large volume of information dealt with in a rapid and timely fashion.

NASA launched ERTS-1 (renamed LANDSAT-1) into a near-polar orbit on 23 July 1972 to remotely sense the surface of the earth with a multispectral scanner and a set of three return beam vidicons. Multispectral imagery obtained from this spacecraft, with its capacity for repetitive coverage and synoptic view, has provided a better tool to monitor the dynamic nature of the earth's natural resources. This characteristic is particularly important to the dynamic processes of agricultural and forest management and land use planning. Often, for example, a land use map has been out of date when it was first published. The use of LANDSAT type images can complement the

map revision procedures, providing a capability to monitor trends in land utilization on a nearly real-time basis (Place, 1973).

Recently, Taiwan has investigated the potential use of the larger scope of remote sensing data collection for natural resource inventories (Chang, 1974; Miller, 1974; Pan, 1974; and Wang, 1974). Four excellent LANDSAT images of Taiwan were taken on November 1, 1972 with over 90% cloud free conditions. Ninety percent of the land area of the island was covered by the center two images of the four. The direct visual interpretation of LANDSAT imagery of Taiwan was first applied to regional geologic studies (Wang, 1976). Density slicing and image enhancement techniques were also tested to help delineate special features. However, the inadequate scale of the photographic format of the LANDSAT images and its attendant limitations on the spatial resolution discouraged Taiwan resource managers. The question often brought out was, "does LANDSAT imagery have sufficient spatial resolution for resource management in Taiwan?"

Taiwan is a mountainous island and heavily vegetated with subtropical forests. The land use patterns are small and complicated. Thus, Taiwan requires detailed spatial information in a larger scale for resource management purposes. LANDSAT imagery in the photographic form does not currently meet these requirements. Recently special processing and photographic display has been prepared and the test portions of LANDSAT images of selected small sites in the

United States comparable to high altitude airphotos. These promising results are far superior to the standard LANDSAT products commercially available for Taiwan. The digital form of the LANDSAT images contains considerably more spatial information than is contained in the more commonly available LANDSAT photographic form, since some of the original image's resolution is lost in the photographic reproduction processes being currently applied. The digital form of these images also lend themselves to computer-aided methods of interpretation. The resulting map product can be made through computer processing techniques at a proper scale for the resource management. Moreover, the computer multispectral analysis approach significantly improves the amount and accuracies of the interpretation relative to direct visual interpretations of the LANDSAT photographs.

Computer processing of remote sensing imagery (automated image processing) has been widely tested by many disciplines for such applications as urban planning, crop and forestry inventory, water resource management, geologic mapping, etc. This previous work established the value of computer processing of LANDSAT images for resource inventories, however, most of this work was restricted to areas of minimal topographic relief. Larger variations in topographic slope and aspect may significantly affect the accuracy of the analysis of LANDSAT data collected over mountainous terrain (Hoffer, 1974). The ground resolution for LANDSAT imagery is

about 60 by 80 meters. Each resolution cell represents an averaging of the spectral return from this nominal 60 by 80 meter ground cell. The land use pattern of Taiwan is small scale and heterogenous and considerably more complicated than the United States where agricultural practices employ large homogenous fields. Thus, the reliability of the identification of the varieties of Taiwan land use and land cover by computer analysis of LANDSAT imagery must be specifically tested.

A remote sensing program in Taiwan was initiated on several fronts in the early 1970s (Miller, Chang and Wang, 1974). Although the advantages and disadvantages of satellite imagery were well recognized by these programs, the potential use of the digital LANDSAT imagery could not be demonstrated. Recently a more detailed and more expensive approach to crop and forest inventory of Taiwan was initiated using infrared aerial photographs of the coastal plains. The study described here investigated the possibility of applying computer image analysis techniques to the available LANDSAT images of Taiwan. The specific purpose was to extract land cover maps for use in land use planning and thus to provide an additional stepping stone to promote the use of remote sensing in Taiwan.

1.2 Study Objectives

This study was designed to test the applicability of digital computer-aided analysis techniques of LANDSAT multispectral scanner images to identify and classify major land cover types of Taiwan with a minimal amount of ground control data. The specific objectives of this study were:

1. to develop a land use/land cover hierarchical classification system for use with remote sensing data,

2. to design a practical method to collect the ground control data needed to establish the training sets used in the computer classification processes,

3. to select the optimal combination of image spectral bands and ratios for use in LANDSAT mapping of Taiwan land cover types evaluated in terms of the accuracy and economies of the process,

4. to produce land cover maps by computer classification of LANDSAT imagery at a scale of 1:25,000, and

5. to design a reasonable scheme for the verification of the accuracy of these results using limited ground control information.

The general objective of this study was to demonstrate by example the nature and capability of automated image processing of remote sensing imagery collected from aircraft and satellite. It is hoped that by reviewing the results of this research that these new remote sensing techniques can be more fully

appreciated and the approach more widely employed in Taiwan in the near future.

1.3 Study Outline

This study was carried out at Colorado State University for the past year using the computer software system entitled the LANDSAT Mapping System (LMS) operating on a Control Data Computer (CDC 6400) (Appendix A). A limited study area was selected to represent the wide spectrum of land cover present in Taiwan. A land use/land cover classification scheme was evolved in a step by step fashion for use with airphotos and LANDSAT imagery. The only available, good quality, single date LANDSAT multispectral image taken on November 1, 1972 was analyzed using supervised computer image processing techniques. Three methods were tested for the collection of the training sets needed to establish the "spectral signatures" of the land uses sought due to the difficulties of retrospective collection of representative ground control data. Computer preprocessing techniques were applied to the digital images to improve the final classification results. The impacts of the application of these techniques on the test accuracies achieved were investigated in detail. The techniques applied included geometric corrections, spectral band or image ratioing and statistical cleaning of the representative training sets. The investigation led to the optimal selection of spectral bands or images and their ratios. Subsequently, final

land cover classification maps were produced at a scale of 1:25,000 using the favorable techniques and imagery. A computer cost evaluation of these processes was completed relative to the time and dollar costs of using the Colorado State University CDC 6400 computer. The statistical verification of the accuracy of the classification map results was hard to complete within the United States due to the paucity of ground control data. However, a minimal level of statistical verification was possible to substantiate the quality of the maps produced.

II. DEVELOPMENT OF A HIERARCHICAL LAND USE/LAND COVER CLASSIFICATION SCHEME FOR TAIWAN

2.1 Description of Study Area

2.1.1 Introduction

Taiwan island is 394 kilometers long and 144 kilometers broad at the widest point. It lies between 21°45' and 25°38' north latitude and 119°18' and 122°7' east longitude with an area of 35,961 square kilometers (Fig. 2.1). The very dominant topographic feature of Taiwan is the central range of high mountains running from the northeast corner to the southern tip of the island. This backbone of the island contains 62 peaks with elevations above 3000 meters and which rise abruptly from the sea along the eastern Pacific coast. The western half of the island facing the China mainland and shallower Taiwan Strait is a terraced succession of uplands and coastal plains and basins. Approximately one-third of the total land area of 35,961 square kilometers is arable and occurs on the gentler western slopes. The mountain areas are forested or heavily revegetated where the forests have been removed.

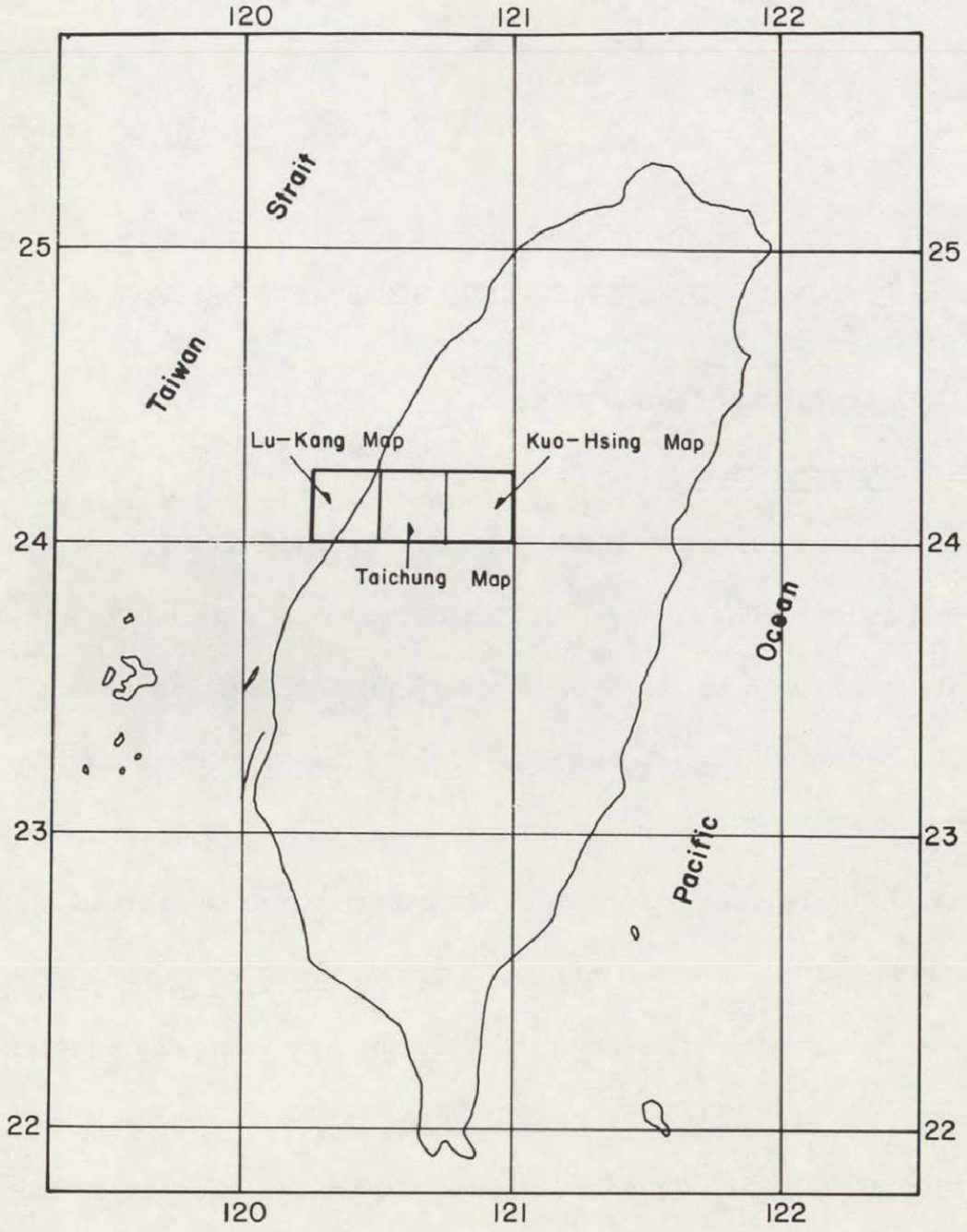

Fig. 2.1. GEOGRAPHIC POSITION OF TAIWAN AND THE AREA SELECTED FOR LAND USE/LAND COVER MAPPING. The three squares constitute the general study area and indicate the three of 1/50,000 topographic maps to be mapped at a scale of 1/25,000. Scale ∿ 1/2,500,000.

2.1.2 Physiography

The study site is located in the western side of central Taiwan and represents 2,100 square kilometers which is about 6% of the total land area. It constitutes the area of three 1:50,000 topographic maps, namely the Lu-Kang, Taichung and Kuo-Hsing maps respectively from west to east (Fig. 2.1). Beginning at the west coast of the island at the Taiwan Strait, the area selected extends eastward through the coastal plains, terrace tablelands and Taichung basin to the foothills of the central range (Fig. 2.2). The area was selected to contain a complete sampling of the types of land uses practiced in Taiwan. Variations in land use do occur in a north-south sense over Taiwan but are considerably less than those differences induced by the topographical extremes represented in the site selected. The elevation of the site increases eastward from sea level to 2307 meters which is the highest peak in the general area. The Wu river dominates the drainage and winds its ways across the site to the Taichung basin cutting through the tableland to reach the sea at the upper left corner of the area. The average elevation of the tableland is about 200 meters above sea level.

The climate of central Taiwan is subtropical. The mean monthly temperature in winter is above 15^{o}C except for the mountain region. This is favorable for the cultivation of rice and other crops, including sugar cane, pineapples and bananas. The mean annual

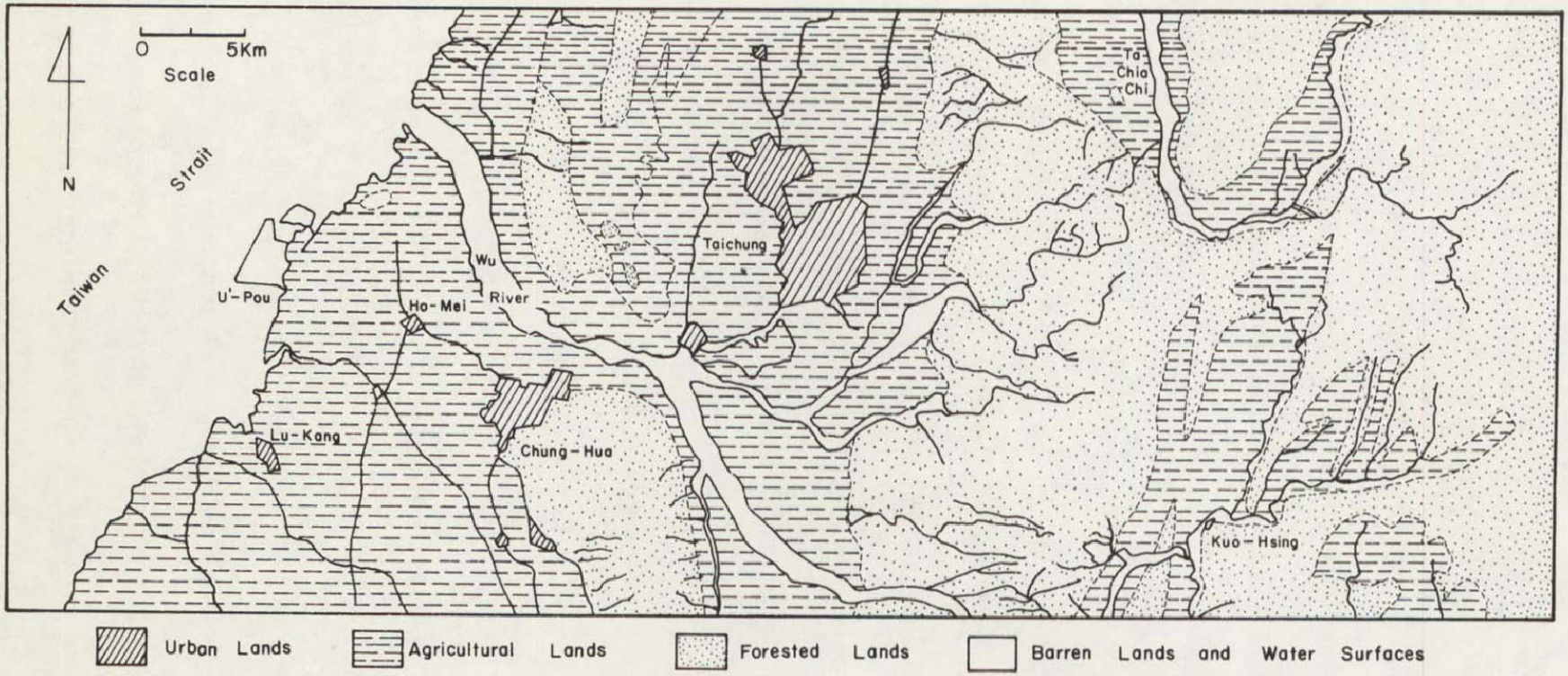

Fig. 2.2. THE DRAINAGE PATTERN AND MAJOR LAND USES OF THE STUDY AREA. Prepared by photointerpretation from 9" X 9" color print of LANDSAT-1 imagery of November 1, 1972. Transferred to the map base by the aid of a Zoom Transfer Scope. Scale ∿ 1/300,000.

precipitation of the area is around 1.7 meters. The wet season, from May to September, contributes almost 80% of the annual precipitation. Typhoons and thundershowers are the major types of rainfall. The winter monsoon prevails from October to March with mean maximum wind velocity as high as 17 m/sec. The monsoon can cause heavy damage to field crops on the coastal plains. A typhoon or thundershower may cause a flood and very severe erosion and redeposition due to the precipitous terrain and the short steep river courses.

2.1.3 Agriculture

The study site contains the central portion of the Taichung basin and was selected to be representative of Taiwan in physiography and agriculture. The site contains a sample of the coastal plains, terrace tablelands, and basin and foothills where most of the major economic activities of the island occur. Taichung basin is where the provincial government of Taiwan is located and contains some of the most productive agricultural lands. Taichung is the third largest city in Taiwan and is the cultural, economic, industrial, and recreational center of central Taiwan. Taichung Harbor has recently been built to the north of the Wu River mouth. The study area contains these features and thus is an area which will play an increasingly important role in the future economic development of the Republic of China.

The important agricultural products of the basin area are rice, sugar cane and sweet potatoes and the miscellaneous crops include corn, sorghum, peanuts, etc. Bananas and grapes are the common fruits planted in the coastal low lands, while oranges and other fruits are cultivated in the foothills. However, most upland and lowland orchards are small areas scattered throughout the rice paddies or among other natural tree growth. Deciduous trees are the major forest type in the basin area. Acacia is the dominant type, especially on the terrace tablelands. Conifers dominate the mountain slopes with elevations above 1000 meters.

Tidal flats extend a few kilometers into the sea during low tide and 820 hectares of reclaimed land have been developed in this area. Fish ponds and rice paddies are the main type of land uses in and adjacent to these tidal flats.

2.2 LANDSAT Multispectral Scanner Imagery of Taiwan Available for Analysis

2.2.1 Introduction to the LANDSAT System

NASA launched the Earth Resources Technology Satellite-1 (subsequently renamed LANDSAT-1) into a near-polar, sun-synchronous, circular orbit on July 23, 1972. It achieved a successful orbit of about 920 kilometers (570 miles) above the surface of the earth circling the globe every 103 minutes or 14 times a day (LANDSAT Users Handbook, 1976). LANDSAT-1 is able to view the

same spot anywhere on the surface of the earth at the same local day time every 18 days. Subsequently LANDSAT-2 was launched into a similar orbit so that imagery became available alternately with a 9 day interval. About February 1, 1977 the orbit of LANDSAT-1 was readjusted so that the intervals between the imaging paths of the two satellites is now 6 days and 12 days. These satellites both carry a television camera system (Return Beam Vidicon or RBV) and a radiometric scanner (Multispectral Scanner or MSS) which together obtain imagery in seven different optical spectral ranges of visible and photoinfrared energy reflected from the earth's surface. Four spectral ranges are covered by the Multispectral Scanner (MSS) imagery (Table 2.1).

Table 2.1. LANDSAT MULTISPECTRAL SCANNER SPECTRAL RANGES OR BANDS.

MSS Band	"Color" Range	Wavelength Interval (in micrometers)	(in Angstroms)
4	Green	0.5 to 0.6 μm	5000 to 6000 Å
5	Red	0.6 to 0.7 μm	6000 to 7000 Å
6	Photoinfrared	0.7 to 0.8 μm	7000 to 8000 Å
7	Photoinfrared	0.8 to 1.1 μm	8000 to 11000 Å

2.2.2 Introduction to the Multispectral Scanner System

Incident solar electromagnetic energy reflected from the surface of the earth to the satellite is focused by an oscillating scan mirror onto a set of 24 sensors or detectors in the MSS (Multispectral Scanner) device. These sensors form an array which one may picture schematically as a set of four columns, of six sensors each, with one column for each MSS spectral band (Fig. 2.3).

The instantaneous view which each sensor has of the ground is a square of approximately 79 m by 79 m (259 ft by 259 ft). The six sensors in a given band view collinear and contiguous resolution elements. Thus the set of six sensors in a given column instantaneously sweeps out or views a strip approximately 474 m by 79 m (1554 ft by 259 ft) (LANDSAT Users Handbook, 1976).

The region on the ground viewed by the sensors in a given spectral band in one sweep of the mirror from west to east is called a swath (Fig. 2.3). It is 474 m wide and sweeps out a length of about 185 km (1554 ft by 115 mi). That region within a swath which is viewed by a single sensor, or a set of the four different sensors in a multispectral sense, is called a scan line of the resulting image.

The lines and swaths do not lie perpendicular to the ground orbit track of the satellite because, while the mirror is scanning, the satellite is moving and the earth is rotating. The velocity of the mirror and satellite relative to the earth is such that when the mirror

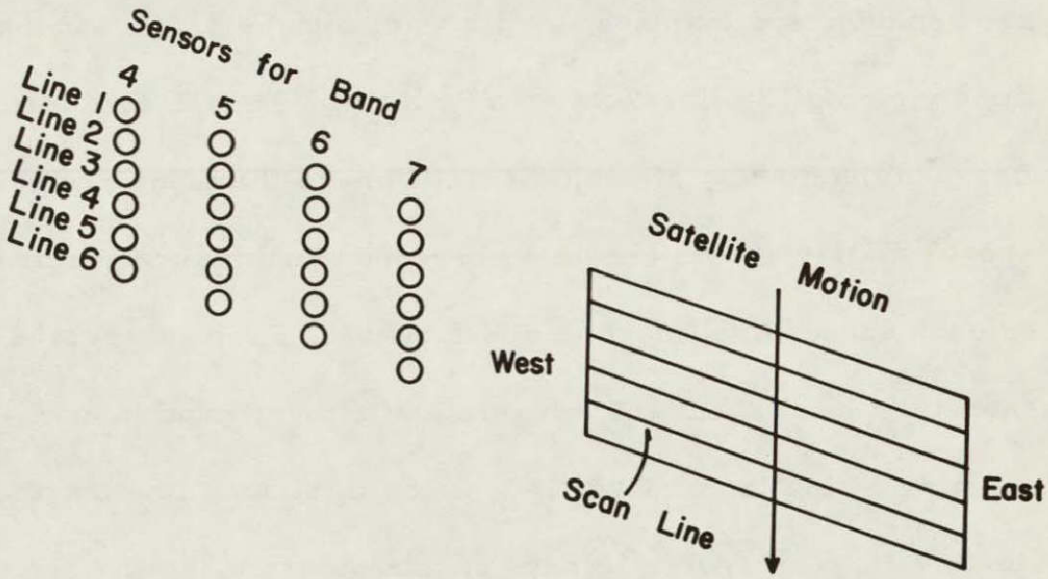

Fig. 2.3. SCHEMATIC DIAGRAM OF LANDSAT'S MULTISPECTRAL SCANNER CONCEPT. Six scan lines constituting a swath are swept out as shown for each mirror scan. The angle of the scan lines is caused by the relative motion between the satellite and the earth's surface. The length of each scan line is ~ 185 km while its width is 79 m.

has returned to its starting point and is ready to begin its next contiguous swath the satellite has moved forward relative to the earth's surface such that there is no gap or overlap between swaths. The imagery obtained in this fashion is continuous as the satellite continues around the earth. Analog magnetic tape of these images is recorded at a ground tracking station whenever the satellite is within range. The image may be temporarily stored on board the spacecraft for subsequent retransmission when it is in the range of a

ground station. Subsequently, these tapes of the continuous image are replayed and displayed as discrete images of 390 swaths of 2340 lines yielding 125 lines/cm on a $9\frac{1}{2}$ inch by $9\frac{1}{2}$ inch film format. Between the display of each discrete image the tapes are rewound approximately 10% to create a corresponding duplication or overlap on each successive image in a N-S sense. Each successive day the satellite moves about 165 km relative to the ground in an E-W sense creating a side lap of about 10% as the total scan line length is approximately 185 km. After 18 days of this sideskipping the given satellite closely repeats the same ground path over Taiwan.

2.2.3 Introduction to the Digital or Discrete Nature of the LANDSAT Images

The signal recorded at the ground station is in analog form and when played back as outlined above provides the basis to produce the commonly available black and white or color photographs of the LANDSAT images. Each of the 24 MSS sensors measures the intensity of the reflected solar energy it receives in its respective wavelength interval or spectral band and produces a separate output of the continuously varying or analog signal. Thus individual black and white photographs of each of the four spectral bands or color combinations can be produced on the ground. The analog recording of these signals also provides the source for the digital or discrete picture element format of the LANDSAT imagery which is compatible

with digital computer analysis. This process digitally or numerically samples the analog recorded, continuously variable, electronic signal from each sensor. This sampling occurs on the average of 3,216 times on one satellite scan line of 185 km and the string of numbers obtained is recorded on a second magnetic tape in a digital format which is compatible with standard digital tape of the electronic computer. This is called the Computer Compatible Tape (CCT) form of the LANDSAT image.

The region on the ground for which the reflected solar energy intensity is measured and numerically recorded is called a pixel which is short for picture element. A computation of 3,216 times the 79 m ground resolution noted earlier yields a line length greater than 185 km as the pixels overlap about 29% along the scan lines. This yields an effective ground resolution of 79 m (N-S) by 57 m (E-W) for each pixel. Each pixel is represented by a discrete number for each spectral band on the CCT. These values range from 0 to 63 in MSS band 7 and from 0 to 127 in MSS band 4, 5 and 6 with 0 the lowest energy level and 63 or 127 the highest. Each and every MSS pixel is represented on the CCT by a set of four numbers for the instantaneous reflected solar energy values measured in each of the four MSS bands.

2.2.4 LANDSAT Imagery of Taiwan

Four contiguous LANDSAT-1 MSS images of Taiwan were obtained shortly after launch on November 1, 1972 (Fig. 2.4). One of these was selected for analysis. Computer compatible tapes (CCT's) were purchased from the EROS (Earth Resources Observation System) Data Center of the U.S.G.S. located at Sioux Falls, South Dakota (Table 2.2). One 185 km by 185 km image consists of four CCT's, each representing all of the four MSS values for each pixel for an 46 km wide strip of the image.

Table 2.2. SPECIFICATIONS OF THE LANDSAT-1 IMAGE ANALYZED.

Date image taken	November 1, 1972
Scene ID No.	1101-01550
Sun angle	43°
Sun azimuth	144°
Cloud cover	10%
Quality assessment	good
MSS Bands used	4, 5, 6, 7 (all)
Center coordinates of frame	N $24^{\circ}24'$ E $121^{\circ}05'$
Type of product available	20" X 20" B/W prints of Bands 5 & 7 CCT's - 7 track 800 BPI Seq. # 1, 2 and 3 of 4

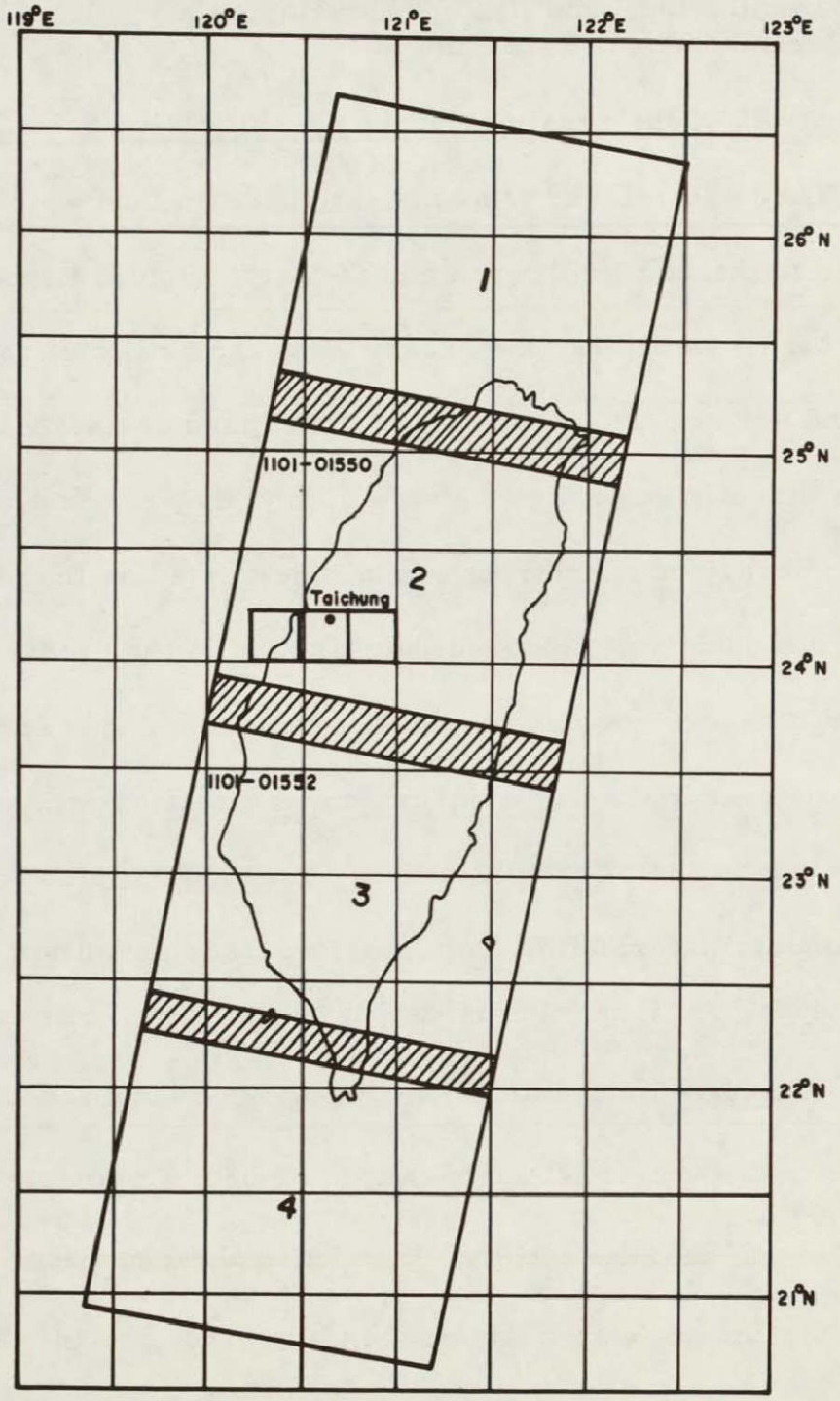

Fig. 2.4. FOUR LANDSAT-1 FRAMES COVERING TAIWAN ON NOVEMBER 1, 1972. NASA LANDSAT ID# shown on upper left corner of the images. The location of three of the 1/50,000 topographic maps to be mapped at a scale of 1/25,000 and identified in Fig. 2.1 is indicated within image #2.

2.3 Sampling the Land Use and Developing a Ground Control Data Base

2.3.1 Basic Considerations of the Classification Scheme

Land use refers to "man's activities on land which are directly related to the land" (Clawson and Stewart, 1965). Land cover, on the other hand, describes "the vegetational and artificial coverings of the land surface" (Burley, 1961). Some land use activities of man can be directly related to the type of land cover. For instance, using imagery on which rice can be interpreted as the land cover, it may subsequently be inferred that farming is the present land use activity although not actually visible as such. Other activities, especially recreational activities, can only be related with difficulty to land cover by use of remote-sensing techniques. However, use of supplemental information from other sources permits a more functional approach to the classification of land use (Anderson, Hardy, and Roach, 1971 and 1976). Variation in land cover is therefore the basis for any land use classification system employing remote sensing imagery. The title of "land use mapping" is often applied to remote sensing image classification activities as a whole which tends, as in this study, to amalgamate the distinct concepts of mapping land use and land cover.

The ground resolution of the LANDSAT image has been shown to be nominally 57 m by 79 m or 0.45 hectare. At orbital altitudes the single 0.45 hectare pixel recorded for each of the four MSS bands

may represent the integration of a variety of spectral responses for the land covers it contains. Thus an individual pixel may represent a gross generalization (or aggregation) of the 0.45 hectare area it is measuring (Anderson, 1971). An area of 0.45 hectare in Taiwan may consist of several different specific types of land use/land cover. Therefore, the relationship between the reliability of LANDSAT images for land use identification and its dependence on distinct spectral returns for the various land covers must be tested for the Taiwan case.

2.3.2 Testing the Scheme on Low Altitude Airphotos

The aforementioned considerations led to the adoption of a land use/land cover hierarchical scheme for initial testing with the interpretation of low altitude airphotos (Table 2.3). This scheme was subsequently revised by use and provides a logical basis for the collection of the ground control (ground truth) data to be used as training and verification data in the automated image processing procedures employed. Subsequently this same airphoto classification scheme provided the basis for the abridged classification scheme applied to the LANDSAT imagery.

2.3.2.1 Assembling Grid Sampled Ground Control Data

A grid sampling method tied to the LANDSAT image grid was devised to test this airphoto classification system, collect specific point type ground control data and estimate the relative amounts of

TABLE 2.3. LAND USE CLASSIFICATION SYSTEM CHECKED FOR USE WITH LOW ALTITUDE BLACK AND WHITE AIR-PHOTOGRAPHS. Revised from the Anderson system (Anderson, Hardy, and Roach, 1971). This system intercombines land use and land cover. Upon actual application Level III was deleted as it could not be reliably applied to low altitude black and white air-photos.

Code	*Level I*	*Code*	*Level II*	*Code*	*Level III*
100	Urban and built-up lands	110	Commercial and service		
		120	Residential and new community		
		130	Industrial		
		140	Transportation and irrigation		
		150	Institutional		
		160	Strip and clustered settlement		
		170	Mixed		
200	Agricultural lands	210	Grains		
		220	Crops	221	Sugar cane
				222	Vegetable
				223	Sweet potato
				224	Peanut
				225	Others
		230	Orchards	231	Grapes
				232	Banana
				233	Oranges
				234	Others
300	Forested lands	310	Hardwoods	311	Acacia
				312	Mixed
		320	Conifers	321	China firs
		330	Bamboo		
400	Barren lands	410	Gravels		
		420	Tidal flat		
500	Water surfaces	510	Water ways		
		520	Ponds and reservoirs		
		530	Estuaries		
		540	Sediment-laden water		
600	Range lands	610	Grassland		
		620	Scattered grass		

land uses in the study area for final map accuracy verification. Symbolic images were prepared from the LANDSAT CCTs using a computer line printer. This was accomplished by assigning an alphabetic symbol to a range of the values stored on the digital computer tapes for the various pixels. These symbols for a particular one of the four MSS band values are then printed by a computer line printer in their proper spatial or geographic position. For example, the intensity of the reflected radiation recorded on the CCT for a given pixel and specific one of the four MSS bands takes on values 0 to 63, thus we might print the letter

M = "M" overprinted with "I" for the 0-10 range of reflected energy,

U for the 21-30 range,

\+ for the 31-40 range,

\- for the 41-50 range,

θ = "0" overprinted with "-" for the 50-60 range, and leave blank for the range over 60.

This yields a symbolic image clearly representing each pixel on the ground area imaged by the satellite (Fig. 2.5). This graymap, as it will be called hereafter, provides a large scale, photographic-like rendition of the reflected radiation reaching the satellite in one of the four MSS bands. It differs from a conventional black and white photograph in that each of the pixels or ground resolution cells is a discrete symbol. Also, a panchromatic airphoto records all the

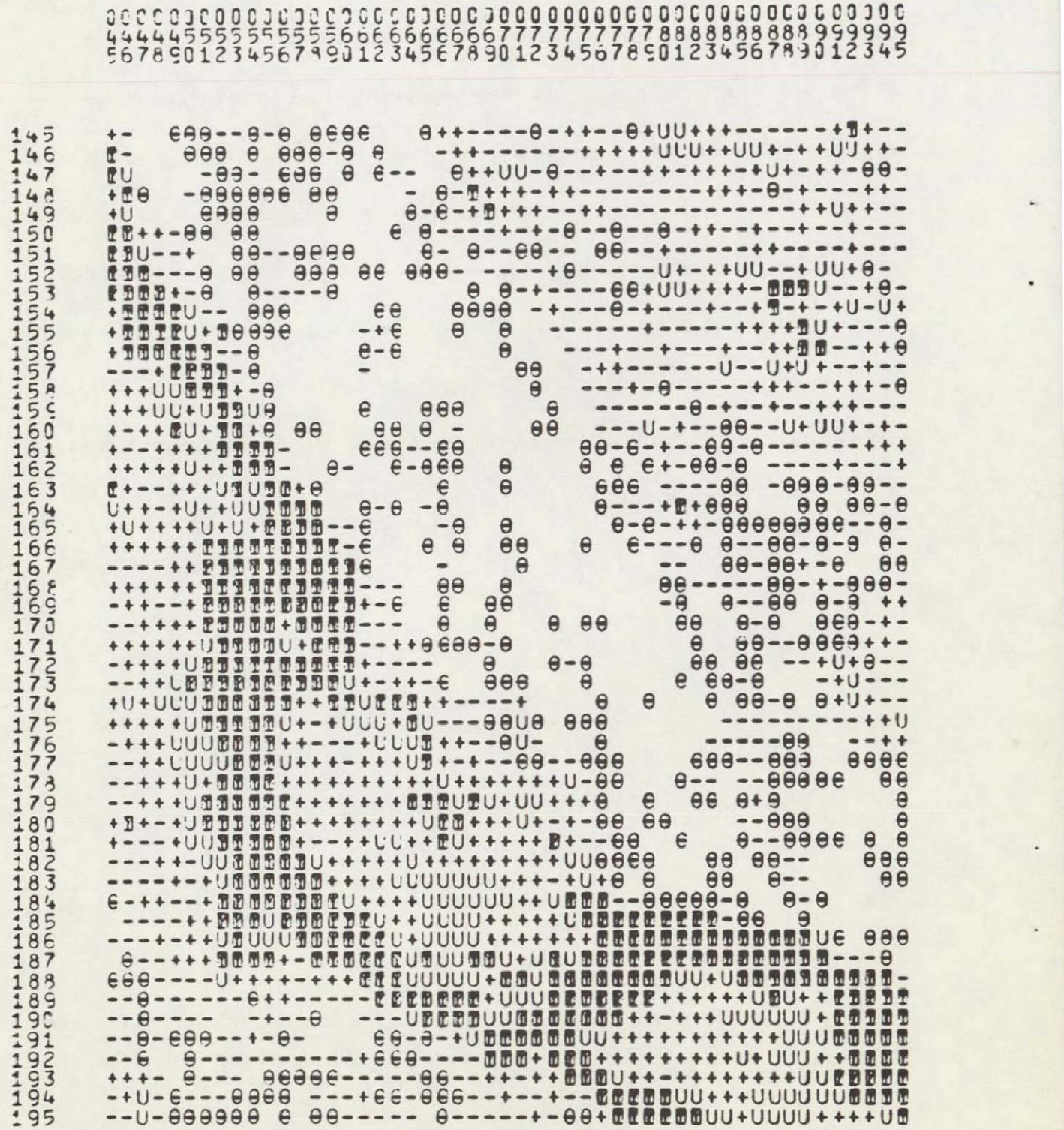

Fig. 2.5. A SMALL PORTION OF THE LANDSAT MSS BAND 7 LINE PRINTER GRAYMAP OF THE TAICHUNG MAP. 1:25,000 scale in true geometry. Line number and column number are designated to identify the relative location of each pixel.

reflected solar energy from about 0.4 to 0.7 μm while the above techniques produces four graymaps each representing a narrower spectral interval or band, e.g. MSS band 5 yields a graymap of the 0.4 to 0.5 μm reflected energy.

The study area is exactly coincident with three of the Taiwan basic series of 1:50,000 topographic maps (Fig. 2.1). Each of these maps was photographically enlarged exactly two times to provide a transparent map at a scale of precisely 1:25,000 and approximately 1 by 1 meter (40" by 40"). During the preparation of the LANDSAT image each pixel is resampled from the CCT in such a fashion that the resulting graymaps represent 1:25,000 scale line printer symbol maps upon which the transparent topographic map may be overlaid. The geometric rectification procedure employed in this operation will be discussed in more detail in the next chapter. Original picture elements or pixels have been resampled or reformed in this process and will now be referred to as discrete ground cells or simply "cells." Suffice to say at this point that the large, transparent 1:25,000 topographic map could be registered upon the LANDSAT graymaps for each of the four of MSS bands to an accuracy of $\pm$ 0.5 cell or alphabetic symbol (Fig. 2.6).

A sampling grid was laid out upon each combination of topographic map and graymap so as to mark out every 30th column and every 30th line of graymap symbols (Fig. 2.6). This provided the

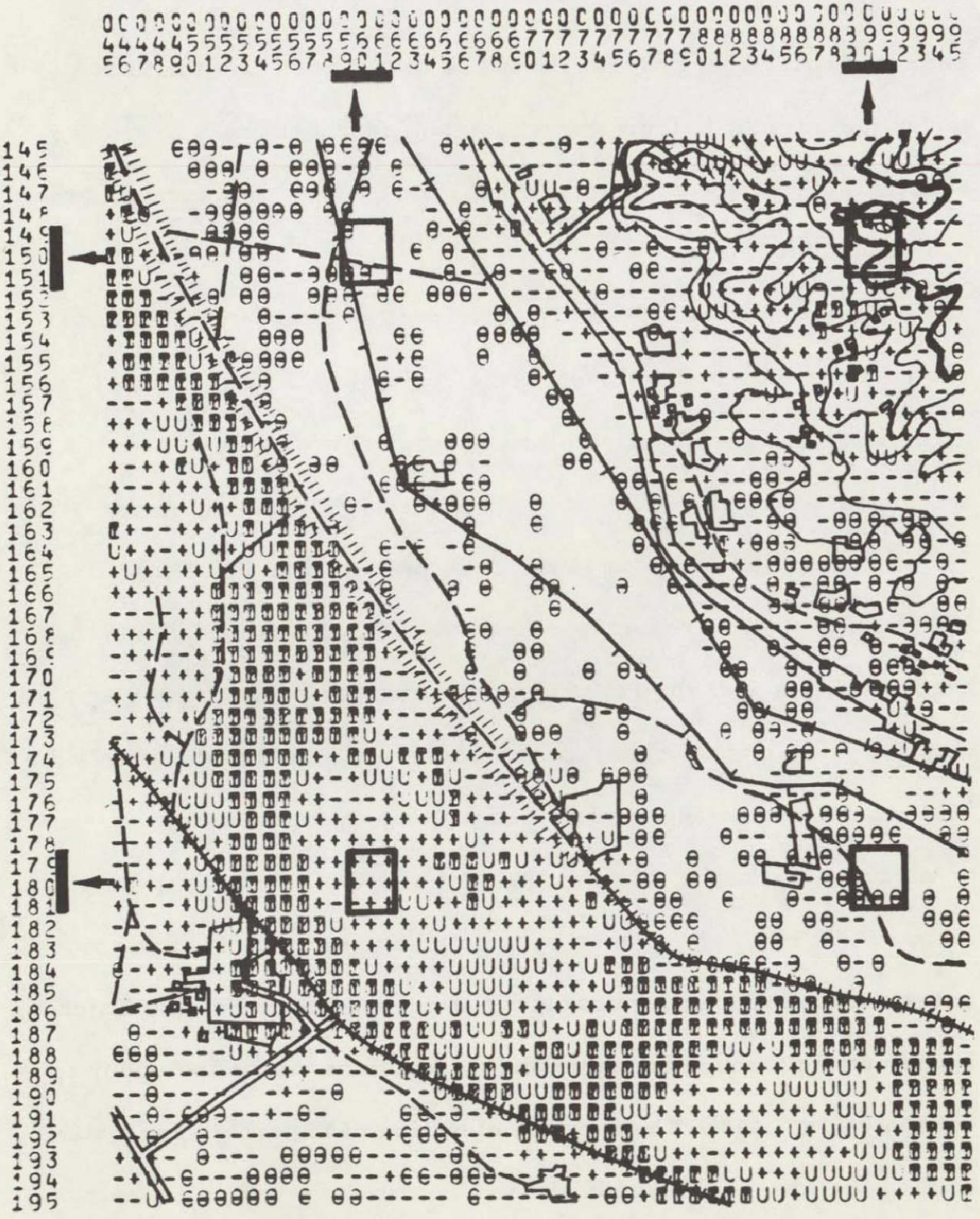

Fig. 2.6. EXAMPLE OF THE REGISTRATION OF A SMALL PORTION OF THE TAI-CHUNG TOPOGRAPHIC MAP UPON THE LANDSAT MSS BAND 7 GRAYMAP. 1:25,000 scale in the true geometry. Line number and column number which are designated by the arrows and bars locate the 30 by 30 sample grid and 3 by 3 array, respectively. The interior rectangles further emphasize the 3 by 3 arrays selected for airphoto interpretation.

regular sampling grid whose actual land use/land cover was estimated by airphoto interpretation. This sampling grid, while regular in spacing, provides a random sample of the land uses/land covers which occur in the area to be mapped. The two maps could be misregistered by as much as $\pm$ 0.5 line printer symbol thus a group of 3 by 3 symbols were identified for photointerpretation with the 30 by 30 sample cell as the center of the 3 by 3 array (Fig. 2.6). The topographic map was annotated so as to show the ground location of each of the 3 by 3 symbol arrays which represent $\sim$1710 m by $\sim$ 2370 m on the ground. Aerial photographs of Taiwan are treated as sensitive material. Thus a blue print 1:25,000 copy of each of the annotated topographic maps together with a preliminary classification scheme (Table 2.3) was returned to Taiwan for photointerpretation. Several hundred low altitude, black and white airphotos with scale of 1:16,700 were used as the basis for interpreting the land uses/land covers within the sampled 3 by 3 rectangular arrays of cells. Most of the airphotos used were taken during November and December, 1973 or about one year after the available LANDSAT image. A small portion of the airphotos were taken in the spring, 1974. A Zoom Transfer Scope was used to change scale and superimpose a local area of the 1:25,000 topographic map upon the corresponding airphotos. Localized terrain and cultural features were used to match the group of 3 by 3 cells annotated on the map to their proper position

upon the airphotos. This rectangular group of nine cells was then annotated upon the airphotos. Three hundred twenty three arrays of nine cells each were annotated in this fashion upon their respective sets of photographs. These photographs were next interpreted for the land use/land cover which occurred in each of the arrays of nine cells using the preliminary classification system (Table 2.3). The interpretation was completed by a professional staff member of the Mining Research and Service Organization of Taiwan and checked by the Taiwan Forest Bureau. A data form containing a sketch of the 3 by 3 cells was completed for each sample array by the interpreter (Fig. 2.7). Upon it was sketched the land use/land cover of the array identified by the respective codes. Additional ancillary data was also noted on the form such as the date, quality, etc. of the airphotos used together with any comments.

The land use/land cover of each of the topographic maps was summarized by tabulating its occurrence in numbers of individual cells (Table 2.4). The majority of the cells were interpreted as having a single dominant land use/land cover. However, quite a number of cells were identified as containing two different land uses and these were counted as 0.5 cell to each of the two categories. The third order of detail (Level III) land uses were not tabulated and were dropped from the preliminary classification scheme at this point as

their photointerpretation proved unreliable from the low altitude black and white airphotos.

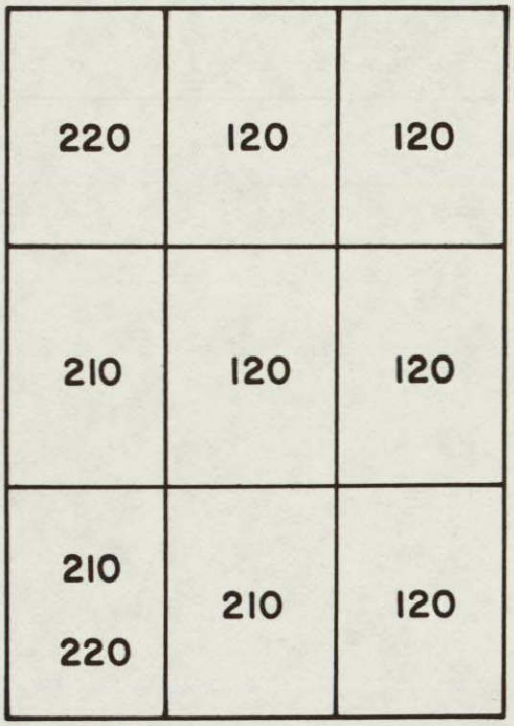

Fig. 2.7. SKETCH OF THE MAP PORTION OF THE DATA FORM COMPLETED BY AIRPHOTO INTERPRETATION. The center cell occurs every 30 by 30 cells on the 1:25,000 graymaps. A 3 by 3 array of cells is interpreted to minimize the impact of misregistration between the transparent topographic map overlay and graymap. Each rectangular cell is ~ 0.45 hectare (~1.1 acre) on the ground. Land uses/land covers are identified in each cell by three digit code numbers (Table 2.3).

The assemblage of this data provides a distributed type of training set for later input to the LANDSAT image classification procedure. At this point it provides an accurate review of the land use of 2760 sampled points distributed over the study site and three maps (Table 2.4). Since the sample points used were assembled

TABLE 2.4. INVENTORY OF THE LARGE SAMPLE OF GROUND CONTROL CELLS INTERPRETED FROM BLACK AND WHITE AIRPHOTOS. Based on 3 topographic maps of 1/50,000. Land areas only were sampled for 3 by 3 array of cells yielding 2370 m x 1710 m (on the ground). A cell covers 0.45 hectare.

Land Use Class				*Lu-Kang Map*		*Taichung Map*		*Kuo-Hsing Map*		*3 Maps Combined*	
Code	*Level I*	*Code*	*Level II*	*I*	*II*	*I*	*II*	*I*	*II*	*I*	*II*
100	Urban lands			38 cells		185 cells		27 cells		250 cells	
		110	Commercial		0 cells		15 cells		0 cells		15 cells
		120	Residential		1		58		0		59
		130	Industrial		0		24		0		24
		140	Transportation		10		15		0		25
		150	Institutional		0		10		9		19
		160	Clustered		20		63		18		101
		170	Mixed		7		0		0		7
200	Agricultural lands			300		681		247		1228	
		210	Grains		46		265		25		336
		220	Crops		248		334		87		669
		230	Orchards		6		82		135		223
300	Forested lands			3		233		777		1013	
		310	Hardwoods		3		191		618		812
		320	Mixed woods		0		12		117		129
		330	Conifers		0		29		38		67
		340	Bamboo		0		1		4		5
400	Barren lands			41		26		31		98	
		410	Gravels		10		26		31		67
		420	Tidal flat		31		0		0		31
500	Water surfaces			40		13		3		56	
		510	Water ways		10		10		3		23
		520	Ponds and reservoirs		27		3		0		30
		530	Estuaries		3		0		0		3
		540	Sediment-laden water		–		–		–		–
600	Range land			3		33		79		115	
		610	Grassland		3		10		7		20
		620	Scattered grass		0		23		72		95
Total				425 cells		1171 cells		1164 cells		2760 cells	

from a regular grid, the relative populations of each land use can now be computed to provide a basis for the subsequent verification of the maps produced by computer interpretation of the LANDSAT image (Table 2.5).

2.3.2.2 Assembling Areal Ground Control Data

Areal ground control data was collected by the same procedure. Twenty-five rectangular or square sample areas were selected from the LANDSAT graymap/topographic map combinations. These areas were distributed over the land area of the three topographic maps so as to provide a reasonable sample of the variety of land uses which occurred in the study area. These small map areas ranged from 30 by 30 cells on the graymap (2370 m by 1710 m) to 100 by 100 cells (7900 m by 5700 m). The map areas were transferred to, and annotated upon, the same airphotos employed in the previous sample data collection using the Zoom Transfer Scope for scale change and local topographic fit. The land use inside the sample areas noted on the photos was interpreted and sketched on the maps by the same photo-interpreter noted earlier. Nominally 1:16,700 sketch maps were prepared of each sample site map (Fig. 2.8). Some residual air-photo distortions remain in these maps as they were not retransferred back to the 1:25,000 graymap/topographic map composite. However, their rigorous geometric relationship to the LANDSAT imagery is not critical.

TABLE 2.5. ESTIMATION OF THE RELATIVE AMOUNTS OF LAND USE OF THE AREA TO BE MAPPED. Based on the photointerpretation of the 2760 ground cells provided in Table 2.4 for the area of the 3 of 1/50,000 topographic maps. Values shown are the percentage of the total land area projected from the sample data to be of the given land use type.

Land Use Class				*Lu-Kang Map*		*Taichung Map*		*Kuo-Hsing Map*		*3 Maps Combined*	
Code	*Level I*	*Code*	*Level II*	*I*	*II*	*I*	*II*	*I*	*II*	*I*	*II*
100	Urban lands			9%		16%		2%		9%	
		110	Commercial		0%		1%		0%		0.9%
		120	Residential		0		5		0		2
		130	Industrial		0		2		0		1
		140	Transportation		2		1		0		1
		150	Institutional		0		1		0.5		1
		160	Clustered		5		6		1.5		3
		170	Mixed		2		0		0		0.3
200	Agricultural lands			71		58		21		45	
		210	Grains		11		23		2		13
		220	Crops		58		29		7		24
		230	Orchards		2		6		12		8
300	Forested lands			1		20		67		37	
		310	Hardwoods		1		16		53		29
		320	Mixed woods		0		1		10		5
		330	Conifers		0		3		3		3
		340	Bamboo		0		0		1		0
400	Barren lands			9		2		3		3	
		410	Gravels		2		2		3		2
		420	Tidal flat		7		0		0		1
500	Water surfaces			9		1		0		2	
		510	Water ways		2		1		0		1
		520	Ponds and reservoirs		6		0		0		1
		530	Estuaries		1		0		0		0
		540	Sediment-laden water		—		—		—		—
600	Range land			1		3		7		4	
		610	Grassland		1		1		1		1
		620	Scattered grass		0		2		6		3

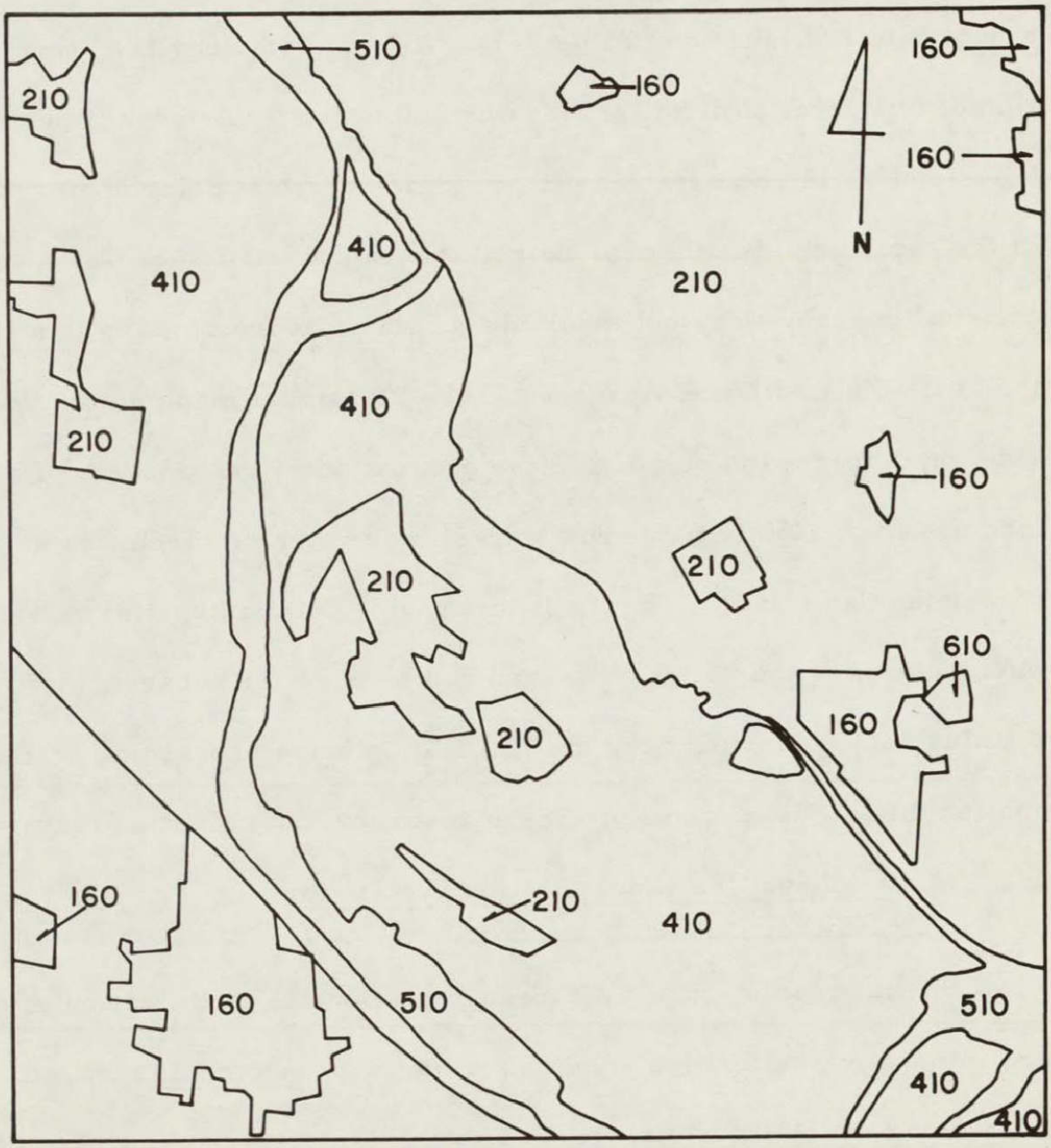

Fig. 2.8. LAND USE SKETCH MAP ORIGINALLY PREPARED AT 1:16,700 ON BLACK AND WHITE AIRPHOTOS. Representative of 25 such square or rectangular sample land use maps distributed over the study area. Small town in lower left corner noted as land use 160 is Chung-Liao-Li. Three digit code numbers designate current land use/land cover (Table 2.3). This area is a slightly enlarged portion of the LANDSAT graymap shown on Figs. 2.5 and 2.6 from lines 159 to 188 and columns 48 to 78.

The sketch maps do not show the originally proposed third order of detail of land use (Table 2.3). As was noted earlier, extraction of this level of detail proved unreliable from the low altitude black and white photographs. It was concluded that color photographs of the same scale would provide reliable interpretation at this level of detail but they were not available for dates approximating those of the available LANDSAT images. These 25 sample maps do not provide any information relative to the estimation of the amounts of each land use in the total study area such as was extracted from the sampled data (Table 2.5). The maps do provide detailed spatial or areal information for the 25 locations and can be used for subsequent training set development for the LANDSAT image processing activity and for direct visual checking of the resulting classification maps.

2.3.3 Initial Land Use Classification System for Testing with LANDSAT Imagery

Spatial resolution has a direct impact on the modification of the preliminary classification scheme for use with automated computer processing of LANDSAT imagery (Table 2.3). This usually results in the inability of the computer to specify the exact function of man's activity on the land surface as noted earlier. This means that the LANDSAT approach will more readily yield land cover information and do poorly on identifying the function which the land cover may represent. For example, a photointerpreter can distinguish between a grass strip denoting a power transmission line or a grass strip

along a railway. He uses the increased resolution available to him as well as shape information. He may see the poles of the power line or the rails and ties and thereby designate the specific function of the wider grass strip. The coarser 0.45 hectare LANDSAT resolution precludes this level of detail in the computer analysis of land use unless ancillary, i.e. non-image, data is employed in the classification scheme. Image processing schemes for use with LANDSAT imagery are currently being developed which overlay other ancillary information such as power line maps and road maps, etc. (Tom and Miller, 1976). This enables the computer to use known information on the distribution of known functions to further identify the activity which might be conducted in a 0.45 hectare cell.

The advanced image processing schemes using ancillary map data were available in the computer programs used in this study but were not tested here. Thus, further modification of the original land use/land cover hierarchical scheme was necessary (Table 2.3). Urban classes such as industrial (130), institutional (150) and transportation and irrigation (140) refer specifically to land function and were removed. The urban type of strip and cluster settlement (160) in Taiwan is usually sparsely distributed among agricultural lands. The integration of the reflected solar energy in the 0.45 hectare resolution cell does not usually resolve such narrow, sparse urban land functions. Waterways (510) and ponds and reservoirs (520)

refer to spatial as well as functional information available to airphoto interpreters and are not distinguished by LANDSAT. The difference between clear water and sediment-laden water or clear water of varying depths is very distinct and categorization of water areas was rebased upon these characteristics. Rangelands (grasslands) are usually small and sparse in Taiwan (Table 2.5) and are confused with agricultural lands and were omitted. Land use categories were retained or added wherever they corresponded with a specific land cover type such as commercial (110).

These considerations in light of the known capabilities of LANDSAT imagery yielded a revised classification scheme for a combination of land use and land cover (Table 2.6). This test scheme contained five gross categories at the first level of detail namely urban, agricultural, forested, barren lands and water surfaces. It is subdivided into 14 more detailed second level classes. Subsequent testing of this land use/land cover classification scheme on LANDSAT imagery will result in a further modification such as subdivision of selected second level land cover classes into third level land cover classes where it was clear that LANDSAT imagery would support such a refinement.

TABLE 2.6. THE PROPOSED LAND USE CLASSIFICATION SYSTEM FOR TESTING ON LANDSAT IMAGERY. Modified from the low altitude airphoto scheme (Table 2.3). This scheme actually denotes land cover. Water classes may denote water depth or sediment concentration and may be interpreted as either.

Code	*Level I*	*Code*	*Level II*
100	Urban lands	110	Commercial
		120	Mixed
200	Agricultural lands	210	Grains
		220	Crops
		230	Orchards
300	Forested lands	310	Hardwoods
		320	Conifers
		330	Mixed
400	Barren lands	410	Gravels
		420	Tidal flat
500	Water surfaces	510	Shallow seawater
		520	Medium seawater
		530	Deep seawater
		540	Fresh water

III. DEVELOPMENT OF LANDSAT TRAINING SETS TO REPRESENT THE LAND USE/LAND COVER OF TAIWAN

3.1 Methodology Used to Improve the LANDSAT Imagery

3.1.1 Introduction

Fourteen times a day each of the two U.S. National Aeronautics and Space Administration's (NASA) LANDSAT satellites orbits the earth collecting resources information from the surface. A brief introduction to the Multispectral Scanner (MSS) imaging system on each satellite was presented earlier (Section 2.2) and is reviewed and supplemented here. These MSS systems aboard the spacecraft convert the hue (i.e. four bands) and intensity of the reflected sunlight from earth below into an analog signal representing a series of images. These signals are stored on on-board tape recorders for subsequent retransmission when the satellite is within range of a U.S. tracking station or they are transmitted directly. Additional tracking and recording stations are in construction or operation in S. America, Africa, Australia, Japan, etc. Taiwan is within direct readout range of the Japanese recording station under construction although the images used in this study were recorded and retransmitted to a U.S. station.

The four overlapping, simultaneous MSS images received at the ground station as analog signals are recorded and processed and made available to potential users in a photographic form. These space photos each cover an area of nominally 185 km by 185 km and are available as black and white or color composite photographs ranging from scales of 1:250,000 to 1:3,369,000. This multiple date coverage of most of the world land area may be purchased from the U.S. Department of Interior, EROS Data Center, Sioux Falls, South Dakota which acts as the agent of public distribution of these images for the U. S. Government.

The analog signals representing each MSS four band image may also be digitized as described earlier to provide numeric values for discrete pixels or ground resolution cells. The resulting computer compatible tapes (CCTs) may thus be obtained from the EROS Data Center for any imagery which has been recorded (Appendix B). However, before this digital imagery can be used it must be corrected or preprocessed to remove as many of the systematic errors as possible such as those geometric errors caused by the rotation of the earth and motion of the satellite. There are also several kinds of non-systematic errors or noise involved in the images which may at first appear to discourage their quantitative analysis. The effects of spatially varying clouds, haze and other atmospheric constituents on the propagation of the electromagnetic energy from sun to ground and

ground to the satellite produce non-systematic noise within the individual LANDSAT image. The variations in signal caused by the surface features sought such as topography, soil types, vegetation changes, etc., also provide a spatially varying component in each of the four different MSS bands constituting one LANDSAT scene. The MSS sensing system also adds additional systematic and non-systematic noise to the data; for instance, the six-line problem caused by the imbalance in the calibration of the six sensors used in a swath for a given band.

The task presented by this imagery is thus much like that in cryptography--to break the code and extract the desired information from the available signal. Surprisingly, although many competing factors affect the recorded image on the CCT, it is still possible by appropriate simplification and calibration to extract very quantitative information about surface features.

The tests completed and discussed in detail in the balance of this section review the methods used for removal of several of the systematic errors and for minimizing the impact of undesirable noise. These include geometric rectification of the images and ratioing between various two combinations of the four of MSS bands. Training sets or sample data were developed to statistically represent each of the desired Taiwan land uses and land covers. Three different procedures for assembling this training data were tested. These sets of

training data were statistically cleaned to remove noise, i.e., other surface material types, which might have been inadvertently included when selecting representative samples. Finally, the image processing algorithms were tested on the three different sets of training data. These tests determined which combination of training data and algorithm would produce the most suitable land use/land cover maps.

3.1.2 Geometric Correction Applied

The systematic geometric corrections such as scaling and skew that could be predicted reasonably well were performed without direct use of ground geometric control points. More advanced LANDSAT geometric rectification procedures necessitate supplying a collection of known ground positions which must be located to $\pm$ 1 cell in the uncorrected image graymaps. This approach may work well in countries with extensively developed large scale road and other transportation nets with very rectangular agricultural cropping patterns to supply geometric control points which can readily be located in the unrectified graymaps. Obtaining such a collection of geometric ground control points is not nearly so reliable in the many countries dominated by smaller scale, irregularly laid out agricultural and transportation systems. The system employed here worked very well on a map by map basis without the direct incorporation of any geometric ground control points into the rectification process. The

correction consists of applying five linear transformations which act on the entire image without direct reference to ground control.

The LANDSAT image consists of discrete samples of reflected solar energy over a two-dimensional image space. The image can be thought of as a three-dimensional array P(i, j, k) where i are the rows or lines of image cells, j are the columns of image cells across the scene and k are the four MSS spectral bands. The data values for each pixel are non-negative integers having values between 0 and 127.* The four MSS bands are assumed to be in perfect registration so that the problem can be studied as a two-dimensional, single band image problem. Linear transformation of elements of the original unrectified two-dimensional image space into another more geometrically correct two-dimensional space is accomplished by the simultaneous application of the following matrices as linear transformations.

$$\underline{Y} = \underline{A}\,\underline{X}$$

$$\underline{Y} = \begin{bmatrix} Y_1 \\ Y_2 \end{bmatrix} \qquad \underline{X} = \begin{bmatrix} X_1 \\ X_2 \end{bmatrix} \qquad \underline{A} = \begin{bmatrix} A_{11} & A_{12} \\ A_{21} & A_{22} \end{bmatrix}$$

---

*Data values range from 0 to 127 in MSS band 4, 5 and 6, while they range from 0 to 63 in MSS band 7 because of the differences in dynamic ranges of the sensors.

The application of these linear transformations can be depicted (Fig. 3.1). The nodes of the X grid represents original LANDSAT numeric samples of pixels of reflected energy from discrete resolution cells on the earth. The desired geometrically rectified sample cells are represented by the Y grid. The new samples are oriented in a rescaled, rotated, and deskewed coordinate system. The geometric correction process assigns reflected energy values to nodes (or cells) in the new Y grid using the pixel values available from the original LANDSAT data on the X grid. The linear transformations $\underline{A}$ denote matrices representing the systematic adjustments for 1. scale change, 2. rotation, 3. skew due to the earth rotation, and 4. output scale factor. Correction for the non-linear, sinusoidal variation in the oscillation rate of the scan mirror are also applied.

Application of the total geometric transformation to an input image requires new samples on the new Y grid between existing samples on the input X grid where there is no sample value. Thus, some interpolation scheme is required to resample points if an uniform completely filled output grid is desired. The resampling technique used was the nearest-neighbor assignment, in which the value of the closest input sample on the X grid is assigned to the sample point on the output Y grid. The average position error introduced by this geometric transformation of LANDSAT data using the

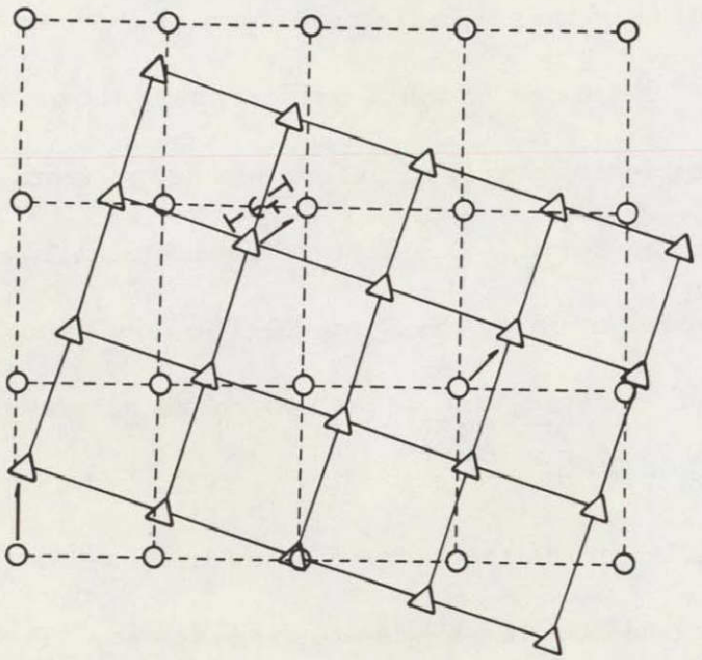

Fig. 3.1. RELATIONSHIP OF ORIGINAL AND TRANSFORMED LANDSAT IMAGE CELLS. The new or output grid represents a clockwise rotation and rescaling of the original input grid. ϵ_T is the total Euclidian Error Distance introduced by the resampling technique (after P. E. Anuta, 1973).

nearest-neighbor assignment is about 20 meters or 66 feet (Anuta, 1973). This error is only slightly more than the 50 feet tolerance for 1:24,000 scale topographic maps generated by the U.S. Geological Survey. The tolerance of this 1:24,000 map is presumed similar to or better than that of the 1:50,000 scale topographic maps of Taiwan.

The geometric correction procedure outlined above was applied to the available LANDSAT imagery of the study area. The actual

computer program applied to compute the transformation was part of Colorado State University package of computer programs entitled the LANDSAT Mapping System or LMS for short (Appendix A). The computer line printer provided the most economic display device for reproducing and checking the geometrically corrected four band underlay of the three 1:25,000 enlarged, transparent topographic maps. Thus the line printer was used to output symbolic graymaps of each image band as described earlier and the land use/land cover classification maps to be subsequently produced. This line printer produces 8 lines per inch and 10 symbols per inch along the line. Thus the output grid from geometric adjustment must be rectangular in the ratio of 8 to 10 and scaled so that the line printer graymap is printed at 1:25,000. The interaction of the output grid (Y grid) of these dimensions with the input grid (X grid) of the LANDSAT pixels is quite good. The output sample cell size to be displayed on the line printer by one symbol at 1:25,000 scale represents nominally 79 m N-S and 64 m E-W. The original LANDSAT pixel has already been shown to be a rectangle of nominally 79 m by 57 m inclined about 12° to the east of north by the inclination of the orbit. The application of the nearest-neighbor resampling to original inclined LANDSAT grid by the N-S and E-W output grid is quite satisfactory due to the similar size and shape of input and output cells. Should a more varied transformation be undertaken, e.g. to match some other map

scale or to a square cell grid, a more significant mismatch would occur resulting in significant oversampling or undersampling. The simple nearest-neighbor resampling for 8 by 10 line printer display of 1:24,000 to 1:25,000 scale is about optimal when using this procedure to rectify LANDSAT imagery (Fig. 3.2). At the 1:25,000 scale 87.8% of the original LANDSAT cells are sampled once, 1.4% are sampled more than once, and 10.8% are not sampled (Miller, 1975).

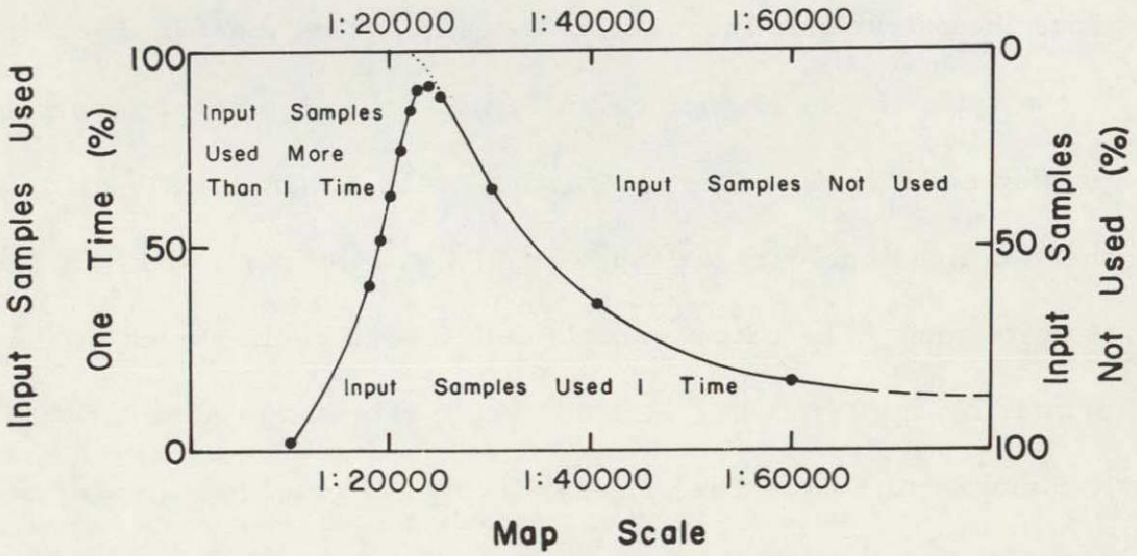

Fig. 3.2. RESAMPLING EFFICIENCIES OF THE GEOMETRIC ADJUSTMENT. Application of the nearest-neighbor approach in the resampling at various map scales transfers percentages of the samples shown from the input grid (X grid) to output grid (Y grid). The curves apply to maps resampled in the ratio 8 N-S to 10 E-W for display at the scales shown on the 8 line/inch printer (Miller, 1975).

Four new revised LANDSAT images are produced upon completion of this operation from the four original MSS LANDSAT bands. Each new set of four resampled images is deliberately prepared for an area slightly greater than each of the three respective 1:25,000 topographic maps. A graymap at the scale of 1:25,000 is printed on the line printer for one of the resulting new four band image files as they will now be called. The respective topographic map in the form of a 1:25,000 transparency is overlaid upon this line printer map and translated N-S and E-W until an accurate match is obtained between the topographic map and the graymap features related to the topography. This introduces geometric ground control which does not require the identification of specific control points on the graymap. It is a regional overall fitting of the two maps of the same scale and geometry. Once the best fit has been selected the excess or boundary cells in the graymap are trimmed off by the computer so that the resulting image file exactly matches the map area on the respective topographic map (Appendix A). One four band image file is produced in this fashion to match each of the three topographic maps (Fig. 2.1). These three small image files contain all the image cells dealt with in the balance of this study and are much smaller than the original 185 km by 185 km total image (Fig. 2.4).

3.1.3 Ratioing MSS Bands

Ratioing has been proposed by a number of experimenters as a means of reducing non-systematic errors within a multispectral image. Ratioing is simply dividing the reflected solar energy or radiance recorded in one MSS band by that of another on a cell by cell basis. Similar surface cover materials may have been recorded at different radiance values in a given spectral band because they occur on varying topography (i.e. differing solar lighting conditions), in areas of spatially varying atmospheric effects and so on. Should these perturbing effects be multiplicative in the same amount for the two spectral bands, the ratio of the two spectral bands will cancel the effect as it multiplies both numerator and denominator.

A ratio of the near infrared and chlorophyll absorption bands is well correlated with the amount of functioning green biomass on the ground surface in grassland areas (Pearson, Tucker and Miller, 1976). The ratio of MSS bands 7/5 might be an important variable for surface biomass classification as MSS band 5 (0.6 to 0.7 micrometers) contains the region of highest chlorophyll absorption and MSS band 7 (0.8 to 1.1 micrometers) is a spectral band characterized by high levels of reflectance for green vegetation (Maxwell, 1974). Also, since MSS band 4 (0.5 to 0.6 micrometers) does not contain the center of either of the two chlorophyll absorption bands, the ratio 5/4 might also be an important derived image. An advantage which

adjacent ratios should give for vegetation classification is an improved signal to noise ratio (Maxwell, 1976).

MSS ratios have been shown to be effective for quantitative mapping of suspended solids in water of up to at least 900 ppm. Typical mid-continent values for variables such as sun angle and wind speed do not significantly affect MSS ratios for this application (Yarger and McCauley, 1975).

Each of the three topographic map oriented image files created earlier contain the four MSS bands in the form of four radiance values for each cell. These four bands are designated 4, 5, 6 and 7. Twelve ratios can be computed for the four bands taken two at a time. One half or six of these ratios will be the inverse of the remaining six. The spatial variation in the ratio of two spectral bands is just the same as in the ratio of the inverse of the two bands except in an inverse sense. Thus, no unique differences are available in the inverse ratios and they were omitted. Six ratios between the four original MSS bands were thus computed and interspliced back into the four band image file using the LMS programs (Appendix A). Each cell in this 10 band/ratio image file is represented by 10 values, one for MSS bands 4, 5, 6, and 7 and ratios 5/4, 6/4, 7/4, 6/5, 7/5, and 7/6.

3.2 Selection and Evaluation of Training Sets

3.2.1 Introduction to Computer Image Classification

A land use/land cover map is prepared by computer classification using a process which recognizes groups of image cells or classes whose members have selected multispectral characteristics in common. This is a statistical process which may be implemented on a digital or analog computer. Ideally, these classes or groups of cells should be mutually exclusive and exhaustive. This states in a statistical sense that there should be one and only one class to which a cell belongs and can be assigned and all cells in the domain of interest may be so assigned to one of the classes based on its multispectral characteristics. These rigorous requirements are difficult to fulfill and often are not totally achieved in practice. The land use/land cover classes or groups of cells sought in this application are based on the 10 band/ratio multispectral properties possessed by the cells in the image files. A class is formed by grouping together a small, representative number of those cells in the image files that are alike and represent a known, selected land use or land cover. Likeness of the cells assembled together to represent one class is specified by statistical similarity in the radiance values recorded for those cells for one or more of the MSS bands/ratios. Optimum classification will group image cells together into classes which are separated from one another in one or more MSS bands/ratios by

discontinuities in the ranges of their observed radiances (Siegal, 1976).

There are two basically different, general approaches to classification mapping with LANDSAT images. The classification can be "unsupervised" in which the boundaries between land cover types are objectively determined from a computer algorithm to delineate natural clusters in a spectral sense. The "supervised" approach, on the other hand, uses training areas of sample cells selected to represent each class by the human analyst. Supervised classification requires each training area or group of image cells to be representative of a specific land cover of interest based upon "a priori" knowledge referred to as ground control or "ground truth" data. "A priori" ground control or "ground truth" information may be collected on the ground, with airphotos or, more logically, a combination of both. Statistics such as mean and variance are computed for all selected cells for each class and spectral band. These statistical representations of each land use/land cover are used "to train" various automated techniques to identify all other unknown cells within the LANDSAT image file which have statistically similar multispectral characteristics. The supervised approach is the only approach tested in this study. However, the unsupervised approach is very useful and should not be overlooked, especially when dealing with areas where ground control data is non-existent or difficult to obtain.

The supervised classification scheme requires that at least one training set or group of image cells be selected to define each land use/land cover class or theme. These training sets should be representative of each of the land use/land cover classes to be investigated. They in turn constitute a small subset of the original image file in n-dimensional multispectral space, where n = 10 and each dimension is a spectral band or a ratio of bands. The classification scheme tested here is discriminant analysis which uses the selected training sets to define "volumes" in this n space. Each of the remaining cells in the image file which are not part of the training sets may subsequently be checked to see which of these n-dimensional volumes it best fits in a statistical sense thus defining its unknown land cover. A more technical, mathematical expression of this approach has been included (Appendix B).

3.2.2 Factors Affecting Selection

The previous discussion shows that the selection of the training sets to represent each land use/land cover class is the most important part of this computer analysis of LANDSAT imagery. These training sets must be a collection of sample cells which is representative of the total population of the land use/land cover class in the related image files. The quality of the final classification map for each land use/land cover class depends to a large part on how well the training set represents it.

The population of a well defined land use/land cover class should approximate a multivariate, normal distribution. A random sampling method might be employed to get an unbiased training set which is representative of each specific class. This sampling procedure will be tested here although it incorporates difficulties in economy and timeliness.

The size of training set representing each land use/land cover class is also a critical point. It may appear that the bigger the sample the more representative and better the training set will be. The subsequent development of the statistical representation of a land use/land cover class is usually an iterative procedure and if sample size is big the cost is consequently high. Also, the larger the sample the greater the risk of including cells which are not related to the land cover sought. However, the minimum number of sample cells should be at least greater than the number of spectral bands and ratios should it be necessary to invert the covariance matrices to obtain the discriminant functions. Finally, it would not be surprising if several times that minimum number of samples was needed to smooth out statistical fluctuations and obtain a really good estimate of the population (Duda and Hart, 1973). As a rule of thumb, 30 times the number of spectral bands/ratios is a reasonable lower limit on the size of training set for a given class (Smith, 1976).

Three major problems were encountered in this study during the selection of the training sets. They were (1) temporal inconsistency between the date of the collection of the LANDSAT image and ground control data, (2) misregistration of the ground control data, and (3) lack of rapid, direct communication between this study and those responsible for collecting the ground control data.

(1) Temporal inconsistency between the images and ground truth was inevitable in this application and many others. The only available LANDSAT imagery was taken on November 1, 1972. The ground control information available for this study included three 1:50,000 topographic maps published in 1970 and a collection of 1:16,700 B & W airphotos taken on various dates one or two years after the LANDSAT image.

(2) Misregistration between the ground control cells and image cells was particularly critical in the test of the grid cell sampling method. Specific geometric control points were not available for the geometric corrections applied. The average position error which resulted was $\pm$ 1 or 2 cells.* Misregistration thus occurs while transferring the ground control cells from graymap to airphoto for identification. The error in its final location could

---

*LANDSAT geometric rectification programs are currently available using ground control points which achieve accuracies of RMS = $\pm$ 0.5 cells for the entire LANDSAT image.

easily be on the average of one cell. This one cell displacement problem may not be so serious in areas of large scale homogeneous land uses. But, it may markedly effect the representative nature of training sets collected for "noisy" or small scale land use patterns as in Taiwan.

(3) Lack of rapid, direct communications between the collector of the ground control and those performing the image analysis in the U.S. was caused mainly by the large distance between the two countries. It takes at least two weeks to have a two-way exchange by air mail. Better communications between these two functions would yield better training sets.

3.2.3 Statistical Cleaning Applied

A training set is usually obtained by selecting one or more rectangular or irregular bounded groups of cells within a larger region previously identified on the ground or with airphotos as representing the desired land cover class. A training set can also be assembled from a sampled group of discrete cells which have been previously identified as representing the desired class. The first or area method overlooks the possibility that some of the individual cells within the specified training sets may not be of the desired class or may be excessively noisy. The second or point method is very sensitive to miss-selected points due to the misregistration of the point ground control data on the graymaps. Statistical cleaning of training

sets has been proposed as a method to reduce the noise incorporated into the training sets by these and other related errors (Maxwell, 1976). However, one might argue that the class heterogeneousness is really not noise but an integral part of the land use/land cover class. Thus, if a considerable percentage of the cells representing a class were removed from its training sets, the remaining cells might be too specific to represent the real, diverse nature of that land use/land cover class. The procedure tested and described below uses as a rule-of-thumb that no more than 20% of the cells representing a class will be removed in a given iteration.

The statistical cleaning was accomplished iteratively by computing the mean vector and covariance matrix, the spectral signatures, for each class based on the original, unaltered training sets. Then the "posteriori" probabilities were computed for the possibility that each cell in each training set belonged to each land use/land cover class. Cells were deleted from a given training set if they had a low probability of belonging to the class which they were originally selected to represent and/or a high probability of belonging to one of the other classes. Proceeding iteratively, a new mean and covariance matrix was computed for the cells which remained to represent each class ($\geq$ 80%) and additional cells deleted by the same criterion. Usually two or three iterations were enough to provide adequate cleaning which was indicated by high "posteriori" probabilities for

the remaining cells (Maxwell, 1976). Placing a limit on removing no more than 20% of the cells in a training set for any given iteration "points" the training set toward the numerically dominant land use/land cover in the set.

The impact of statistical cleaning on the classification results for three methods of selecting training sets was carefully investigated. The discriminant functions were computed from and applied back to the cells of the training sets as an indication of their accuracy to discriminate or map the unknown cells. Deleting those cells with low probability of belonging to the training set representing the class was tested to determine if the remaining cells yielded a "better" training set. A new discriminant analysis and cleaning activity is iteratively performed with the remaining points as noted above. A measure of the ability of the modified training sets to represent discrete, mappable land use/land cover types can be obtained after each cleaning iteration. Apparent training set accuracy provides a measure of the total number of the cells in a given class(es) which are actually assigned to the correct class(es) by the discriminant function at that iteration or cleaning level. The cells which are correctly assigned to the proper class(es) are divided by the number of cells input to that step representing the class(es) and multiplied by 100 to yield this measure of accuracy in percent. Thus at any level of cleaning the

$$\text{Apparent Training Set Accuracy} = 100 \times \frac{\text{Correctly Classified Cells}}{\text{Cells Input to Form the Discriminant Function}} .$$

The numerator of this fraction can be expected to hold reasonably well while the denominator decreases as the number of cells representing a class(es) decreases with successive cleanings. Thus, the apparent training set accuracy increases as cells are cleaned or removed from the original training sets.

Actual training set accuracy is computed by dividing the cells which are correctly assigned to a class(es) at any level of cleaning by the original number of cells selected to represent that class before any statistical cleaning is applied. The fraction obtained is multiplied by 100 to convert it to percent as

$$\text{Actual Training Set Accuracy} = 100 \times \frac{\text{Correctly Classified Cells}}{\text{Original Cells Selected to Represent the Class(es)}} .$$

The denominator of this fraction is fixed at the original number of cells for each successive cleaning of a class(es) while the numerator fluctuates to indicate the actual impact of the cleaning procedures on the classification matricies. Statistical cleaning is designed to remove those cells erroneously included in the group of cells selected to represent a class. The revised classification matricies computed after each cleaning are applied to all the cells originally selected to represent the class. The revised matricies have been improved by the cleaning process if some of the members of the original group of

cells which were incorrectly classified are now "pulled back" or correctly classified.

Further understanding of these two measures of evaluating statistical cleaning may be achieved by example. A specific agricultural field is selected as a training set to represent a given agricultural crop cover class. The field contains areas of good homogeneous crop canopy and small areas of trees and areas of the crop mixed with weeds. Statistical cleaning may remove the cells representing trees as they have low probability of being the crop and high probability of belonging to another class representing trees. A portion of the cells representing the weed/crop mix would have been incorrectly classified before cleaning. Statistical cleaning is applied to improve the classification matricies for the crop by removing the tree cells and the value of this is measured by what happens to the weed/crop mixed cells. Pulling them back into the crop class may provide the best and appropriate map of the distribution of this crop type. This may be evaluated by examining the actual training set accuracy at each successive level of cleaning where the numerator should increase as error or tree cells are removed from the training set for the given class.

Apparent and actual training set accuracy is computed and examined for each of the three approaches used to compose the training sets. At the outset it should be clearly understood that if the

training sets are roughly picked by an inexperienced user a meaningful increase in actual training set accuracy might accompany the statistical cleaning. Training sets which are carefully selected to represent each desired class may show little improvement with successive cleaning.

The final determination of the impact of this statistical cleaning must be made by consideration of what it does to improve the accuracy of the final, total classification map. Examination of the training set accuracies computed in this effort only hint at the impact of the procedure on the actual map production.

3.2.4 Non-Supervised Method

The initial training set selection was completed without benefit of airphoto or other direct ground control information. The only information available was the 1:25,000 graymaps of MSS band 5 and 7, the 1:25,000 topographic overlay, and the knowledge of the test area possessed by four Taiwan resource specialists present in the U.S. The supervised method of collecting training sets has come to imply that specific ground control information was used as a basis for training set selection. Unsupervised image classification is a quite different analysis procedure employed when no ground control data is known and no training sets are to be employed. The procedure evaluated here used the supervised approach without benefit of ground

control and is termed "non-supervised" to avoid confusion with either of these two accepted procedures.

The graymaps of MSS band 5 and 7 were carefully examined. Homogeneous areas in gray tones were visually selected by examining both graymaps simultaneously. Eighteen potentially separable, homogeneous land use/land cover classes were selected and their estimated land use/land cover or water type class assigned based upon the 1:25,000 topographic map overlay and the judgment of the panel of four Taiwan resource specialists. This procedure may be graphically represented as a plot in two dimensions with each axis showing the magnitude of the radiance values recorded for each cell in MSS band 5 and 7. This plot is referred to as two dimensional spectral space and can be used to visually estimate the separability of each potential land use/land cover class. The cell values* in area A range from 35 to 45 in Band 5 and from 73 to 255 in Band 7 (Fig. 3.3). The cell values in area B range from 43 to 255 in Band 5 and from 59 to 75 in Band 7 (Fig. 3.3). Cell values in area C range from 0 to 36 in Band 5 and from 0 to 75 in Band 7. MSS band 4 is reasonably similar to Band 5 and 6 is similar to 7 thus these three ground areas represent three different surface materials which may

---

*The cell values were multiplied by 2 for MSS band 4, 5 and 6, by 4 for band 7 in order to increase the data range to an uniform 0 to 255 for use in the LMS software package.

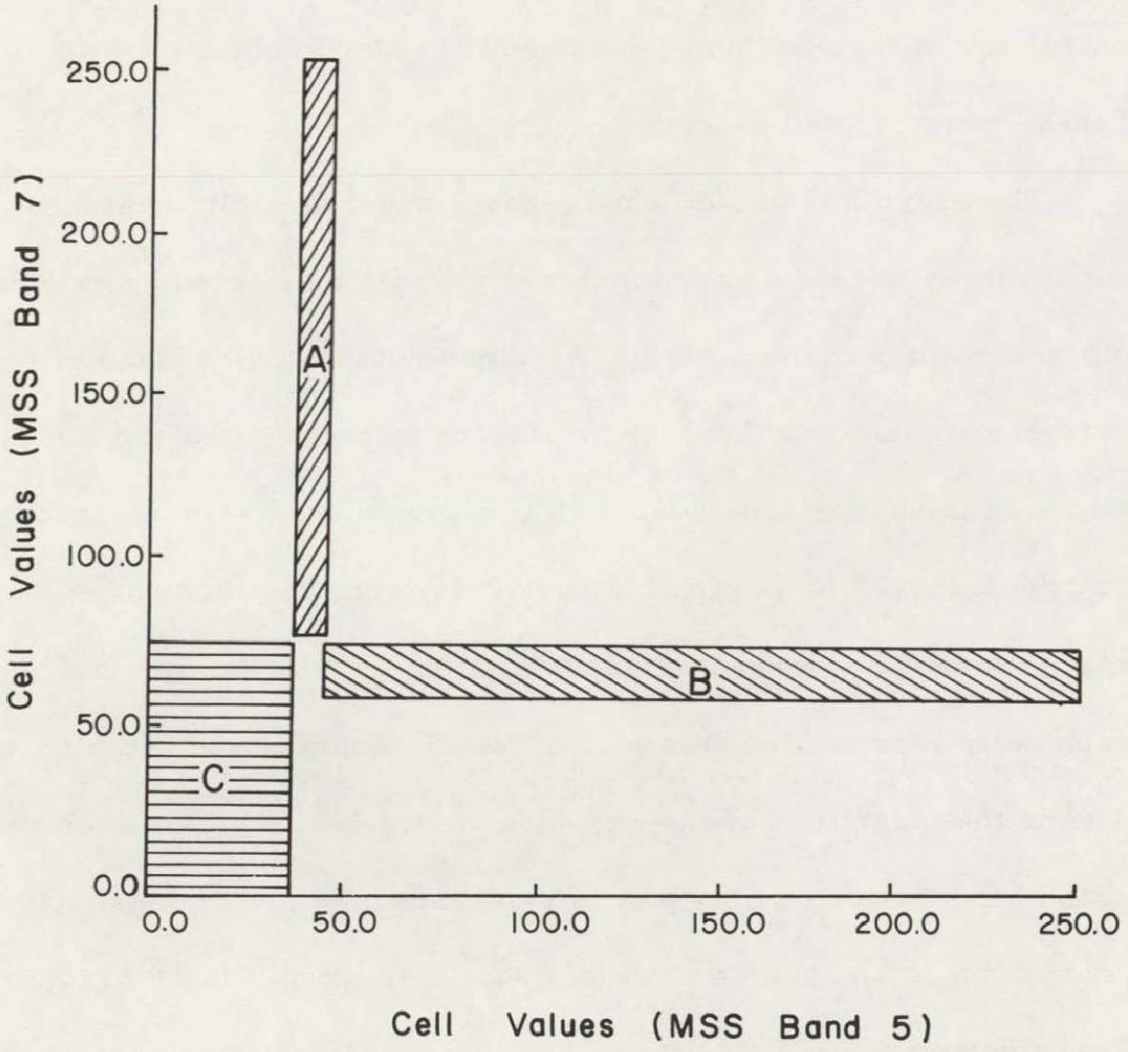

Fig. 3.3. SIMPLE SEPARATION OF CLASSES A, B AND C IN TWO DIMENSIONAL SPECTRAL SPACE. This simple definition is often referred to level slicing.

be mapped reasonably well in the larger four spectral space represented by all four MSS bands. Training sets were thus selected to represent 18 land use/land cover classes using only the hierarchical classification scheme (Table 2.5), graymaps, topographic information, and available knowledge of the area.

The procedure yielded five classes of grains representing distinctly different fields of rice probably in different stages of

growth. Since no ground control was collected at the time of the LANDSAT imaging, it was not possible to place specific names on these and other individual agricultural classes. At this point they may only be identified as distinct, mappable classes. Offshore water classes were designated by selecting training set rectangles in the homogeneous areas of progressively deeper water identified on the topographic map. Less than 10 meters was designated shallow seawater, 10 to 20 meters as medium and more than 20 meters as deep. Considerable confusion between water depth and sediment load were thus possible and cannot be resolved without more known information on actual suspended sediment and turbidity distribution at the time of imaging. Confusion was encountered between the urban land use classes and grain classes as rice is grown in and about the urban portions of the test area. Specific training sets for urban classes are thus difficult to identify and several proposed urban categories were omitted.

The training sets selected in this fashion consisted of several rectangular groups of cells totaling 50 to 250 cells and representative of each of the 18 land cover/water type classes sought. These collections of cells were used to compute a discriminant function which was then tested back upon the same cells to provide an evaluation of how well it can separate or map the cells from which it was prepared. The resultant assignment of all the known training set cells into the 18 classes provides a training set accuracy matrix which indicates

how well the mapping function will perform (Table 3.1). This matrix shows how each of the original training set cells in each class (horizontal dimension of matrix) were assigned to each class by the discriminant function (vertical dimension). The cells which were correctly assigned occur on the diagonal--i.e. they were selected to represent rice and are subsequently classified as rice. Those cells which were incorrectly identified or miss-classified occur off the diagonal. The number of cells on the diagonal for each class divided by the number of cells representing that class is a figure of merit called training set accuracy and is multiplied by 100 to obtain a percentage. All the cells on the diagonal divided by all the cells in all the training sets provide an overall figures-of-merit or training set accuracy for the mapping or discriminant function being tested. The overall training set accuracy for this initial test of the non-supervised training sets using all 10 MSS bands/ratios was 68.6% and varies widely within the 18 classes (Table 3.1).

Discriminant analysis can be made to proceed in a stepwise fashion so that each of the successive 10 MSS bands/ratios are added in their optimal order. This approach does not alter the final accuracy achieved using all 10 MSS bands/ratios but the approach determines if some lesser combination of bands and ratios will achieve an acceptable portion of this final 10 band/ratio accuracy. The greater the number of bands and ratios selected for the final discriminant

TABLE 3.1. TRAINING SET CLASSIFICATION ACCURACY USING THE "NON-SUPERVISED" TRAINING SETS. 18 classes showing training set accuracy *in percent* using 10 channels (4 LANDSAT MSS bands and their 6 ratios).

Land Use Class				*No. of Points*	*Ur-*	*Agricultural*									*Forested*		*Barren*		*Water*				
Code	*Level I*	*Code*	*Levels II and III*	*in T.S.*	*ban*	*211*	*212*	*213*	*214*	*215*	*221*	*222*	*223*	*231*	*311*	*312*	*410*	*420*	*510*	*520*	*530*	*540*	*550*
100	Urban lands					—	—	—	—	—	—	—	—	—	—	—	—	—	—	—	—	—	—
200	Agricultural lands	211	Grain A	63		59	0	0	5	19	0	0	0	17	0	0	0	0	0	0	0	0	0
		212	Grain B	54		0	100	0	0	0	0	0	0	0	0	0	0	0	0	0	0	0	0
		213	Grain C	49		0	0	76	0	0	0	0	0	0	0	0	0	24	0	0	0	0	0
		214	Grain D	63		10	0	0	71	3	0	11	0	0	0	0	5	0	0	0	0	0	0
		215	Grain E	233		17	0	0	4	54	19	0	2	4	0	0	0	0	0	0	0	0	0
		221	Upland crop	147		3	0	0	0	25	59	0	6	6	0	0	0	0	0	0	0	0	0
		222	Sugar cane	187		7	0	0	9	0	0	73	0	7	0	0	3	0	0	0	0	0	0
		223	Citrus	228		1	0	0	0	0	7	0	55	17	19	0	0	0	0	0	0	0	0
		231	Pears	224		11	0	0	2	1	4	4	5	64	10	0	0	0	0	0	0	0	0
300	Forested lands	311	Deciduous low	168		2	0	0	0	1	1	0	9	9	79	0	0	0	0	0	0	0	0
		312	Deciduous high	130		5	0	0	0	0	0	0	0	0	0	95	0	0	0	0	0	0	0
400	Barren lands	410	Gravels	256		0	2	0	21	0	7	0	0	0	0	0	69	1	0	0	0	0	0
		420	Tidal flat	175		0	0	30	0	0	0	0	0	0	0	0	0	36	33	0	0	0	1
500	Water surfaces	510	Shallow seawater	90		0	0	3	0	0	0	0	0	0	0	0	0	24	70	2	0	0	0
		520	Medium seawater	147		0	0	0	0	0	0	0	0	0	0	0	0	0	0	97	3	0	0
		530	Deep seawater	226		0	0	0	0	0	0	0	0	0	0	0	0	0	0	30	69	1	0
		540	Clear water	60		0	0	3	0	0	0	0	0	0	0	0	0	0	0	0	2	93	2
		550	River	70		1	0	7	0	1	0	0	0	0	0	0	0	1	0	0	0	9	80

Overall accuracy = 68.6% obtained by 1762 correct identifications (diagonal) divided by 2570 total samples in all training sets.

function the greater the cost of its application to the total image file. Once the order of the addition of the bands/ratios has been determined a new training set accuracy matrix (Table 3.1) can be computed after the addition of each band or ratio in the prescribed order. Overall and individual class training set accuracy can thus be determined and plotted for each band or ratio added in the stepwise fashion (Fig. 3.4). This graphically portrays the accuracy achieved at the addition of each intermediate band or ratio relative to that achieved by the last or 10th band/ratio. An easy selection may thus be made as to the number and combination of bands/ratios needed to achieve an acceptable and economic combination.

Statistical cleaning was evaluated for use with these training sets. This necessitates that the two computations of training set accuracy described earlier be performed. It is thus possible to plot apparent training set accuracy for band/ratio added as well as actual training set accuracy (Figs. 3.4 and 3.5). A separate curve for each type of accuracy is achieved for each cleaning operation applied. Three successive iterations of cleaning were performed yielding four training set accuracy curves of each type where the 0 level of cleaning represents the initial case where no cells have been removed (Fig. 3.4). The initial or 1st cleaning imposed on these training sets provides a marked increase in apparent training set accuracy at all bands/ratios added and smaller increases occur for each successive

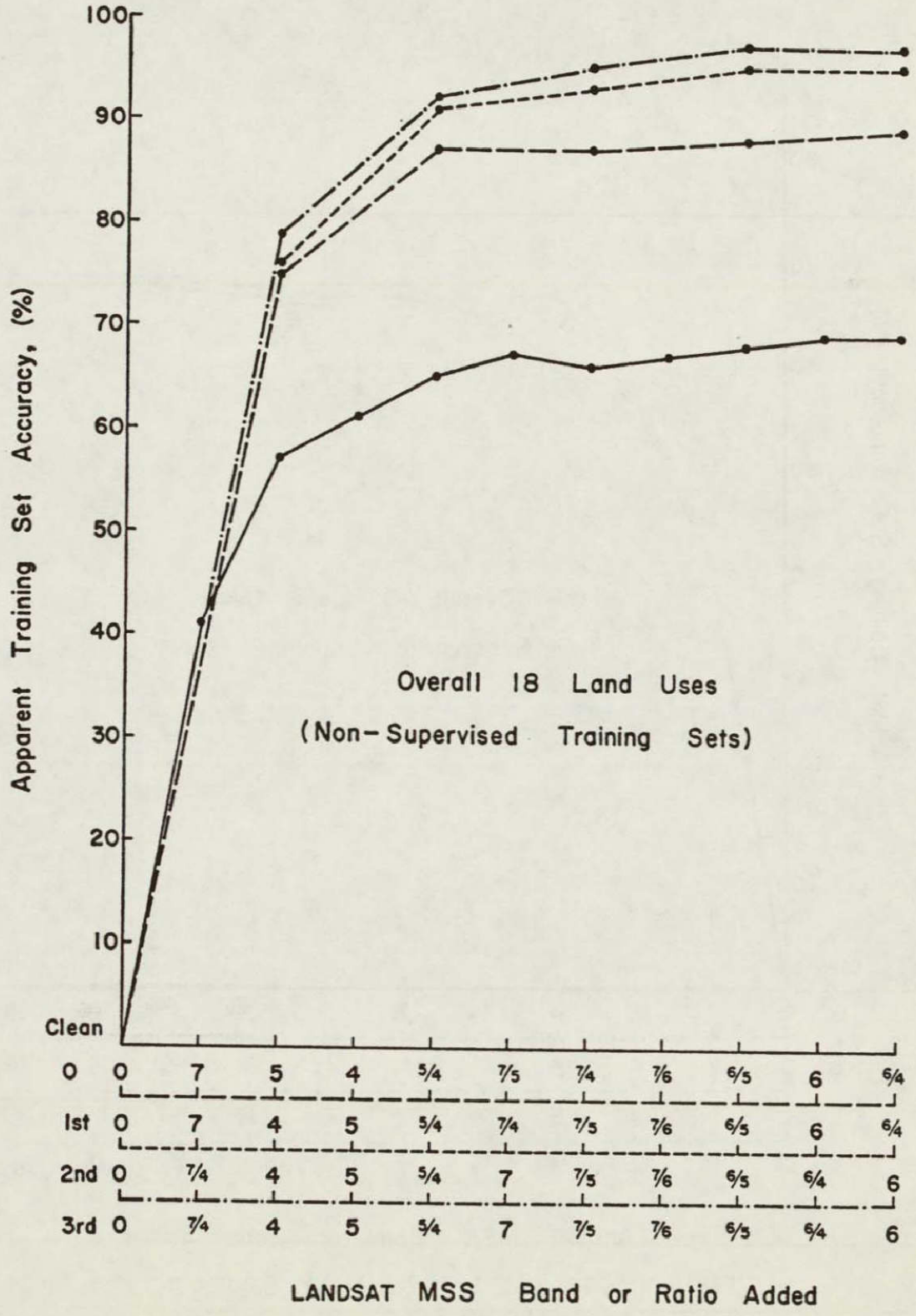

Fig. 3.4. APPARENT INCREASE IN TRAINING SET ACCURACY ACHIEVED AT EACH LEVEL OF STATISTICAL CLEANING. Eighteen classes are represented based on classification by the 10 MSS bands/ratios.

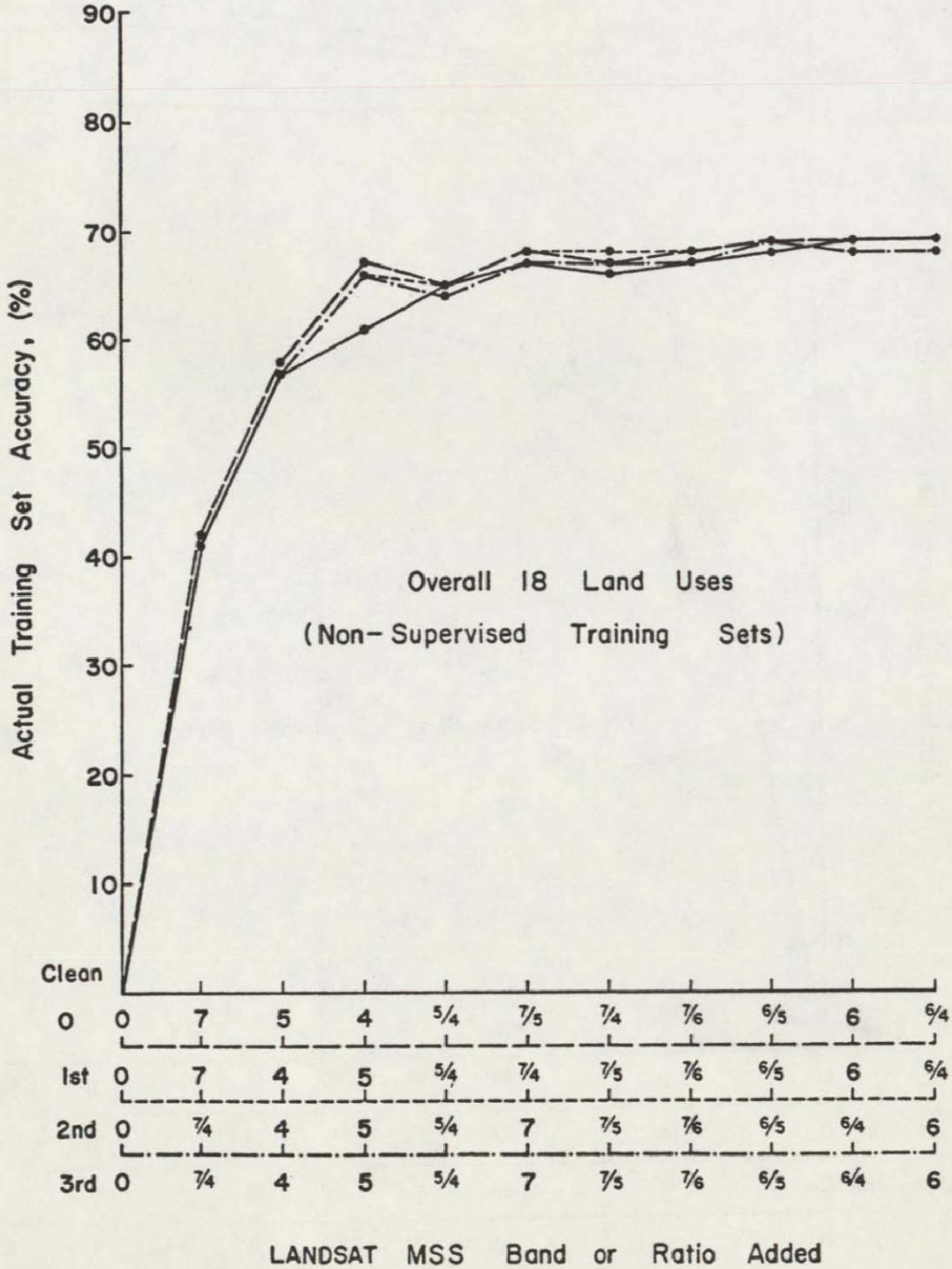

Fig. 3.5. ACTUAL INCREASE IN TRAINING SET ACCURACY ACHIEVED AT EACH LEVEL OF STATISTICAL CLEANING. Eighteen classes are represented based on classification by the 10 MSS bands/ratios.

2nd and 3rd iteration (Fig. 3.4). At the addition of the 10th band after three levels of cleaning an apparent overall training set accuracy of approximately 95% is achieved. Examination of the same graphical portrayal of actual training set accuracy shows no increase due to this statistical cleaning procedure (Fig. 3.5). The cleaning procedure has successively removed cells from the training sets which do not appear to belong to the respective classes based upon their "posteriori" probabilities. This appears to have little effect in "bringing back" or correctly classifying that portion of the cells which were not deleted by the statistical cleaning criteria but had not been correctly classified (Fig. 3.5).

Examination of the curves of actual training set accuracy clearly shows that most of the accuracy was achieved by the addition of the 4th or 5th band or ratio (Fig. 3.5). This indicates that a selection of four or five MSS bands and ratios would suffice without cleaning and produce a final classification map of 18 classes with an accuracy based upon a training set accuracy of 68%.

3.2.5 Supervised Method

The collection of specific ground control data on a grid for an array of 3 by 3 cells at 30 by 30 cell spacing has been described (Section 2.3.2.1). The land use/land cover identity of each of the sample cells was obtained by airphoto interpretation. Those individual cells interpreted as containing two land use or land cover

types were assigned to that one of the two classes which dominated the remainder of the cells in its 3 by 3 array. No sample cells were interpreted for the offshore area of tidal flats and areas of seawater. Thus, the same rectangular training sets were used here for these water type classes as were selected for the non-supervised approach. The 2760 grid sampled cells were reassembled into groups of cells representing each of 14 land use/land cover classes. The number of cells to represent each class is directly proportional to the relative amount of that class in the study area and well represents the natural variability within each class, for example, only 15 cells represent commerical land use while 824 represent the hardwood land cover. Test classification proceeded exactly as outlined for the non-supervised approach. The overall and individual class accuracy can be interpreted from the 10 band/ratio training set accuracy matrix (Table 3.2). An overall accuracy of only 42.3% is achieved ranging from a low of 14% for conifers to a high of 96% for medium seawater.

Three iterations of statistical cleaning were applied to these training sets in a stepwise fashion yielding apparent increases in accuracy at each level (Fig. 3.6). Examination of these four curves of actual training set accuracy implies that no real effect has been achieved (Fig. 3.7). A reasonable approximation of the accuracy achieved by the 10 bands/ratios occurred at the end of only two steps representing the addition of only ratio 6/4 and band 5.

TABLE 3.2. TRAINING SET CLASSIFICATION ACCURACY USING THE "SUPERVISED" TRAINING SETS. 14 classes showing training set accuracy *in percent* using 10 channels (4 LANDSAT MSS bands and their 6 ratios).

Land Use Class				*No. of Points*	*Urban*		*Agricultural*			*Forested*			*Barren*		*Water*			
Code	*Level I*	*Code*	*Level II*	*in T.S.*	*110*	*120*	*210*	*220*	*230*	*310*	*320*	*330*	*410*	*420*	*510*	*520*	*530*	*540*
100	Urban lands	110	Commercial	15	73	27	0	0	0	0	0	0	0	0	0	0	0	0
		120	Mixed	59	7	37	19	15	5	0	0	0	17	0	0	0	0	0
200	Agricultural lands	210	Grains	345	3	14	53	14	13	0	1	0	2	0	0	0	0	0
		220	Crops	699	7	15	38	17	14	1	3	2	3	0	0	0	0	0
		230	Orchards	219	1	5	14	7	30	17	18	6	1	0	0	0	0	0
300	Forested lands	310	Hardwoods	824	0	1	6	3	15	39	20	12	2	0	0	0	0	1
		320	Mixed woods	130	0	2	9	4	22	19	35	8	0	0	0	0	0	0
		330	Conifers	64	3	5	16	3	11	28	13	14	8	0	0	0	0	0
400	Barren lands	410	Gravels	68	19	13	1	6	7	7	10	1	34	0	0	0	0	0
		420	Tidal flat	175	5	0	0	0	0	0	0	0	0	64	31	0	0	0
500	Water surfaces	510	Shallow seawater	90	0	0	0	0	0	0	0	0	0	30	62	8	0	0
		520	Medium seawater	147	0	0	0	0	0	0	0	0	0	0	1	96	3	0
		530	Deep seawater	226	0	0	0	0	0	0	0	0	0	0	0	31	69	0
		540	Fresh water	60	0	0	0	0	0	0	0	0	0	0	0	0	5	95

Overall accuracy = 42.3% obtained by 1321 correct identifications (diagonal) divided by 3121 total samples in all training sets.

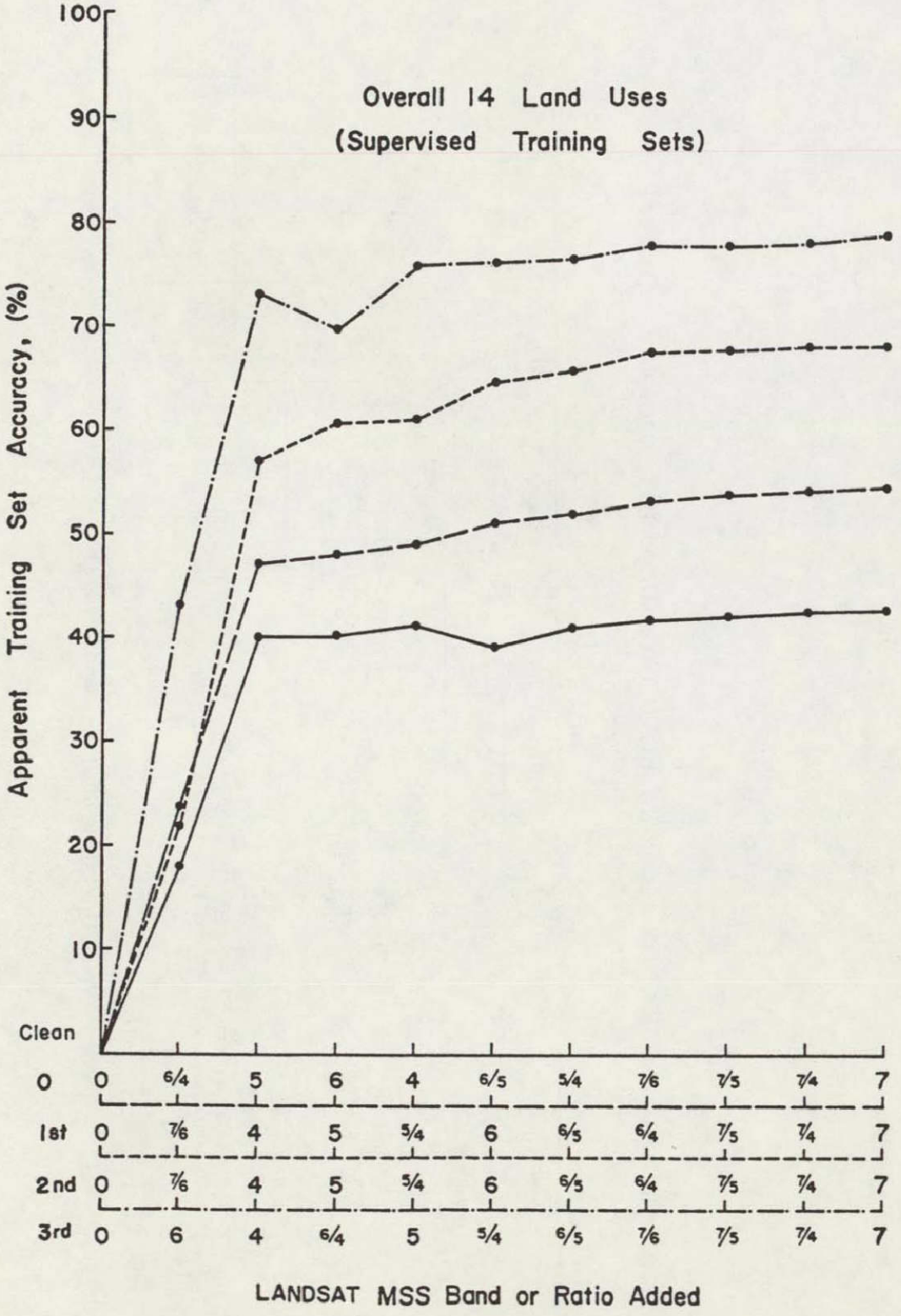

Fig. 3.6. APPARENT INCREASE IN TRAINING SET ACCURACY ACHIEVED AT EACH LEVEL OF STATISTICAL CLEANING. Fourteen classes are represented based on classification by the 10 MSS bands/ratios.

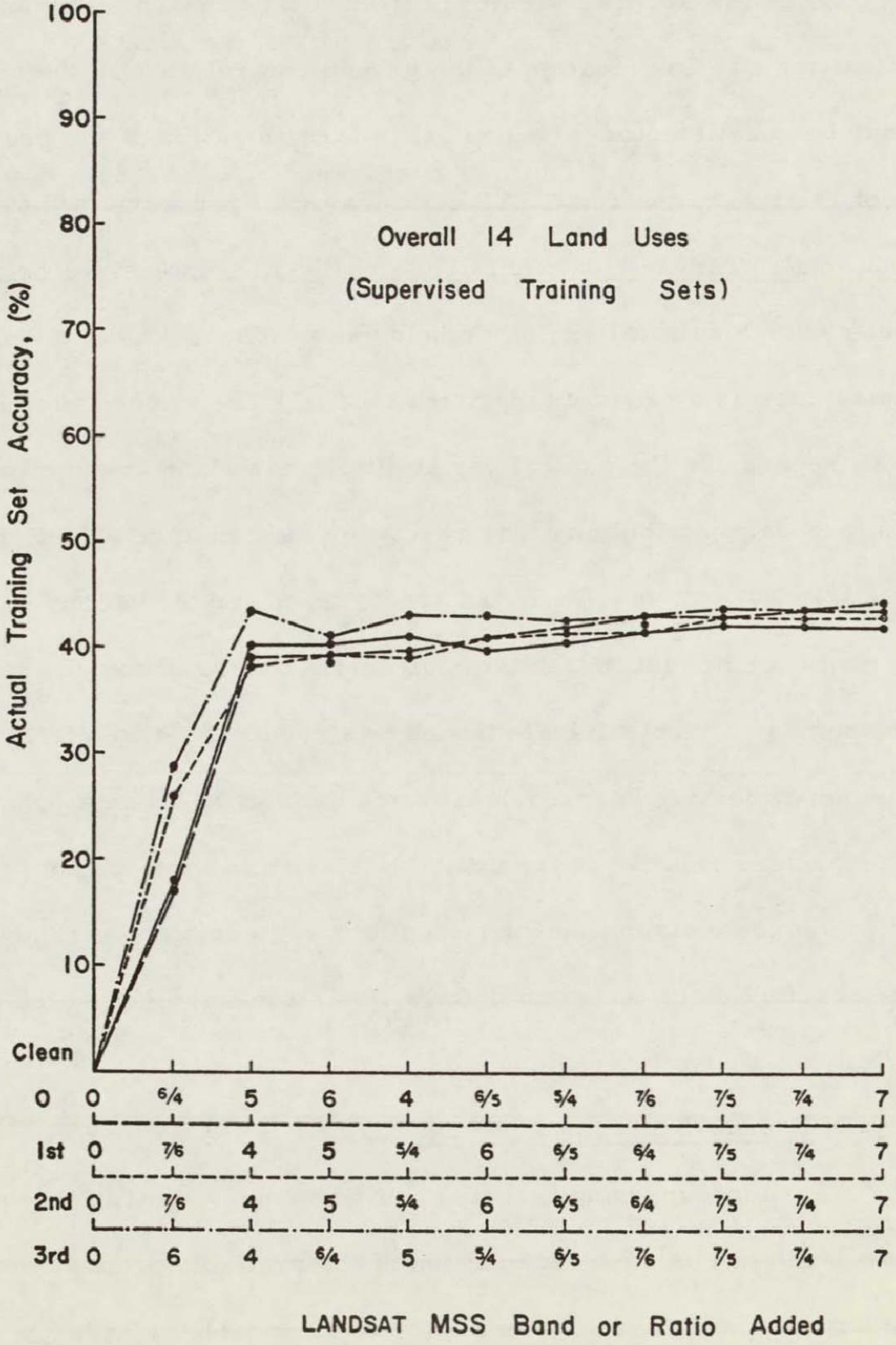

Fig. 3.7. ACTUAL INCREASE IN TRAINING SET ACCURACY ACHIEVED AT EACH LEVEL OF STATISTICAL CLEANING. Fourteen classes are represented based on classification by the 10 MSS bands/ratios.

The low accuracy achieved from this approach is due to two reasons. (1) The location of the ground control data on the graymaps may be unsatisfactory. A one cell misregistration of the ground control relative to the LANDSAT cells may well represent a different material. Taiwan is a country of small scale, intensive, heterogeneous agricultural and other land uses. Thus, a near miss may be as serious as a gross misregistration. (2) The method used here well represents the natural variability in each land cover class. Multimodal distributions may result for the radiance values in a specific band/ratio. The reduction of the number of categories used from 17 to 14 further increases the multimodal nature of the classes. Here the number of agricultural classes was reduced to three from nine in the non-supervised approach to match the ability of the airphoto interpreters relative to the available black and white photos. Thus, the radiance distribution for the cells in a given class may not follow the assumption of Gaussian distribution made in selecting the discriminant analysis technique.

3.2.6 Pseudo-Supervised Method

Pseudo-supervised, that is, "like"-supervised training data was developed using a combination of the available ground control information and careful examination of "mappable" classes by inspection of the natural variation and homogeneousness in MSS band 5 and 7 graymaps. First, the proposed classification scheme (Table 2.3)

was examined with reference to the graymaps to determine if it should be slightly adjusted to represent the number and type of land use/land cover classes which appear mappable. Next, one or more irregular areas were located on the graymaps which were thought to represent these mappable classes and which corresponds to an area covered by one of the 25 ground control maps described earlier (Section 2.3.2.2). Finally, a rectangular or irregular training set selection identified from the ground control map is fit into the homogeneous area on the graymaps (Fig. 3.8). This process was repeated to provide at least three examples of each class containing a total of about 100 cells except for hardwoods type B which contain 246 cells. This procedure overcomes the registration problems of the grid cells approach as the final location of the training set is determined from the graymap while the identity of the class is taken wherever possible from the airphoto interpretations. Actual specific identity was not possible for the agricultural classes due to the mismatch in the dates of the LANDSAT and airphoto images. A small number of the classes could not be represented by reasonably sized rectangular training sets, e.g. the classes which represent highly linear or point distributed land use or land cover. These classes were represented by a larger number of carefully selected irregular shapes and collections of discrete points (e.g. urban land covers). No ground control maps were available for offshore areas of tidal

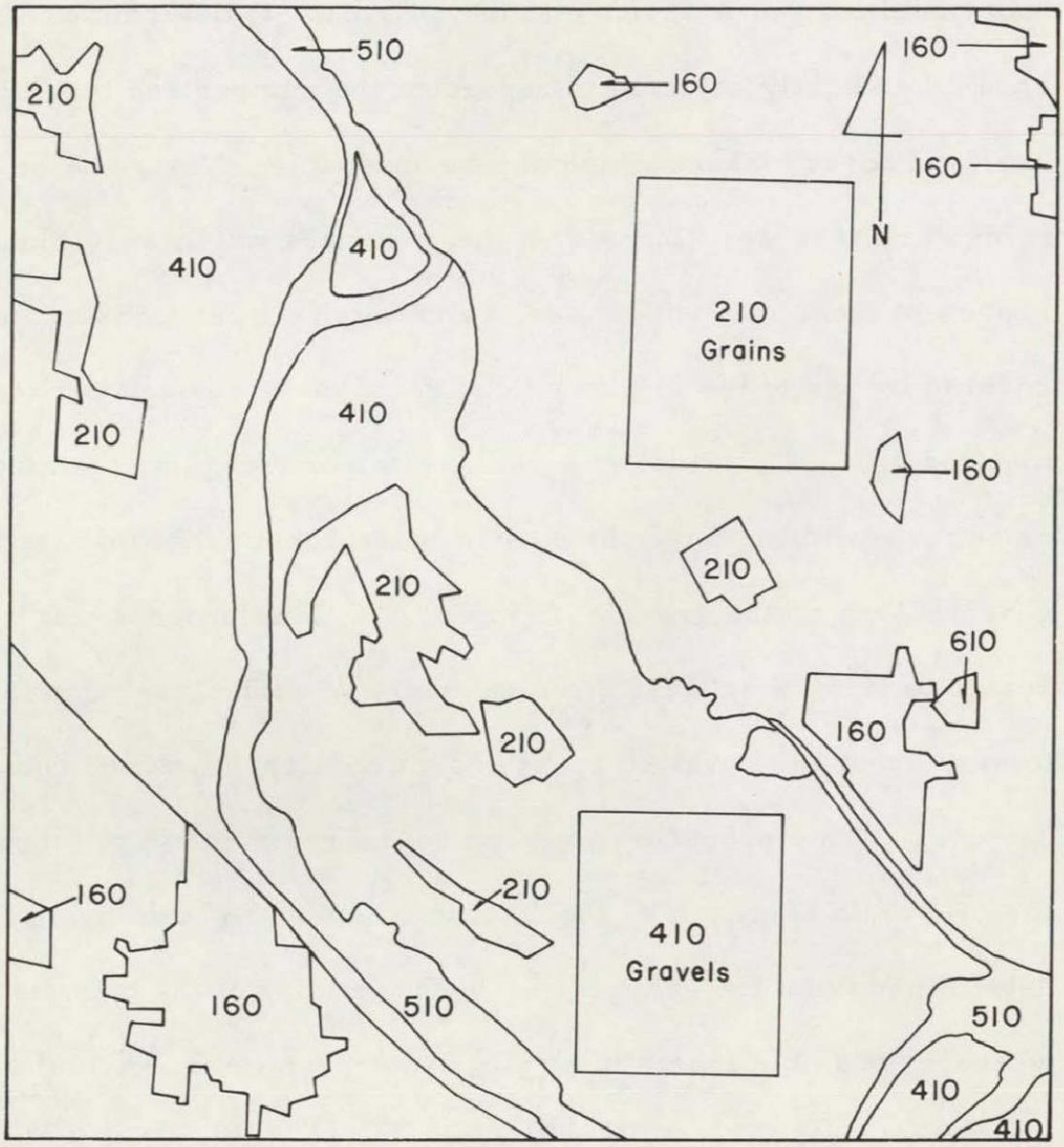

Fig. 3.8. AN EXAMPLE OF THE SELECTION OF TRAINING SETS BY THE "PSEUDO-SUPERVISED" APPROACH. Two rectangles are assigned to the classes of grains and gravels respectively.

flats and areas of seawater. The training sets used here were assembled from a long, narrow strip of cells following a depth contour on the topographic map.

The pseudo-supervised training data assembled performed well as it represented an accumulation of knowledge and experience gained from the two earlier approaches. Test classification and evaluation proceeded as outlined in detail for the non-supervised approach. The overall and individual class accuracies were interpreted from the 10 band/ratio training set accuracy matrix (Table 3.3; Appendices C and D). An overall 20 class accuracy of 77.6% was achieved ranging from 45% for one class of grain to 99% for both medium and deep seawaters.

Lower accuracies were achieved for several of the agricultural classes and for the urban residential classes prompting re-examination of the miss-classification between these classes and their revision to eliminate it. This iterative approach to the selection of the classes was quite in agreement with the type of training set selection approach employed here. The agricultural classes were revised down from 7 to 5 more mappable types and the urban class was combined into the mixed urban class with which it was confused. This reduction of the 20 initial classes to 17 improved the overall training set accuracy to 85% with a low of 71% for one of the crop classes (Table 3.4).

Two iterations of statistical cleaning were applied to the training sets in a stepwise fashion yielding apparent increases in accuracy at each level (Fig. 3.9). Examination of the three curves for actual training set accuracy implies that no real effect has been achieved

TABLE 3.3. TRAINING SET CLASSIFICATION ACCURACY USING THE "PSEUDO-SUPERVISED" TRAINING SETS. 20 classes showing training set accuracy *in percent* using 10 channels (4 LANDSAT MSS bands and their 6 ratios).

Land Use Class				*No. of Points*	*Urban*			*Agricultural*							*Forested*			*Barren*			*Water*			
Code	*Level I*	*Code*	*Levels II and III*	*in T.S.*	*110*	*120*	*130*	*211*	*212*	*213*	*214*	*221*	*222*	*223*	*311*	*312*	*320*	*410*	*420*	*430*	*510*	*520*	*530*	*540*
100	Urban lands	110	Commercial	100	90	3	6	0	0	0	0	0	0	0	0	0	0	0	1	0	0	0	0	0
		120	Residential	85	15	51	24	1	0	0	0	0	0	0	0	0	0	6	4	0	0	0	0	0
		130	Mixed	72	0	31	65	3	0	0	0	0	0	0	0	0	0	1	0	0	0	0	0	0
200	Agri-cultural lands	211	Grain A	82	0	2	6	66	0	22	1	0	2	0	0	0	0	0	0	0	0	0	0	0
		212	Grain B	96	0	0	0	0	100	0	0	0	0	0	0	0	0	0	0	0	0	0	0	0
		213	Grain C	91	0	0	0	23	3	45	0	19	9	0	0	1	0	0	0	0	0	0	0	0
		214	Grain D	101	1	2	2	8	23	1	58	4	0	0	0	1	0	0	0	0	0	0	0	0
		221	Crop A	104	0	0	0	0	0	12	18	50	20	0	0	0	0	0	0	0	0	0	0	0
		222	Crop B	100	0	0	0	2	0	2	0	15	77	0	0	4	0	0	0	0	0	0	0	0
		223	Crop C	75	0	0	0	0	0	0	31	3	0	61	0	0	5	0	0	0	0	0	0	0
300	Forested lands	311	Hardwoods A	156	0	0	0	0	0	0	0	4	1	0	80	14	0	0	0	0	0	0	0	1
		312	Hardwoods B	246	0	0	0	0	2	0	3	4	0	0	13	79	0	0	0	0	0	0	0	0
		320	Conifers	93	0	0	0	0	0	0	0	3	1	0	4	10	82	0	0	0	0	0	0	0
400	Barren lands	410	Gravels	95	0	7	19	1	0	0	0	0	0	0	0	0	0	72	1	0	0	0	0	0
		420	Reclaimed	70	1	3	4	0	0	0	0	0	0	0	0	0	0	0	91	0	0	0	0	0
		430	Tidal flat	96	6	0	0	0	0	0	0	0	0	0	0	0	0	0	0	94	0	0	0	0
500	Water surfaces	510	Shallow seawater	90	0	0	0	0	0	0	0	0	0	0	0	0	0	0	0	4	96	0	0	0
		520	Medium seawater	90	0	0	0	0	0	0	0	0	0	0	0	0	0	0	0	0	0	99	0	1
		530	Deep seawater	90	0	0	0	0	0	0	0	0	0	0	0	0	0	0	0	0	0	0	99	1
		540	Fresh water	84	0	0	0	0	0	0	0	0	0	0	0	0	0	0	0	4	1	0	1	94

Overall average = 77.6% obtained by 1565 correct identifications (diagonal) divided by 2016 total samples in all training sets.

TABLE 3.4. TRAINING SET CLASSIFICATION ACCURACY USING THE "PSEUDO-SUPERVISED" TRAINING SETS.
17 classes showing training set accuracy *in percent* using 10 channels (4 LANDSAT MSS bands and their 6 ratios).

Land Use Class				*No. of Points*	*Urban*		*Agricultural*					*Forested*			*Barren*			*Water*			
Code	*Level I*	*Code*	*Levels II and III*	*in T.S.*	*110*	*120*	*211*	*212*	*221*	*222*	*223*	*311*	*312*	*320*	*410*	*420*	*430*	*510*	*520*	*530*	*540*
100	Urban lands	110	Commercial	100	91	8	0	0	0	0	0	0	0	0	0	1	0	0	0	0	0
		120	Mixed	157	13	73	3	0	0	0	0	0	0	0	10	3	0	0	0	0	0
200	Agricultural lands	211	Grain A	82	0	2	87	0	2	4	0	0	0	0	5	0	0	0	0	0	0
		212	Grain B	96	0	0	0	100	0	0	0	0	0	0	0	0	0	0	0	0	0
		221	Crop A	104	0	0	1	3	75	20	0	0	1	0	0	0	0	0	0	0	0
		222	Crop B	100	0	0	2	0	19	75	0	0	4	0	0	0	0	0	0	0	0
		223	Crop C	75	0	0	0	7	16	0	71	0	7	0	0	0	0	0	0	0	0
300	Forested lands	311	Hardwoods A	156	0	0	0	0	3	1	0	81	13	0	0	0	0	0	0	0	1
		312	Hardwoods B	246	0	0	0	2	4	0	0	14	79	0	0	0	0	0	0	0	0
		320	Conifers	93	0	0	0	1	3	1	0	4	8	83	0	0	0	0	0	0	0
400	Barren lands	410	Gravels	95	0	19	1	0	0	0	0	0	0	0	79	1	0	0	0	0	0
		420	Reclaimed lands	70	4	4	0	0	0	0	0	0	0	0	0	91	0	0	0	0	0
		430	Tidal flat	96	5	0	0	0	0	0	0	0	0	0	0	0	95	0	0	0	0
500	Water surfaces	510	Shallow seawater	90	0	0	0	0	0	0	0	0	0	0	0	0	3	97	0	0	0
		520	Medium seawater	90	0	0	0	0	0	0	0	0	0	0	0	0	0	0	99	0	1
		530	Deep seawater	90	0	0	0	0	0	0	0	0	0	0	0	0	0	0	0	99	1
		540	Fresh water	84	0	0	0	0	0	0	0	0	0	0	0	0	5	0	0	0	95

Overall accuracy = 85% obtained by 1551 correct identifications (diagonal) divided by 1824 total samples in all training sets.

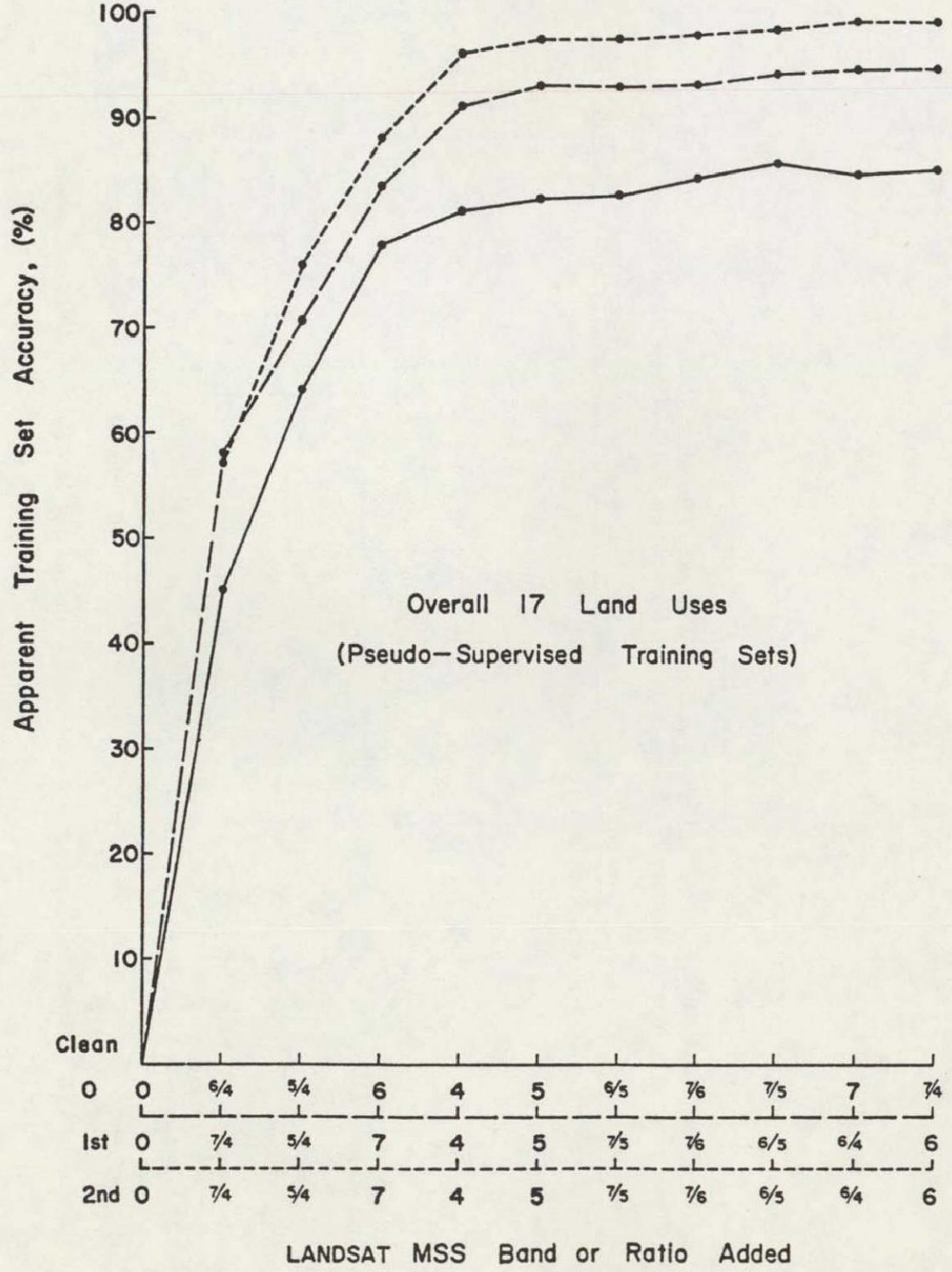

Fig. 3.9. APPARENT INCREASE IN TRAINING SET ACCURACY ACHIEVED AT EACH LEVEL OF STATISTICAL CLEANING. Seventeen classes are represented based on classification by the 10 MSS bands/ratios.

(Fig. 3.10). Approximately 82% actual training set accuracy was achieved with an optimal combination of four bands/ratios versus the 85% achieved with all 10 bands/ratios.

3.2.7 Conclusion and Selection

Statistical cleaning was tested as a method of improving the representation of a class by the cells remaining in the training sets after cleaning. Those cells with low probability of belonging to the class and/or high probability of belonging to another class were deleted. A measure of the effectiveness of the new discriminant function computed after cleaning is the fate of those cells originally selected as part of the training set but which were neither correctly classified nor sufficiently different to be deleted. Cells not classified but not yet deleted were not drawn back into the correct class yielding higher actual training set accuracy with successive cleaning iterations (Fig. 3.11). Apparent training set accuracy will increase in all cases in direct linear proportion to the cells deleted (Fig. 3.11). Just the opposite occurred with two of three training set selection approaches representing a slight decrease in actual training set accuracy with each cleaning. There is a direct linear relation between the number of points deleted from the training sets and the apparent increases in accuracy. Training sets which are noisy may well be improved by statistical cleaning but the best way to improve low

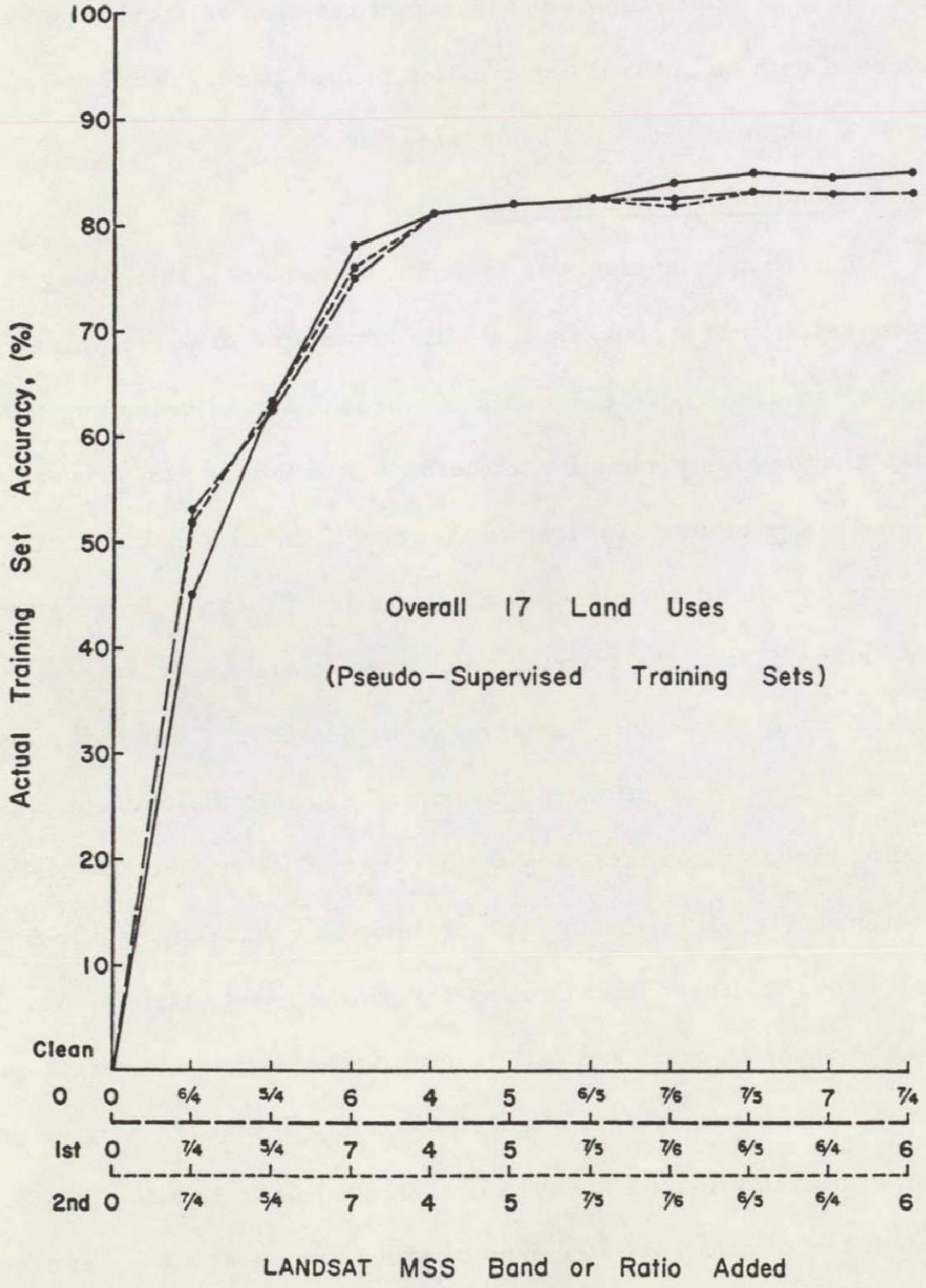

Fig. 3.10. ACTUAL INCREASE IN TRAINING SET ACCURACY ACHIEVED AT EACH LEVEL OF STATISTICAL CLEANING. Seventeen classes are represented based on classification by the 10 MSS bands/ratios.

training set accuracy is to reselect better or more representative training sets.

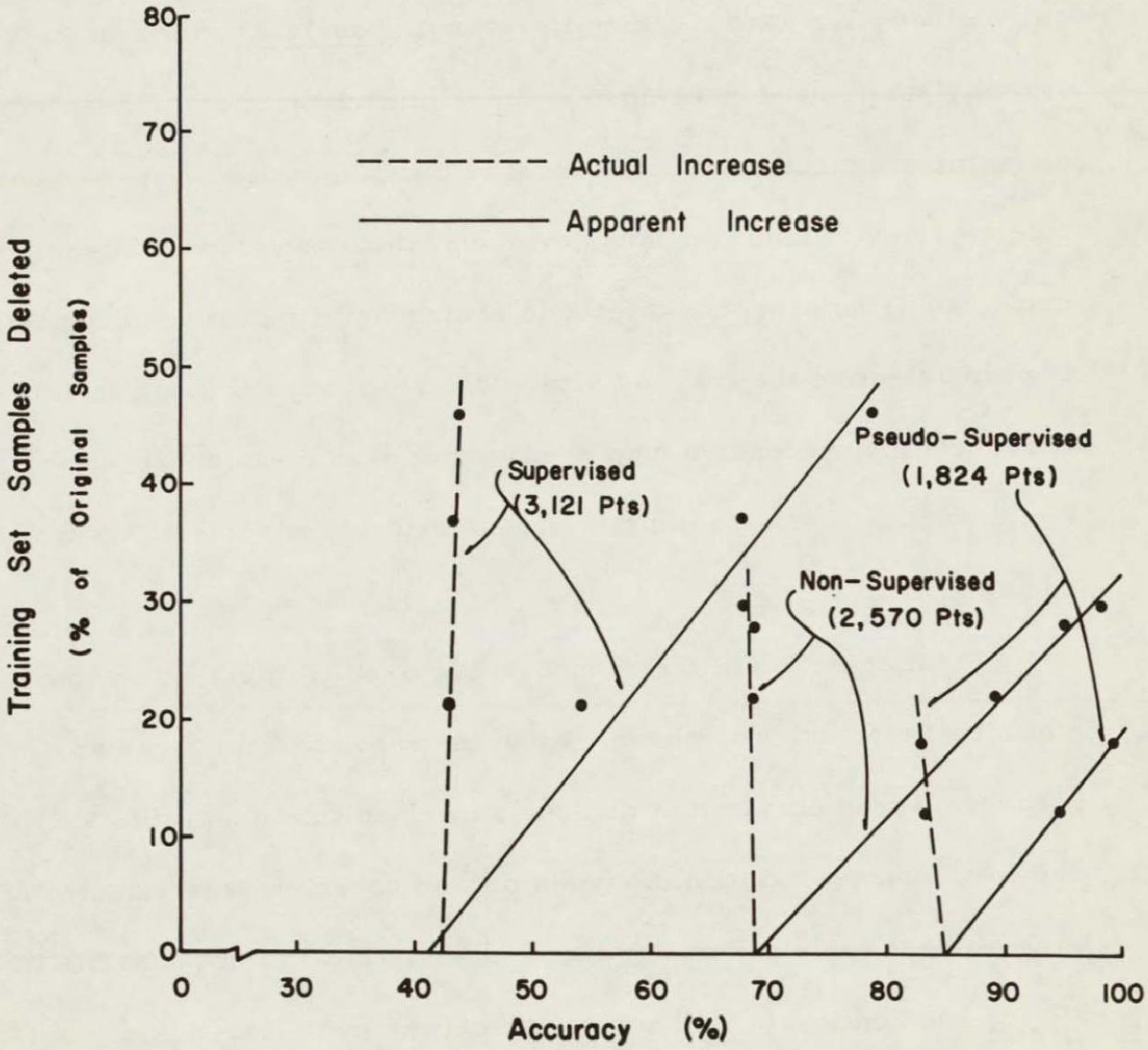

Fig. 3.11. COMPARISON OF THE ACTUAL VERSUS THE APPARENT TRAINING SET ACCURACY RESULTING FROM STATISTICAL CLEANING. All 10 bands/ratios were used. Note that the apparent increase in accuracy is directly proportional to the number of points deleted for each of the three approaches.

A final evaluation of the value of statistical cleaning must await a future test of its impact upon map verification accuracy. This requires that after each cleaning iteration the residual points in the training set be used to compute a discriminant function. These new discriminant functions for each level of cleaning could be used to compute a series of land use/land cover classification maps. These test maps can be compared with ground control information not known or used in selecting the training sets. The resulting verification accuracy for each successive map prepared at each cleaning iteration would provide a more definitive assessment of the value of statistical cleaning.

Final selection of the pseudo-supervised training sets without statistical cleaning was obvious when the results of the three approaches were compared at all levels of classification (Table 3.5). Some differences exist in the types of land cover classes selected for each of these tests and one to one comparisons were not possible in all 2nd and 3rd levels. The final choice was made based upon comparison of the first order accuracy which was quite high for the approach selected. First order class accuracy is computed as 100 times those cells classified into the correct 2nd and 3rd order subclasses of that first order divided by the total of the original number of cells representing those subclasses. The training set accuracies achieved represent how well the training sets would work in preparing

TABLE 3.5. COMPARATIVE TRAINING SET ACCURACY OF THREE APPROACHES TO COMPUTING TAIWAN LAND USE FROM LANDSAT IMAGERY. The percentages indicate the number of training set points placed in the correct class or combination of classes relative to the total number of points originally selected to represent the class(s). NC indicates "not classified." Brackets indicate that there is not a 1 to 1 correspondence in the number of subdivisions attempted in the specific approach.

Land Use Class						*"Non-Supervised" Training Sets*			*"Supervised" Training Sets*			*"Pseudo-Supervised" Training Sets*		
Code	*Level I*	*Code*	*Level II*	*Code*	*Level III*	*I*	*II*	*III*	*I*	*II*	*III*	*I*	*II*	*III*
100	Urban lands					NC			55%			91%		
		110	Commercial				NC			73%			91%	
		120	Residential				NC			37			73	
		130	Mixed				NC							
200	Agricultural lands					93%			69			96		
		210	Grains				80%			53			94	
				211	Rice A			59%			NC			87%
				212	Rice B			100			NC			100
				213	Rice C			76			NC			
				214	Rice D			71			NC			
				215	Rice E			54			NC			
		220	Crops				67			17			92	
				221	Crop A			59			NC			75
				222	Crop B			73			NC			75
				223	Crop C						NC			71
		230	Orchards				71			30			NC	
				231	Citrus			55			NC			NC
				232	Pears			64			NC			NC
300	Forested lands					86			69			94		
		310	Hardwoods				79			58			94	
				311	Type A						39%			81
				312	Type B		95				35			79
		320	Conifers							14			83	
400	Barren lands					56			56			89		
		410	Gravels				69			39			79	
		420	Reclaimed land				36			64			91	
		430	Tidal flat										95	
500	Water surfaces					94			94			98		
		510	Shallow seawater				70			62			97	
		520	Medium seawater				97			96			99	
		530	Deep seawater				69			69			99	
		540	Fresh water				93			95			95	
		550	Clear water				80							

a first order or generalized land use/land cover map with five classes. The pseudo-supervised approach provides the highest training set accuracy for all first order classes ranging from 89% for barren lands to 98% for water surfaces. The overall first order or five class training set accuracy for the pseudo-supervised approach is 94% while it is 79% and 72% for the non-supervised and supervised approaches respectively.

3.3 Selection of Optimal MSS Bands/Ratios

It is not economical to employ all available MSS bands and ratios to classify the complete maps. It is also not necessary as the training set accuracy approaches an upper limit after three or four bands have been added for agricultural and urban land use/land cover classification in terms of overall actual training set accuracy (Fig. 3.12) or first order accuracy (Table 3.6). This conclusion is supported by other experiments employing a similar test procedure in connection with aircraft imagery presenting 12 spectral bands ranging from 0.4 μm to 12.5 μm covering the wider range from the visible spectral region through the thermal infrared (Thompson et al., 1974). No ratios were tested but three of the four aircraft bands selected either overlapped or included the four MSS bands. The study of the aircraft imagery also clearly illustrated the risk of extending these conclusions to all types of classification mapping as 8 of the 12

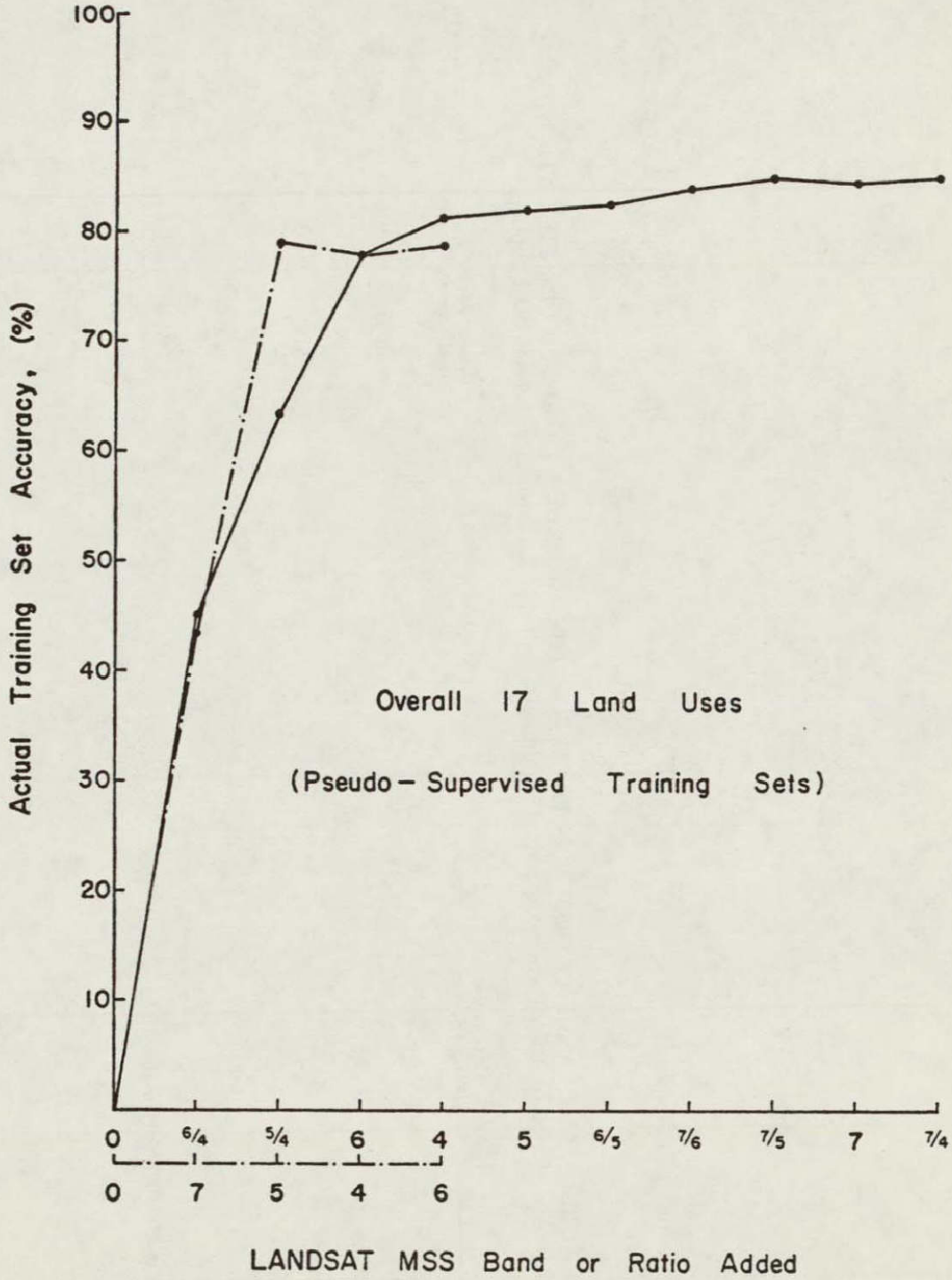

Fig. 3.12. SELECTION OF THE MINIMUM NUMBER OF MSS BANDS/RATIOS FOR PREPARATION OF THE TAIWAN LAND USE/LAND COVER MAPS. Seventeen classes. Based on actual training set accuracy using the "pseudo-supervised" training sets. No cleaning has been applied.

TABLE 3.6. TRAINING SET CLASSIFICATION ACCURACY FOR THE 1st ORDER LAND USE CLASSIFICATION OF TAIWAN. Based on the "Pseudo-Supervised" training sets (Table 3.4). No cleaning has been applied.

Land Use Class		*Maximum Achievable 10-Band/Ratio Accuracy*	*Optimal 4-Band/ Ratio Accuracy*	**Accuracy Gain (+) or Loss (−)*	*Original 4 MSS Band Accuracy*	**Accuracy Gain (+) or Loss (−)*
100	Urban lands	91%	91%	0%	90%	−1%
200	Agricultural lands	96	94	−2	89	−7
300	Forested lands	94	91	−3	91	−3
400	Barren lands	89	92	+3	90	+1
500	Water surfaces	98	98	0	98	0

*Comparison with achievable 10-band accuracy.

spectral bands were required to achieve an optimal accuracy for classifying surficial geology classes.

Four MSS bands/ratios provide the basis for a reasonable 17 class land use/land cover map of Taiwan (Table 3.7). A further test remains as to the actual contribution of the six ratios of MSS bands relative to the use of only the four MSS bands. Ratios of MSS bands as a whole correlated well with one or both of their own numerator or denominator bands (Table 3.8) and thus may contribute little to the classification process selected. A stepwise discriminant analysis of the actual training set accuracy for the 17 classes and using only the four MSS band clearly shows that employing ratios will contribute little to the final accuracy achieved (Fig. 3.12). The four MSS bands alone yield an overall training set accuracy of 79% while the first four MSS bands/ratios provided 81%.

Savings can thus be achieved by omitting the step used to prepare the MSS ratios for related land cover mapping. Also, substantial additional savings can be achieved by noting that bands 5 and 7 of the four MSS bands provide the same overall training accuracy (79%) (Fig. 3.12). Thus, two of the four MSS bands employed with the 17 class pseudo-supervised training sets provide adequate overall accuracy and first order accuracies of better than 90%.

It may appear at this point that a substantial amount of the procedures tested have contributed little to the final processes employed.

TABLE 3.7. FINAL TRAINING SET ACCURACY FOR THE LAND USE CLASSIFICATION MAPS OF TAIWAN. Based on the "Pseudo-Supervised" training sets (Table 3.5). No cleaning has been applied.

Land Use Class						Maximum Achievable 10-Band/Ratio Accuracy			Optimal 4-Band/ Ratio Accuracy			*Accuracy Loss (−) or Gain (+)			Original 4 MSS Band Accuracy			*Accuracy Loss (−) or Gain (+)		
Code	*Level I*	*Code*	*Level II*	*Code*	*Level III*	*I*	*II*	*III*	*I*	*II*	*III*	*I*	*II*	*III*	*I*	*II*	*III*	*I*	*II*	*III*
100	Urban lands					91%			91%			0%			90%			−1%		
		110	Commercial				91%			89%			−2%			92%			+1%	
		120	Mixed				73			69			−4			67			−6	
200	Agricultural lands					96			94			−2			89			−7		
		210	Grains				94			90			−4			93			−1	
				211	Rice A			87%			78%			−9%			85%			−2%
				212	Rice B			100			100			0			98			−2
		220	Crops				92			87			−5			80			−12	
				221	Crop A			75			65			−10			56			−19
				222	Crop B			75			78			+3			72			−3
				223	Crop C			71			61			−10			60			−11
300	Forested lands					94			91			−3			91			−3		
		310	Hardwoods				94			91			−3			86			−8	
				311	Type A			81			67			−14			67			−14
				312	Type B			79			71			−8			68			−11
		320	Conifers				83			75			−8			80			−3	
400	Barren lands					89			92			+3			90			+1		
		410	Gravels				79			83			+4			84			+5	
		420	Reclaimed land				91			94			+3			89			−2	
		430	Tidal flat				95			93			−2			96			+1	
500	Water surfaces					98			98			0			98			0		
		510	Shallow seawater				97			94			−3			97			0	
		520	Medium seawater				99			100			+1			93			−6	
		530	Deep seawater				99			99			0			87			−12	
		540	Fresh water				95			98			+3			91			−4	
Overall accuracy						85%			81%			−4%			79%			−6%		

*Comparison with achievable 10-band accuracy.

TABLE 3.8. CORRELATION MATRICES WITHIN CLASSES (POOLED) FOR THE THREE TYPES OF TRAINING SETS. No cleaning has been applied.

(1) Non-Supervised Training Sets

Bands/Ratios	*Bands/Ratios*									
	4	*5*	*6*	*7*	*5/4*	*6/4*	*7/4*	*6/5*	*7/5*	*7/6*
4	1.00									
5	0.72	1.00								
6	0.34	0.41	1.00							
7	0.16	0.20	0.81	1.00						
5/4	0.20	0.80	0.31	0.18	1.00					
6/4	–0.14	0.01	0.84	0.75	0.16	1.00				
7/4	–0.20	–0.12	0.62	0.89	0.04	0.81	1.00			
6/5	–0.22	–0.40	0.58	0.56	–0.39	0.80	0.70	1.00		
7/5	–0.24	–0.40	0.42	0.70	–0.36	0.65	0.87	0.84	1.00	
7/6	–0.12	–0.08	–0.10	0.36	0.01	–0.03	0.43	–0.02	0.44	1.00

(2) Supervised Training Sets

Bands/Ratios	*Bands/Ratios*									
	4	*5*	*6*	*7*	*5/4*	*6/4*	*7/4*	*6/5*	*7/5*	*7/6*
4	1.00									
5	0.88	1.00								
6	0.43	0.39	1.00							
7	0.19	0.15	0.91	1.00						
5/4	0.55	0.86	0.32	0.15	1.00					
6/4	–0.19	–0.18	0.78	0.85	–0.04	1.00				
7/4	–0.26	–0.26	0.67	0.87	–0.13	0.94	1.00			
6/5	–0.43	–0.57	0.47	0.61	–0.53	0.85	0.84	1.00		
7/5	–0.43	–0.54	0.45	0.68	–0.48	0.83	0.91	0.95	1.00	
7/6	–0.22	–0.22	0.14	0.45	–0.12	0.31	0.54	0.31	0.53	1.00

(3) Pseudo-Supervised Training Sets

Bands/Ratios	*Bands/Ratios*									
	4	*5*	*6*	*7*	*5/4*	*6/4*	*7/4*	*6/5*	*7/5*	*7/6*
4	1.00									
5	0.93	1.00								
6	0.72	0.72	1.00							
7	0.49	0.49	0.87	1.00						
5/4	0.34	0.64	0.41	0.29	1.00					
6/4	–0.18	–0.12	0.53	0.64	0.10	1.00				
7/4	–0.23	–0.19	0.39	0.71	0.01	0.88	1.00			
6/5	–0.28	–0.37	0.29	0.44	–0.41	0.83	0.78	1.00		
7/5	–0.28	–0.35	0.26	0.55	–0.35	0.76	0.90	0.91	1.00	
7/6	–0.14	–0.14	–0.03	0.36	–0.03	0.15	0.50	0.15	0.48	1.00

Hindsight does not substitute for foresight. The impact of these logical test procedures on the Taiwan land use/land cover mapping was unknown at the outset. These subsequent tests provided a logical, scientific basis for the optimal selection of the specific training sets and MSS bands actually used to prepare the final land use/land cover classification maps.

IV. PRODUCTION AND VERIFICATION OF LAND USE/ LAND COVER MAPS OF TAIWAN

4.1 Predictive Accuracy of Training Sets

4.1.1 Additional Consideration of the Classification Algorithm

Two classification algorithms were available for the production of the final maps. These were the maximum likelihood ratio technique (Appendix E) and stepwise discriminant analysis which was discussed in detail earlier (Appendix B). They are basically the same general approach except that stepwise discriminant analysis proceeds in a step by step (band by band) fashion and uses a single, common covariance matrix for all classes. The maximum likelihood technique processes only the designated bands and uses a different, individual covariance matrix for each individual class sought.

The stepwise approach has already proved valuable for examining the various types of training data and the contribution of each spectral band/ratio and establishing that the ratios of spectral bands add little or nothing to the map classification undertaken here (Fig. 3.12). Further, stepwise discriminant analysis established that when it was restricted to select from only the four basic MSS bands it achieved an equally good training set accuracy with only two

basic MSS bands versus a free selection from all 10 MSS bands/ ratios. It now remains to select from one of the two classification techniques and use either the discriminant analysis approach with a single covariance matrix or the maximum likelihood approach with its suite of covariance matrices. Unfortunately, the available likelihood technique cannot currently handle the six ratios of bands and must be restricted to the four basic MSS bands. Ratios of MSS bands contain considerably less variability than the four basic MSS bands and the covariance for some of these band ratios is very small. The available maximum likelihood computer programs cannot, as required, invert these matrices.

At this point it was necessary to devise a method to choose one of these two approaches: discriminant analysis using the optimal subset of 10 bands/ratios determined in stepwise fashion or likelihood ratioing using an optimal combination of the four basic MSS bands. Also, it was important to check how well the earlier interpretations of training set accuracies extended to the actual classification of the maps. These tests were accomplished by preparing a 1/25 sample map of the study area and classifying it with both techniques and the classification matrices computed from the pseudo-supervised training sets. The results for each classification of the sample map were compared to the land use/land cover results obtained from the extensive grid sampled ground control data

procedures outlined earlier. This grid sampled ground control was not employed in forming the pseudo-supervised training sets due principally to its sensitivity to exact registration. However, it does provide a very good measure of the amounts of each land use present on each map for these tests. A verification procedure has thus been designed around this known photointerpretation result to provide a final selection of the technique and the bands to be employed and to predict in advance the general accuracy of the final products.

4.1.2 Sample Map Classification

Cost prohibited classifying each entire map image file with each available technique and combination of bands/ratios as was done with the training data. The pseudo-supervised training sets provide a basis for computing a sample classification map by each technique to obtain a predictive measure of the expected accuracy. A systematic 1/25 sample was extracted for these tests using cells at every fifth line and every fifth column from Taichung and Kuo-Hsing map image files. The Lu-Kang map image file was not sampled as two-thirds of it was water areas whose classification could not be verified by the available airphoto ground control data. These miniature, sampled map image files each contain 5,600 cells which were classified for comparison by both the discriminant analysis and maximum likelihood approaches. Using the results of the prior chapter as a guideline (Fig. 3.12) maximum likelihood was employed on all four MSS

bands and on bands 5 and 7 while discriminant analysis was employed in a stepwise fashion on all 10 MSS bands and ratios. The results of these 12 map classifications are tabulated in terms of the percent of the area of each map which is classified into each land use/land cover by each technique (Tables 4.1 and 4.2).

4.1.3 Verification of Sample Maps

Qualitative and quantitative verification techniques were applied to examine the sample map classification results. The qualitative approach was based upon an examination of the overall appearance of the sample classification maps and tables. The spatial distribution of the three classes of seawater was a good indicator of the general predictive accuracy. The Taichung and Kuo-Hsing classification maps cover only land areas or fresh water, thus the seawater (sediment/depth) classes should not appear on either map. A small area of the class of tidal flats does occur in the upper left corner of the Taichung map but is not confused with shallow (or highest sediment) seawater (Table 4.1). Essentially no sample cells are assigned to the seawater classes on the Taichung map by any of the 12 classifications tested. Proportionally more agricultural lands than forested lands are identified on the Taichung map of the lower coastal plains. Deep (or clearer) seawater is mapped at 3.6% on the higher elevation Kuo-Hsing map by the stepwise discriminant approach by the addition of the fifth band/ratio (6/4, 5/4, 6, 4, and 5)

TABLE 4.1. CLASSIFICATION RESULTS FOR THE TAICHUNG MAP BASED ON 5600 SAMPLED CELLS. 17 classes showing the relative amounts of land uses *in percent* using "pseudo-supervised training data." Sampled points represent every 5th line and column. Stepwise discriminant analysis used for the 10 channels (4 LANDSAT MSS bands and their 6 ratios). Maximum likelihood ratioing technique used for MSS bands 4, 5, 6, 7 and 5, 7.

Land Use Class				*Airphoto*	*MSS Bands and Ratios Added*										*MSS Bands*	*MSS Bands*
Code	*Level I*	*Code*	*Levels II and III*	*Estimates*	*6/4*	*5/4*	*6*	*4*	*5*	*6/5*	*7/6*	*7/5*	*7*	*7/4*	*4, 5, 6, 7*	*5, 7*
100	Urban lands	110	Commercial	6.0%	1.3%	2.1%	1.8%	1.6%	1.5%	1.5%	1.4%	1.4%	1.5%	1.5%	1.2%	1.1%
		120	Mixed		2.4	2.6	3.0	3.1	3.2	3.1	3.3	3.3	3.3	3.3	4.1	3.9
200	Agricultural lands	211	Grain A	71.0	11.8	9.0	15.2	15.1	15.7	15.8	15.5	15.1	15.3	15.4	17.2	15.5
		212	Grain B		16.2	14.9	16.1	16.2	16.7	16.5	16.6	16.8	16.2	16.2	6.8	7.3
		221	Crop A		12.2	19.2	25.7	29.5	33.5	34.3	34.6	35.6	35.4	35.5	35.6	37.5
		222	Crop B		0.1	5.9	5.6	6.1	6.1	5.4	5.5	5.6	5.3	5.1	6.2	9.3
		223	Crop C		15.8	11.5	0.1	0.1	0.2	0.2	0.2	0.2	0.2	0.2	3.8	1.4
300	Forested lands	311	Hardwoods A	20.0	4.9	7.7	4.0	4.2	1.8	1.7	1.8	2.2	2.4	2.3	1.3	2.0
		312	Hardwoods B		28.6	20.9	23.0	20.2	17.4	17.5	17.3	16.9	16.5	16.6	19.6	16.6
		320	Conifers		0.4	0.5	0.2	0.1	0.1	0.1	0.1	0.1	0.1	0.1	0.6	1.8
400	Barren lands	410	Gravels	2.0	5.3	4.6	4.2	2.7	2.6	2.8	2.8	2.8	2.9	2.9	2.3	2.4
		420	Reclaimed lands		0.6	0.5	0.5	0.5	0.5	0.5	0.4	0.4	0.5	0.5	0.3	0.4
		430	Tidal flat		0.4	0.5	0.5	0.6	0.6	0.6	0.5	0.4	0.4	0.4	0.4	0.4
500	Water surfaces	510	Shallow seawater	1.0	0.0	0.0	0.0	0.0	0.0	0.0	0.0	0.0	0.0	0.0	0.0	0.0
		520	Medium seawater		0.0	0.0	0.0	0.0	0.0	0.0	0.0	0.0	0.0	0.0	0.0	0.0
		530	Deep seawater		0.0	0.0	0.0	0.0	0.0	0.0	0.0	0.0	0.0	0.0	0.0	0.0
		540	Fresh water		0.1	0.1	0.1	0.1	0.1	0.1	0.1	0.1	0.1	0.1	0.0	0.1

TABLE 4.2. CLASSIFICATION RESULTS FOR THE KUO-HSING MAP BASED ON 5600 SAMPLED CELLS. 17 classes showing the relative amounts of land uses *in percent* using "pseudo-supervised training data." Sampled points represent every 5th line and column. Stepwise discriminant analysis used for the 10 channels (4 LANDSAT MSS bands and their 6 ratios). Maximum likelihood ratioing technique used for MSS bands 4, 5, 6, 7 and 5, 7.

Land Use Class				*Airphoto Estimates*	*MSS Bands and Ratios Added*										*MSS Bands*	*MSS Bands*
Code	*Level I*	*Code*	*Levels II and III*		*6/4*	*5/4*	*6*	*4*	*5*	*6/5*	*7/6*	*7/5*	*7*	*7/4*	*4, 5, 6, 7*	*5, 7*
100	Urban lands	110	Commercial	0.0%	1.3%	0.6%	0.6%	0.5%	0.3%	0.3%	0.5%	0.5%	0.4%	0.4%	0.3%	0.4%
		120	Mixed		2.7	0.8	1.0	0.9	0.9	0.9	0.9	0.9	0.8	0.8	1.2	1.1
200	Agricultural lands	211	Grain A	30.0	7.5	2.4	3.7	4.7	4.2	3.7	3.2	3.4	3.5	3.6	3.4	5.1
		212	Grain B		21.4	16.4	4.9	3.5	3.0	2.9	3.0	3.0	3.3	3.3	1.0	3.2
		221	Crop A		10.5	17.3	20.0	18.5	18.9	20.5	21.2	21.0	20.8	19.8	13.0	17.4
		222	Crop B		0.6	4.0	5.0	5.6	5.9	4.8	4.6	4.7	4.6	5.5	9.0	3.5
		223	Crop C		10.4	4.7	0.3	0.3	0.3	0.3	0.3	0.3	0.3	0.3	1.2	1.8
300	Forested lands	311	Hardwoods A	67.0	4.6	18.2	24.2	25.7	22.9	24.2	25.4	27.6	28.0	28.1	24.4	22.1
		312	Hardwoods B		26.3	22.1	22.4	21.4	23.3	23.1	22.7	22.4	22.0	21.9	20.6	23.3
		320	Conifers		8.9	9.3	14.2	14.9	15.5	15.3	15.5	14.9	14.8	15.0	24.1	20.6
400	Barren lands	410	Gravels	3.0	3.8	1.0	0.8	0.4	0.3	0.4	0.4	0.4	0.5	0.4	0.3	0.3
		420	Reclaimed lands		1.2	0.2	0.1	0.3	0.3	0.3	0.2	0.2	0.3	0.3	0.2	0.3
		430	Tidal flat		0.6	0.3	0.3	0.1	0.2	0.2	0.1	0.1	0.1	0.1	0.1	0.1
500	Water surfaces	510	Shallow seawater	0.0	0.1	0.0	0.0	0.0	0.0	0.0	0.0	0.0	0.0	0.0	0.0	0.0
		520	Medium seawater		0.0	0.0	0.0	0.0	0.0	0.0	0.0	0.0	0.0	0.0	0.0	0.0
		530	Deep seawater		0.0	0.8	0.8	1.4	3.6	2.4	1.4	0.5	0.5	0.4	0.0	0.1
		540	Fresh water		0.1	1.8	1.9	1.9	0.5	0.9	0.6	0.2	0.2	0.1	0.0	0.1

(Table 4.2). Kuo-Hsing represents an area of considerable topographic relief and yields areas of shadow which are confused with the deep seawater class by the discriminant analysis approach. There is no corresponding confusion in the Kuo-Hsing classification maps prepared from the two or four MSS bands by the maximum likelihood approach. The overall total amounts of each land use/land cover mapped by either approach are approximately the same.

The quantitative test of these results statistically compares the airphoto estimates of the amount of each first order land use/land cover to the corresponding amounts computed for each of the 12 classification maps. It was not possible to make this comparison at a second or third order of land use/land cover due to the slight differences at these levels between the hierarchical classification schemes used on the grid sampled airphotos and the pseudo-supervised training data. The amount of the map occupied by a given first order land use/land cover is computed for each sample classification map in percent (Tables 4.1 and 4.2). It has also been estimated by the grid sample airphoto interpretations (Table 2.5). The LANDSAT image was obtained on November 1, 1972, while the airphotos were obtained in 1973 and 1974 and thus, on the average, there is about a one year separation between these data. A plot can be prepared for each of the 12 sample image classifications comparing the computed amount in percent of each first order land

use/land cover against the airphoto estimates also in percent. Since there are five first order classes mapped for both the Kuo-Hsing and Taichung maps each plot contains 10 points (Fig. 4.1). An exact match between the computed and estimated amounts of land use/land cover would place all 10 points on a 45^{o} line representing a 1 to 1 comparison. A test of how well these points fit the expected line occurs below. A second graph can be prepared which shows the variation in difference between the computed and estimated amounts of each first order land use/land cover for each of the 12 classifications attempted (Fig. 4.2). This graph clearly indicates that MSS bands 5 and 7 with the maximum likelihood approach provide the most accurate rendition of the amounts of each of the major land use/land cover present on both maps. The difference between the computed and estimated results also decreases rapidly for the first four steps and then remains relatively constant. The fact that this measure of comparison does not continue to decrease below a fixed and relatively constant level implies that there is an inherent difference between the computed and estimated results which cannot be further improved by the addition of more spectral bands/ratios. This may represent the amount of real change in land use/land cover between the 1972 LANDSAT and 1973/74 airphoto dates or a systematic difference or "error" in the two different approaches used to obtain the computed and estimated amounts of land use/land cover.

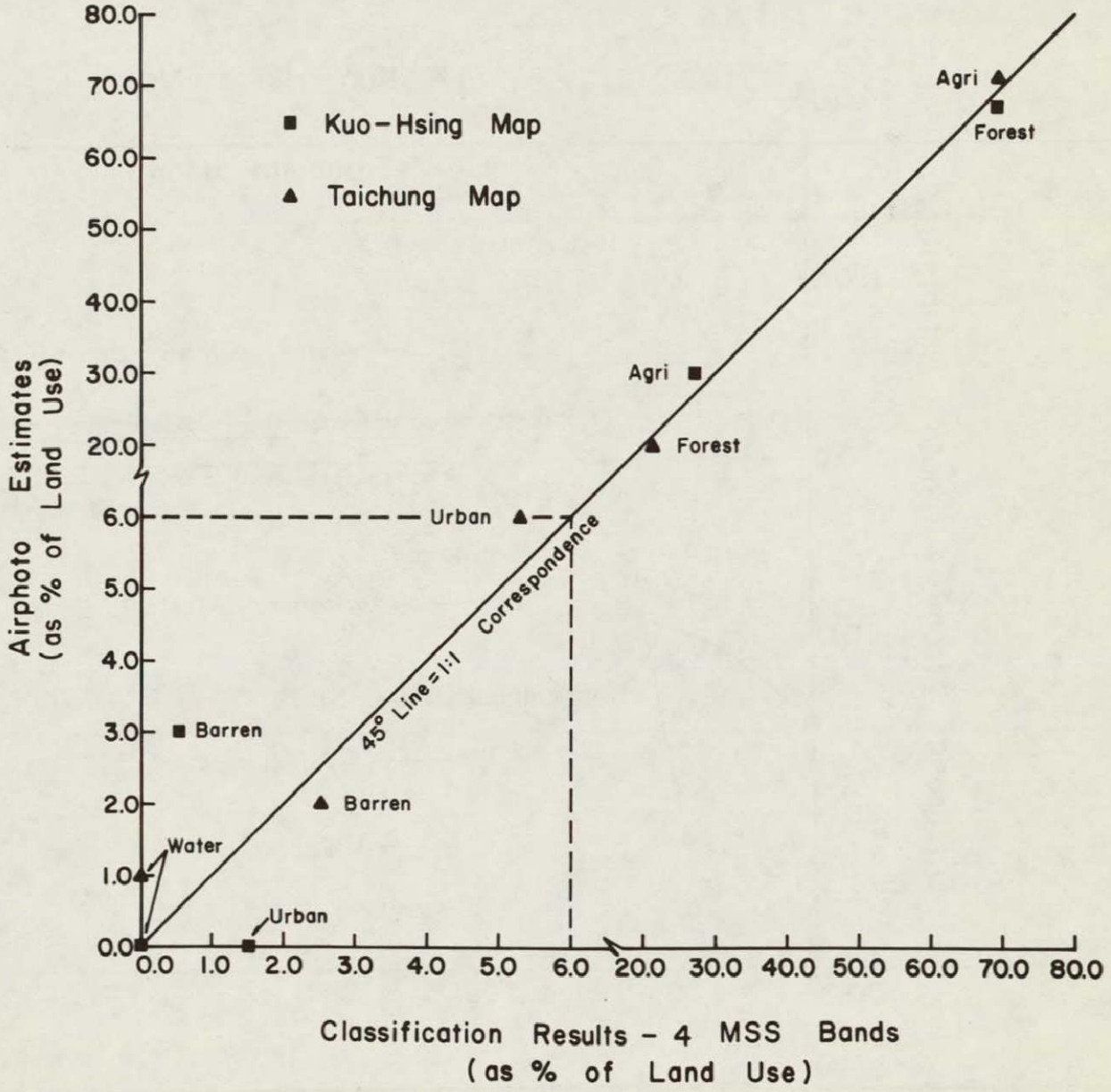

Fig. 4.1. COMPARISON OF THE ESTIMATED TO COMPUTED FIRST ORDER LAND USE/LAND COVER. Maximum likelihood analysis was applied to the four MSS bands. Seventeen second level classes were aggregated into five first level classes for comparison. Airphoto estimates based on 2760 sample cells (Table 2.5). Classification results based on 5600 sample cells (Tables 4.1 and 4.2).

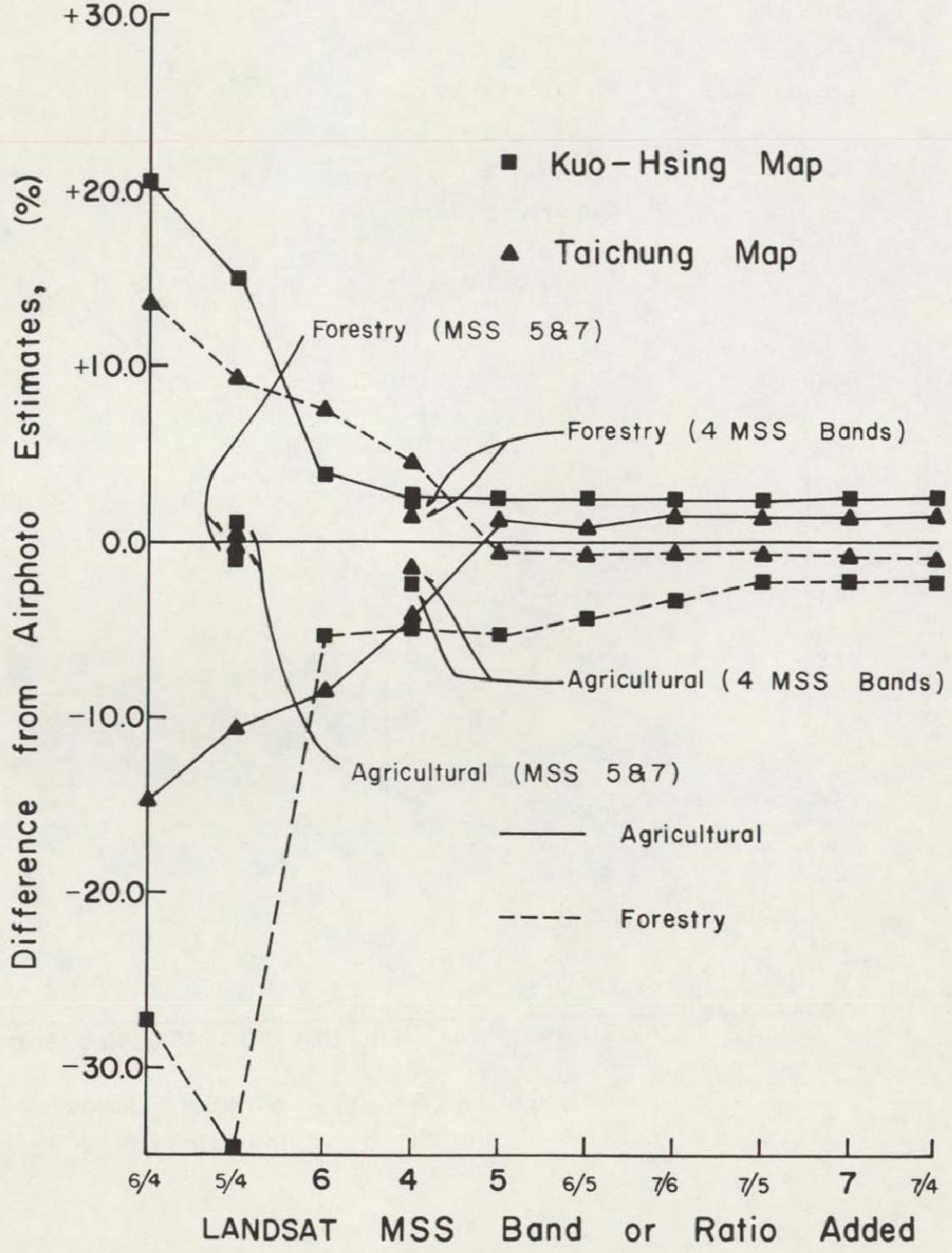

Fig. 4.2. DEVIATION OF FIRST ORDER LAND USE/LAND COVER MAP CLASSIFICATION RESULTS FROM AIRPHOTO ESTIMATES. A negative difference represents an airphoto estimate greater than the classification results. Isolated points for 2 and 4 band cases were computed by maximum likelihood technique. Remaining values connected by lines computed by stepwise discriminant analysis.

4.1.4 Selection of the Final Procedures

Just as with the training set tests the combination of original MSS bands 5 and 7 provide the most economical and accurate results with the available classification algorithms (Fig. 4.2). One additional comparison gives further weight to this conclusion. The comparison of the computed and estimated amounts of first order land use/land cover provide five points to approximate a 45° line, or 10 points if both maps are taken together (Fig. 4.1). These test points do not exactly fit the expected line and the standard error of the estimate provides a means of computing a measure of their misfit as a group. This standard error can be computed and plotted for each of the 12 sample classifications as a function of MSS band or ratio added as was done earlier to examine the training set accuracies (Fig. 4.3). The standard error for MSS bands 5 and 7 processed by the maximum likelihood approach is less than that for all four MSS bands. Further, eight bands/ratios must be used in the stepwise fashion to achieve the same results as with four MSS bands (Fig. 4.3).

The verification procedures employed here are not foolproof but were selected to compensate for differences which evolved into the two hierarchical land use/land cover classification schemes. Certainly a one to one (cell by cell) comparison of the computed and known land use/land cover of a sample of map cells would be more rigorous. It is possible that the overall amounts of the first order

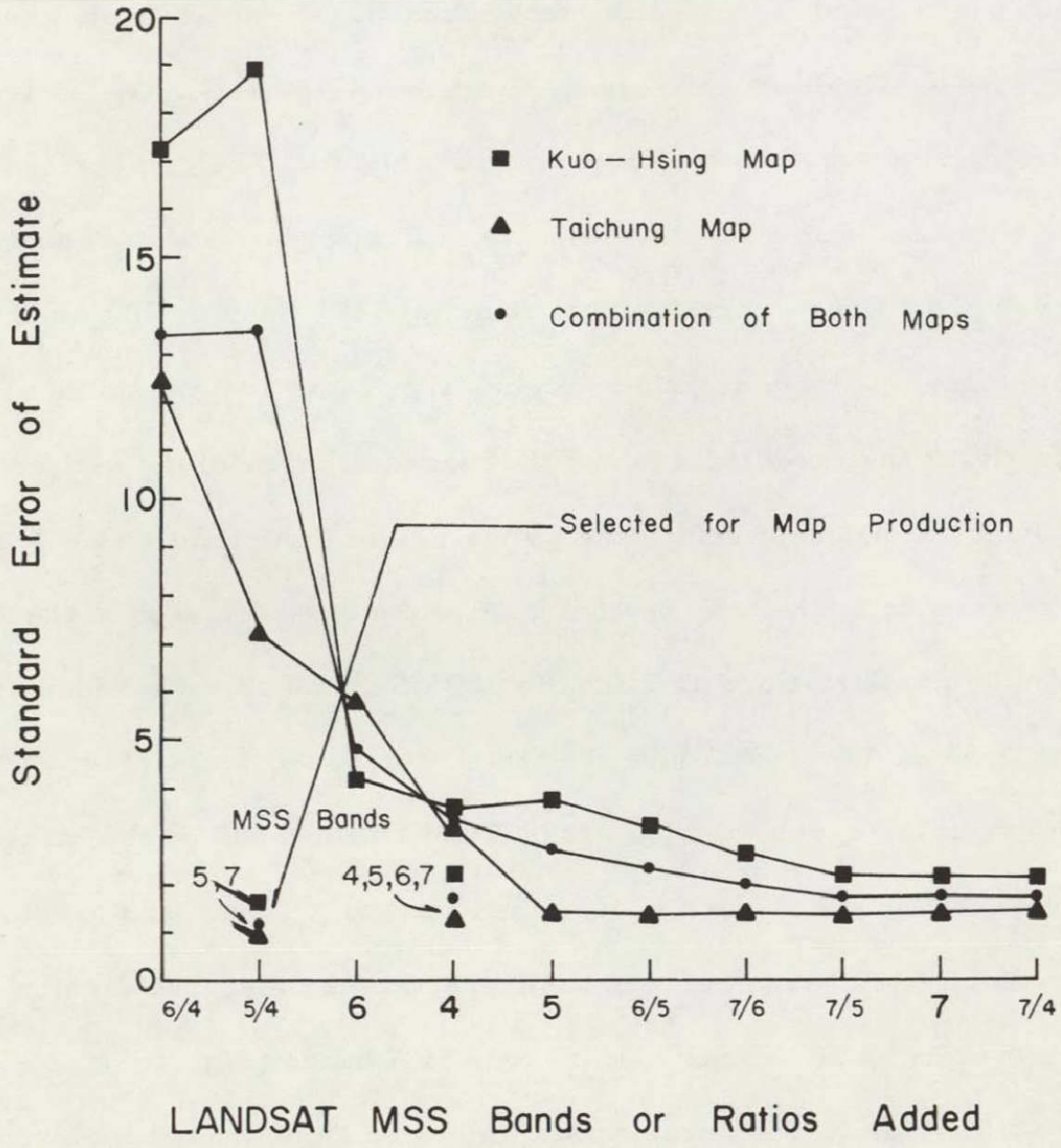

Fig. 4.3. SELECTION OF OPTIMAL LANDSAT BANDS AND RATIOS FOR THE TAIWAN LAND USE/LAND COVER CLASSIFICATION. Standard error of estimate is based upon the difference between airphoto estimates and classification results for the five aggregated first level classes.

land use/land cover can match as has been shown while their spatial distribution does not similarly correspond. The techniques used here do provide a good indication of the optimal bands and technique to be applied for the final map production. The similarity of these results to those obtained earlier by examination of training set accuracy provide additional confidence in these conclusions.

4.2 Map Production

4.2.1 Input

The final land use/land cover classification maps were prepared from MSS bands 5 and 7 by the maximum likelihood approach. Microfilm graymaps of these two bands assign black to the image cells with very low spectral returns and white to those with very high spectral returns (Figs. 4.4 and 4.5). These individual graymaps of MSS bands 5 and 7 clearly show some of the land uses/land covers in detail. The graymap of MSS band 5 for the Taichung map (Fig. 4.4b) displays the drainage pattern and urban lands in white and forests and river channel in black. The rest of land use/land cover types are shown in different intermediate levels of gray. The graymap of MSS band 7 for this same map (Fig. 4.5b) displays the drainage pattern and urban lands in black and most of the agricultural lands in white or light gray. The rough terrain on the eastern side of the Taichung map is emphasized with rougher topography appearing as shaded relief. A

ORIGINAL PAGE IS
OF POOR QUALITY

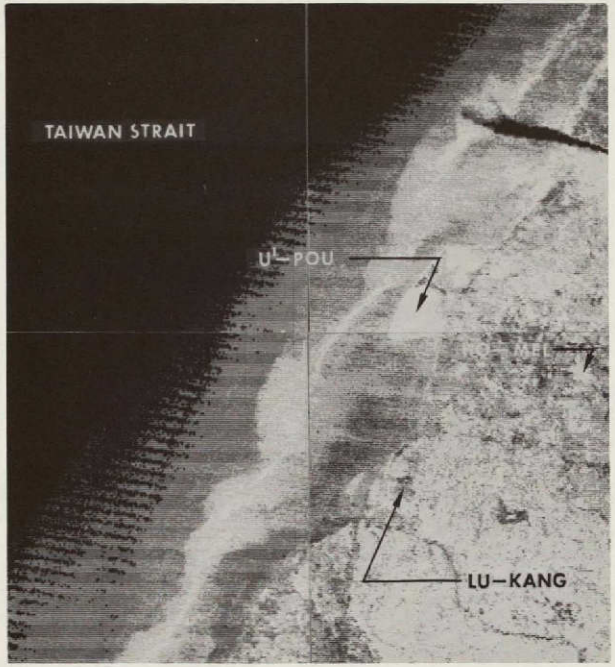

(a) Lu-Kang Map

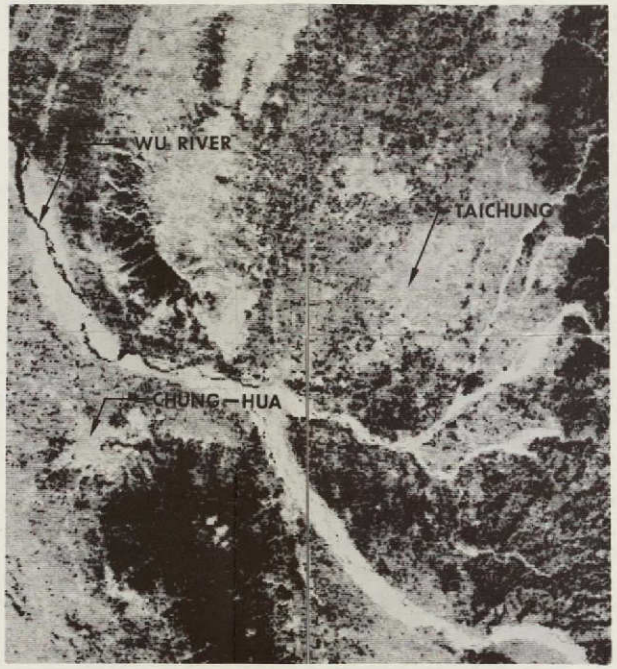

(b) Taichung Map

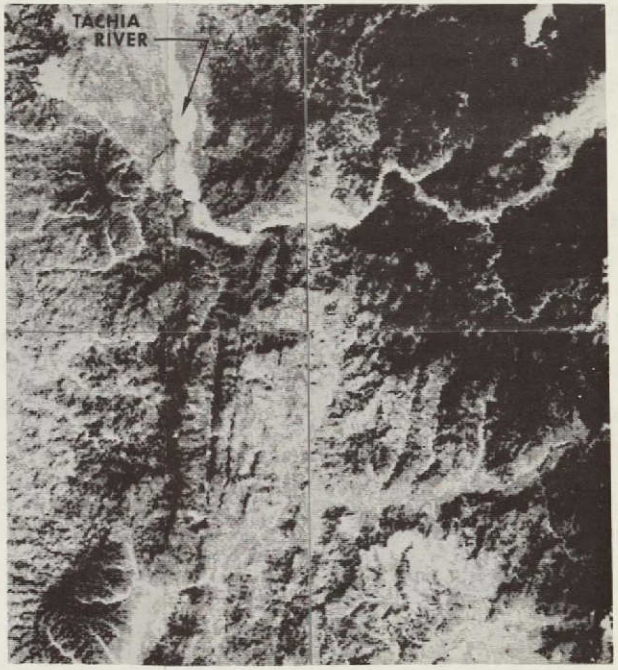

(c) Kuo-Hsing Map

FIGURE 4.4. GRAYMAPS OF LANDSAT MSS BAND 5 FOR THE TEST SITE. Generated on a microfilm plotter from the computer compatible tapes of the November 1, 1972 image. Scale ∿1:200,000. Ten discrete gray levels were displayed. The exact location of these maps is presented in Figure 2.1 (page 10).

ORIGINAL PAGE IS
OF POOR QUALITY

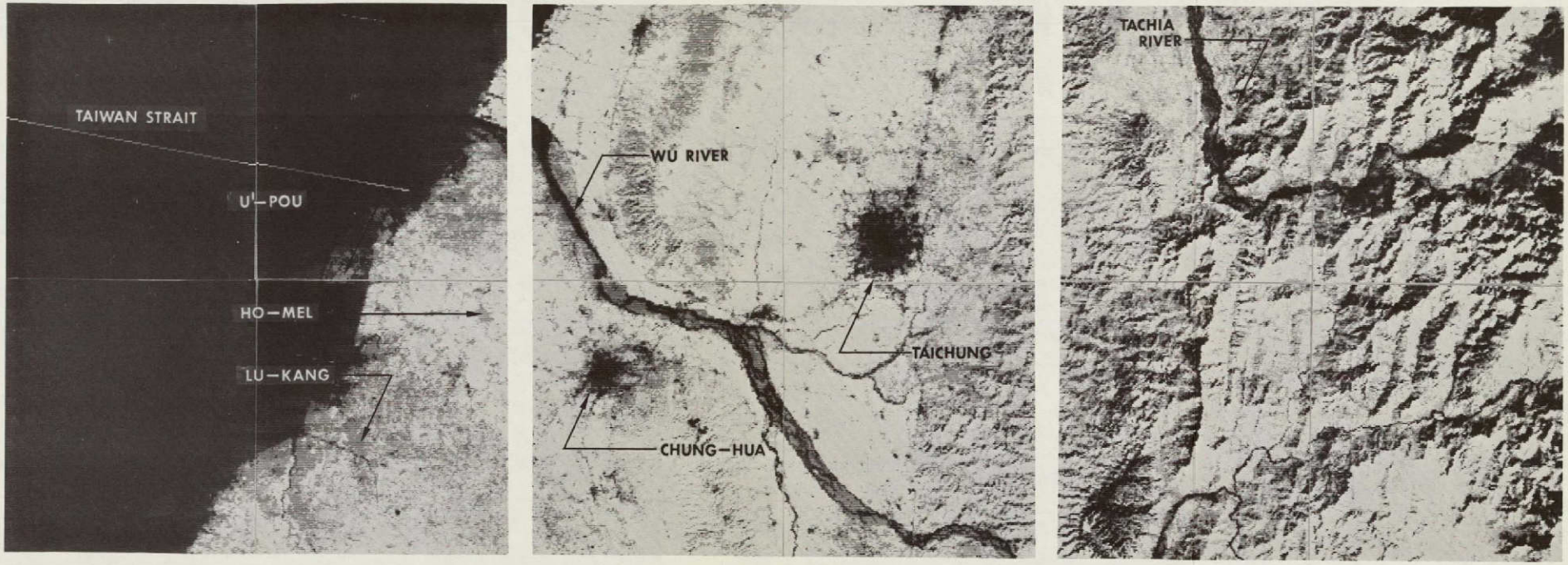

(a) Lu-Kang Map

(b) Taichung Map

(c) Kuo-Hsing Map

FIGURE 4.5. GRAYMAPS OF LANDSAT MSS BAND 7 FOR THE TEST SITE. Generated on a microfilm plotter from the computer compatible tapes of the November 1, 1972 image. Scale ∿1:200,000. Ten discrete gray levels were displayed. The exact location of these maps is presented in Figure 2.1 (page 10).

FOLDOUT FRAME 1

FOLDOUT FRAME 2

ORIGINAL PAGE IS
OF POOR QUALITY

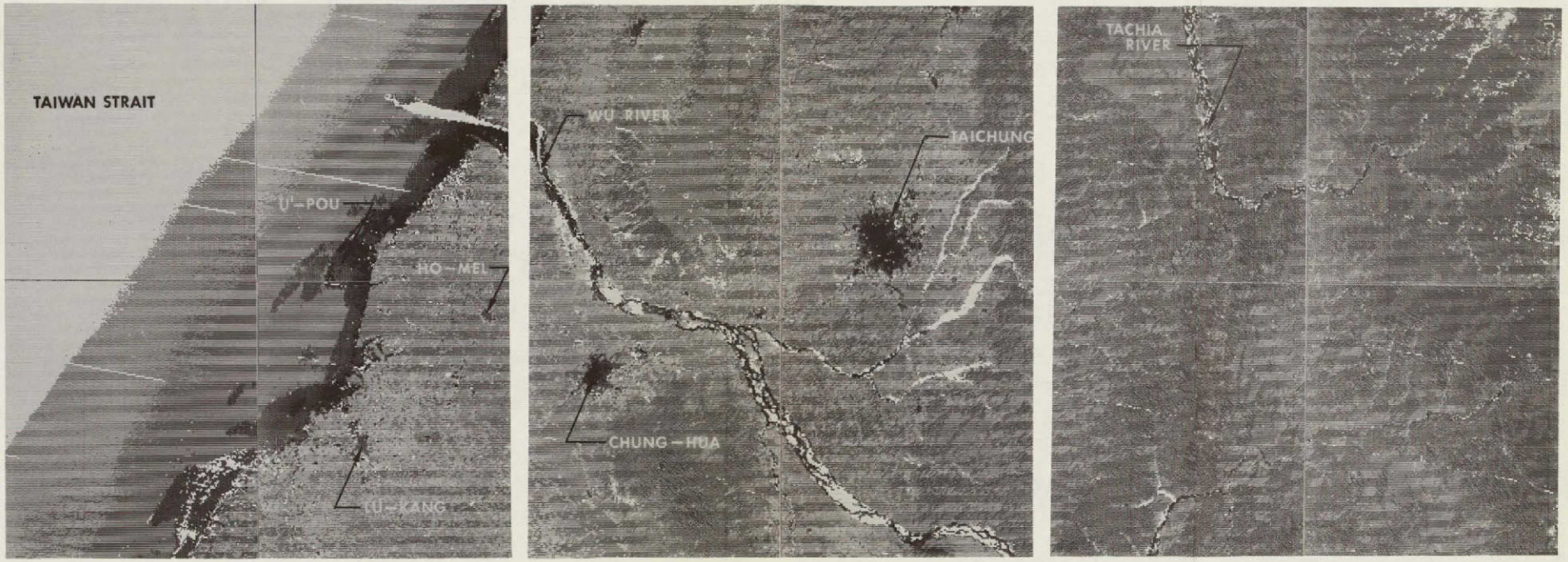

(a) Lu-Kang Map

(b) Taichung Map

(c) Kuo-Hsing Map

FIGURE 4.6. OVERALL 17 LAND USE/LAND COVER CLASSIFICATION MAPS. Extracted by computer analysis of a November 1, 1972 LANDSAT image. Scale ∿1:200,000. Specific second and third order classes are annotated on the theme maps which follow. Compare detail with LANDSAT photo interpretation map in Figure 2.2 (page 12).

FOLDOUT FRAME 1

FOLDOUT FRAME 2

ORIGINAL PAGE IS
OF POOR QUALITY

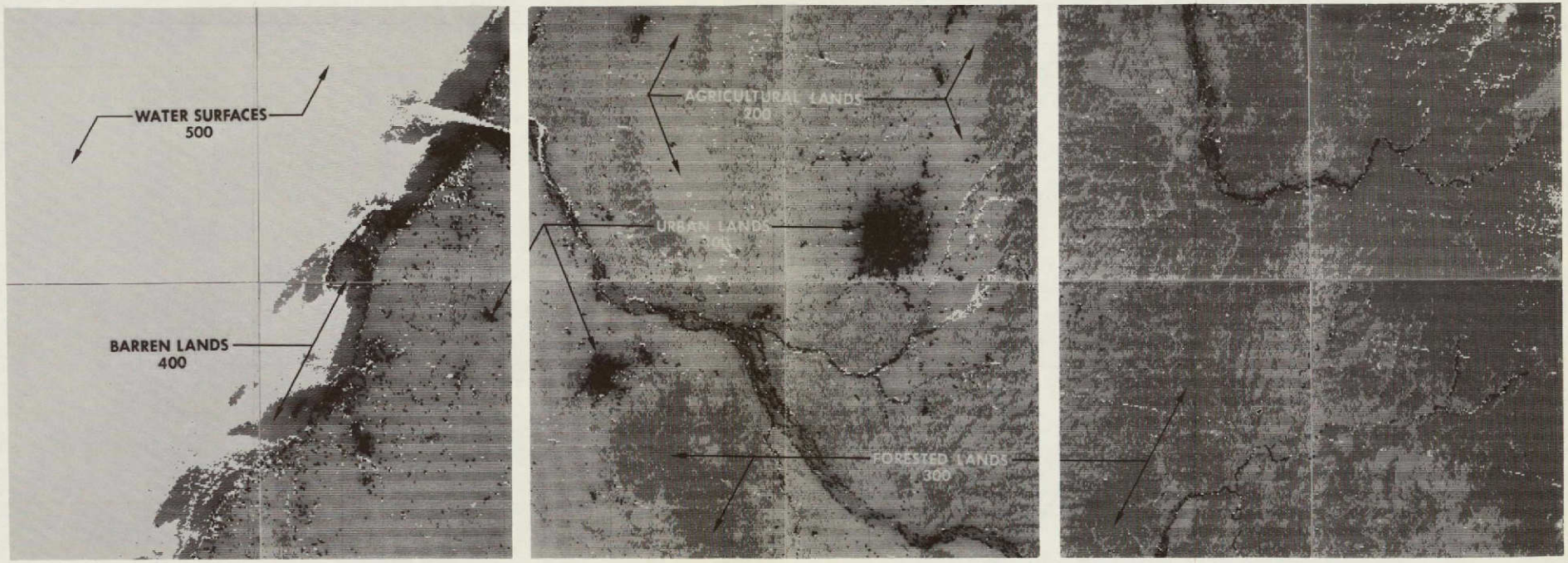

(a) Lu-Kang Map

(b) Taichung Map

(c) Kuo-Hsing Map

FOLDOUT FRAME 1

FIGURE 4.7. FIRST ORDER LAND USE/LAND COVER CLASSIFICATION MAPS. Extracted by computer analysis of a November 1, 1973 LANDSAT image. Scale ∿1:200,000. Specific first order classes are annotated on the maps.

FOLDOUT FRAME 2

order land use within that first order category (Figs. 4.8, 4.9, 4.10, 4.11, and 4.12). Areas of the theme displays belonging to any of the four remaining first order classes are displayed in white. Since no first order category is subdivided into more than five second order classes these theme maps present a reasonable picture of the distribution of each land use/land cover at the second order. Five graylevels or less were used in the first order map and theme maps and can be distinguished by the observer when the land use/land cover is distributed in uniform patches. Highly variable spatial intermixes of cells of various land use are still difficult to distinguish and may only be properly displayed in differing colors, if at all.

4.2.2.1 Verification

Close examination of the theme maps provides a qualitative measure of the accuracy of these final classification maps and the general sources of remaining error. Urban lands were classified along the rivers and coastal lines and appear as "error" in the classification maps (Fig. 4.8). Dry sands occur along the river or coastal embankments and possess very similar spectral characteristics in the two-dimensional spectral space to the concrete roofs of the buildings which dominate the commercial category of urban land use. The addition of spectral bands from LANDSAT images taken on some other date or the overlay of ancillary data, such as the distance from the center of the city to each cell processed, should decrease

ORIGINAL PAGE IS
OF POOR QUALITY

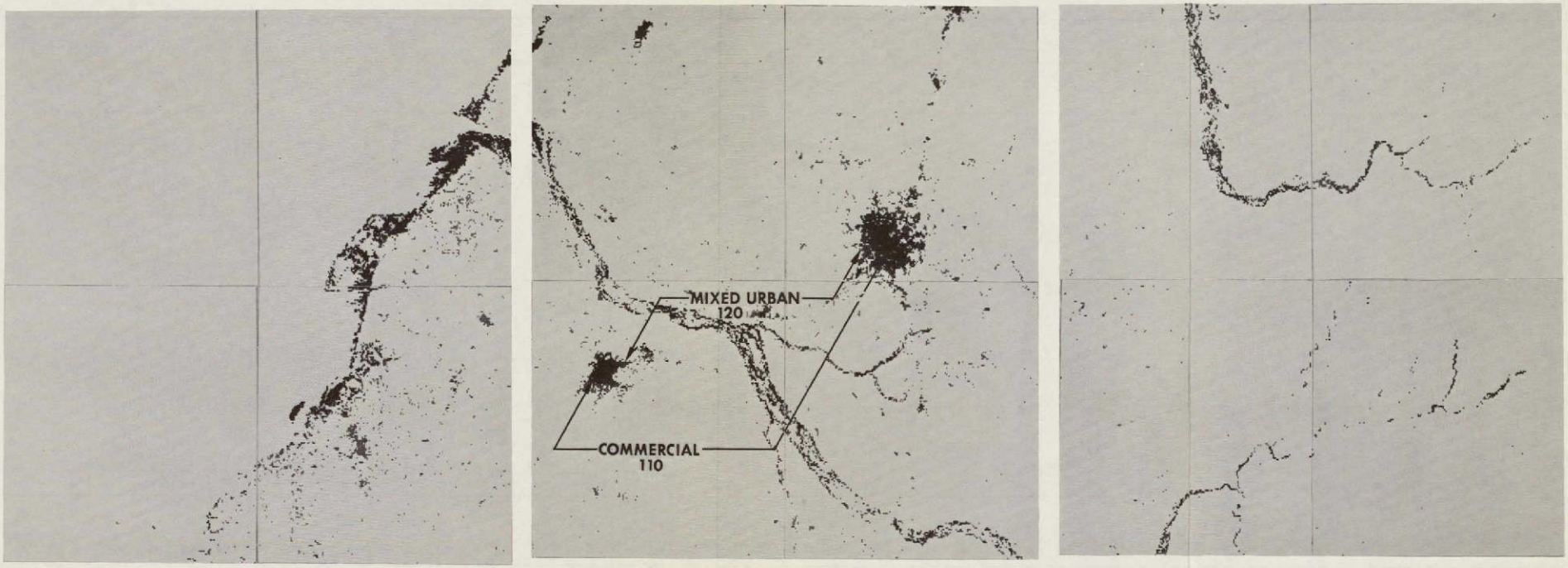

(a) Lu-Kang Map

(b) Taichung Map

(c) Kuo-Hsing Map

FIGURE 4.8. URBAN LAND USE/LAND COVER CLASSIFICATION THEMES. Extracted by computer analysis of a November 1, 1973 LANDSAT image. Scale ∿1:200,000. Specific second order classes are annotated on the maps.

FOLDOUT FRAME 1

FOLDOUT FRAME 2

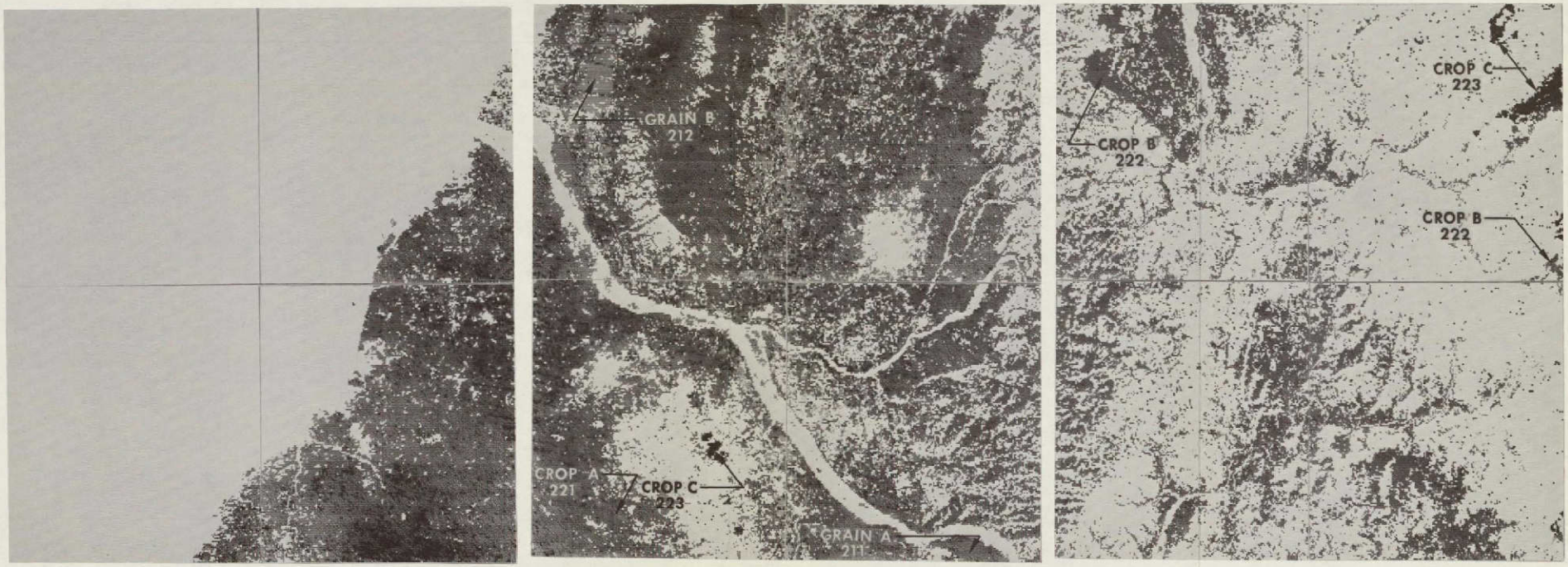

(a) Lu-Kang Map

(b) Taichung Map

(c) Kuo-Hsing Map

FIGURE 4.9. AGRICULTURAL LAND USE/LAND COVER CLASSIFICATION THEMES. Extracted by computer analysis of a November 1, 1973 LANDSAT image. Scale ∿1:200,000. Specific second and third order classes are annotated on the maps.

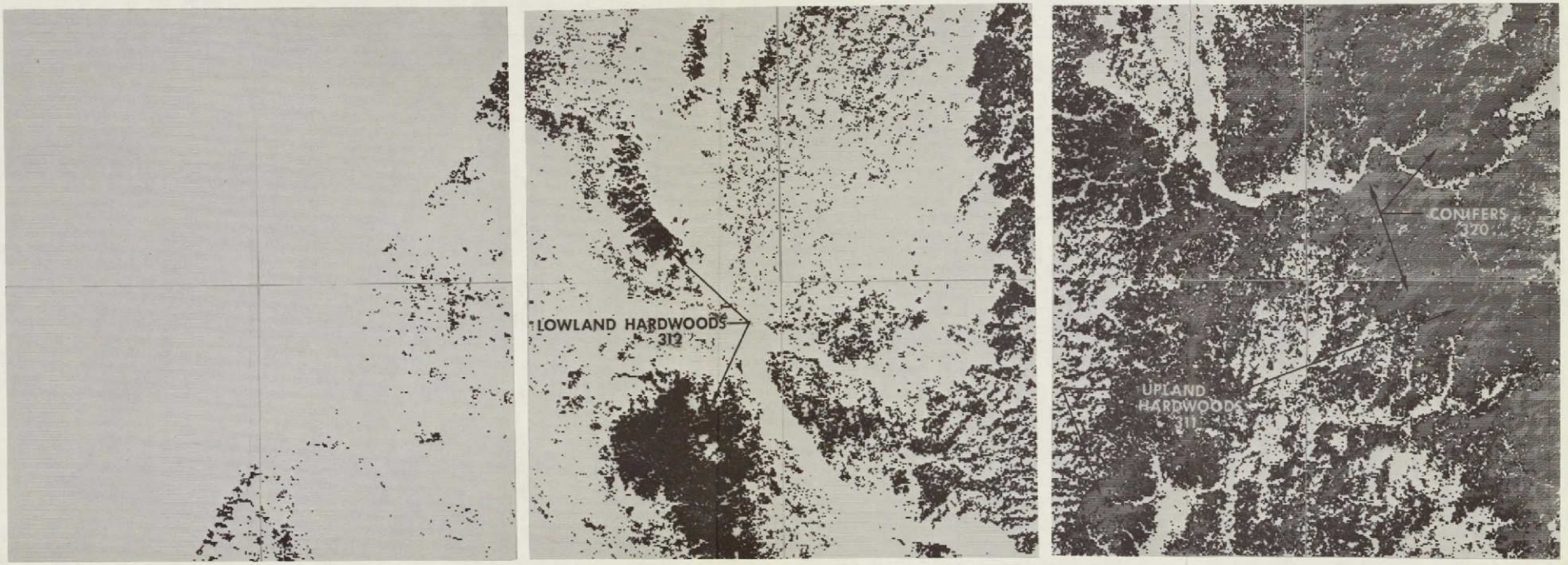

(a) Lu-Kang Map

(b) Taichung Map

(c) Kuo-Hsing Map

FIGURE 4.10. FOREST LAND USE/LAND COVER CLASSIFICATION THEMES. Extracted by computer analysis of a November 1, 1973 LANDSAT image. Scale ≈1:200,000. Specific second and third order classes are annotated on the maps.

ORIGINAL PAGE IS
OF POOR QUALITY

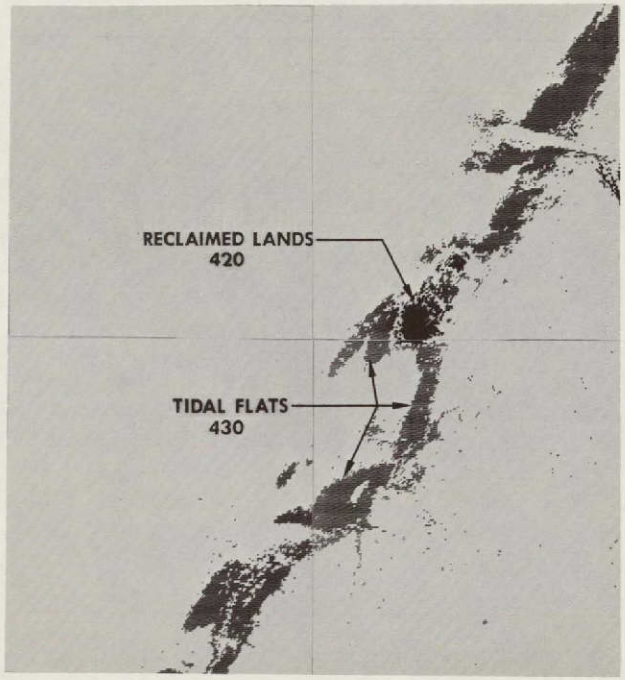

(a) Lu-Kang Map

(b) Taichung Map

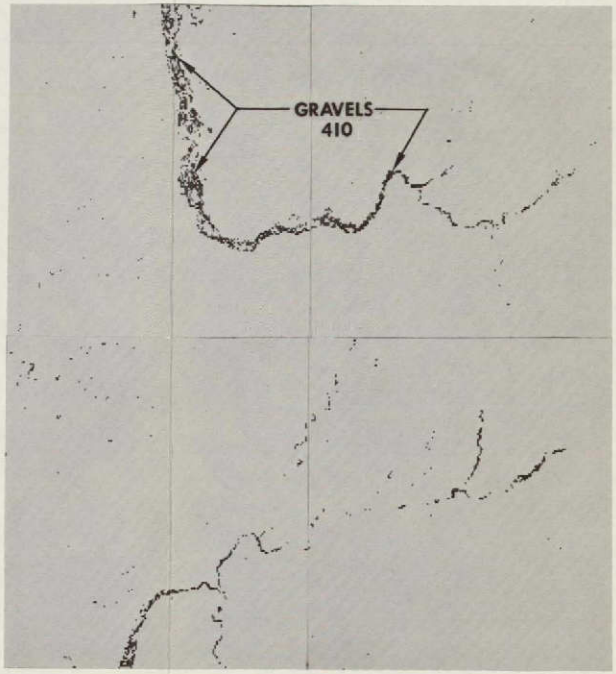

(c) Kuo-Hsing Map

FIGURE 4.11. BARREN LAND USE/LAND COVER CLASSIFICATION THEMES. Extracted by computer analysis of a November 1, 1973 LANDSAT image. Scale ∿1:200,000. Specific second and third order classes are annotated on the maps.

FOLDOUT FRAME 1

FOLDOUT FRAME 2

ORIGINAL PAGE IS
OF POOR QUALITY

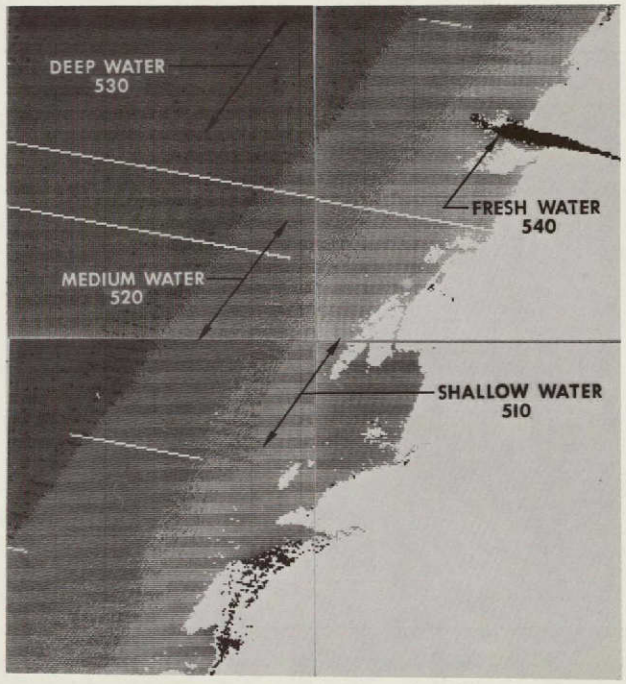

(a) Lu-Kang Map

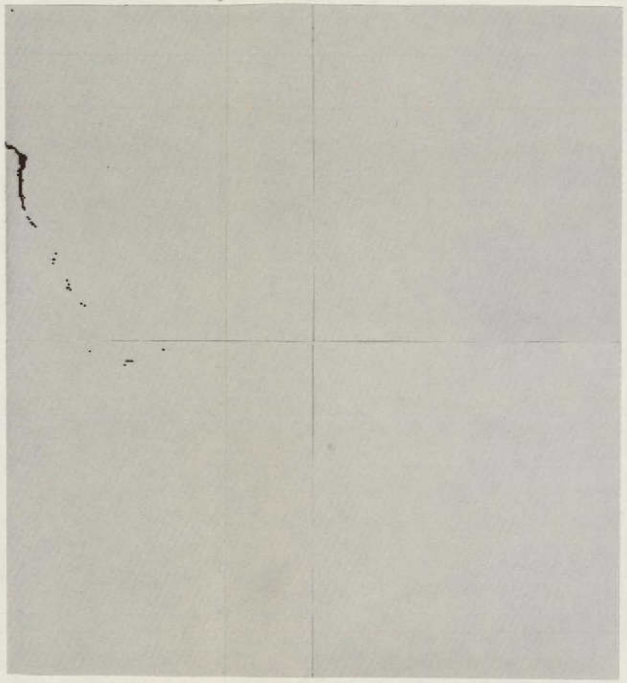

(b) Taichung Map

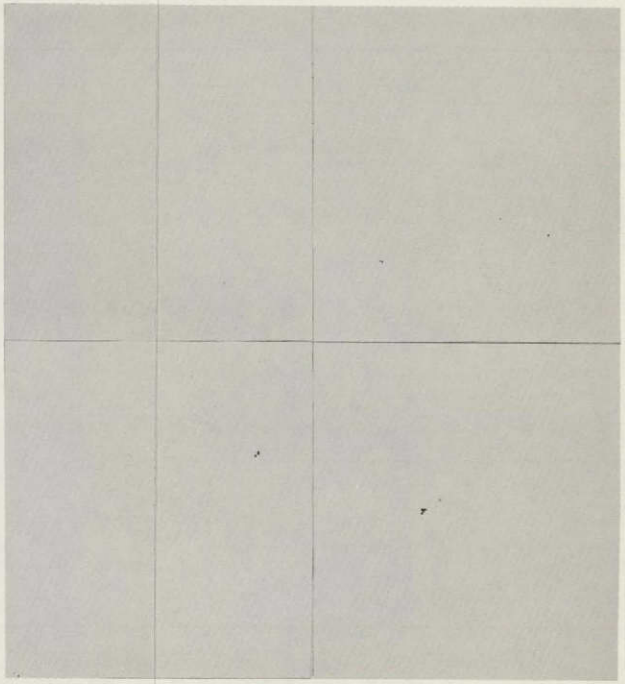

(c) Kuo-Hsing Map

FIGURE 4.12. WATER SURFACE CLASSIFICATION THEMES. Extracted by computer analysis of a November 1, 1973 LANDSAT image. Scale ∿1:200,000. Specific second and third order classes are annotated on the maps. The zigzag diagonal lines in white on the Lu-Kang Map represent missing portions of the original scan lines.

FOLDOUT FRAME

FOLDOUT FRAME 2

this kind of classification error. Generally the distribution of forest types is correlated with the aspect of the terrain. Overlays of slope and aspect data onto the multispectral data should be incorporated into future analysis schemes to improve the accuracy of the categorization of forest types. Overlays of water surfaces of the various categories are distributed parallel to the coastal line but they seem to be more closely related to the suspended sediment content than to the water depth. Adequate ground control information can resolve this question and provide a basis for a separation of these two general water categories. Bad scan lines and the six-line problem due to the imbalance in the calibration of the six sensors in the multispectral scanner were not removed or eliminated in this study. The obvious error in the classification of portions of whole scan lines and banding occurring in water surfaces was caused by these problems. More advanced preprocessing and calibration techniques already demonstrated by others can be employed to reduce the impact of these problems and improve the classification results.

4.2.2.2 Tabulation of Land Use/Land Cover

The area of each of the 17 land uses/land covers in three maps was computed by the maximum likelihood ratioing technique using MSS bands 5 and 7 (Table 4.3). One hundred forty thousand image cells of 0.45 hectares are contained in each of three maps, representing 63,000 hectares per map.

TABLE 4.3. AREA OF EACH LAND USE IN HECTARES AS CLASSIFIED FROM LANDSAT IMAGERY FOR EACH 1:25,000 MAP OF 63,000 HECTARES. 17 classes mapped using "pseudo-supervised" training data and the maximum likelihood ratioing technique applied to MSS bands 5 and 7.

Land Use Class						*Lu-Kang Map*			*Taichung Map*			*Kuo-Hsing Map*		
Code	*Level I*	*Code*	*Level II*	*Code*	*Level III*	*I*	*II*	*III*	*I*	*II*	*III*	*I*	*II*	*III*
100	Urban lands					2,230			3,138			939		
		110	Commercial				1,033			706			145	
		120	Mixed				1,197			2,432			794	
200	Agricultural lands					14,660			43,842			17,394		
		210	Grains				6,936			15,051			3,011	
				211	Rice A			6,596			10,792			2,363
				212	Rice B			340			4,259			649
		220	Crops				7,724			28,791			14,383	
				221	Crop A			6,105			22,504			7,925
				222	Crop B			340			3,975			5,752
				223	Crop C			1,279			2,312			706
300	Forested lands					800			13,678			44,100		
		310	Hardwoods				794			13,243			28,470	
				311	Type A			0			794			15,397
				312	Type B			794			12,449			13,073
		320	Conifers				6			435			15,630	
400	Barren lands					4,473			2,098			434		
		410	Gravels				44			1,556			277	
		420	Reclaimed land				258			246			132	
		430	Tidal flat				4,171			296			25	
500	Water surfaces					40,383			50			6		
		510	Shallow seawater				11,246			0			0	
		520	Medium seawater				12,033			0			0	
		530	Deep seawater				16,437			0			0	
		540	Fresh water				667			50			6	
Unclassified (thresholded out)						454			194			127		

Maximum likelihood ratioing may assign any of the 420,000 cells to an additional 18th class when their probability of belonging to any of the 17 classes specified by training sets is lower than a selected threshold value. Thus, the relationship between classification accuracies and threshold values should be further investigated and additional land uses/land covers will be needed to categorize those unclassified cells.

4.2.3 Costs

Cost is one of the major considerations in a land use/land cover mapping project. The cost for each of 1:25,000 land use/land cover classification maps (about 1 x 1 meter in dimension) was estimated based on the Colorado State University charge system for time on the CDC 6400 computer (Table 4.4). Neither the cost of development and testing of procedures applied to training sets and verification nor the cost of labor was included in this estimate. The cost for computer time only is about U.S. $265 (N.T. $10,070) per map, or N.T. $0.16 per hectare, using two spectral bands and the maximum likelihood ratioing approach. It costs about twice as much to use four spectral bands. Thus, the land use/land cover mapping can be done much less expensively by this approach than by the conventional methods.

TABLE 4.4. COST ESTIMATES FOR EACH 1:25,000 LAND USE/LAND COVER CLASSIFICATION MAP. Does not include cost of development and testing procedures applied to training sets or verification. Based only on Colorado State University charge system of $290 per hour of CDC 6400 time and does not include labor. Based on 17 classes and 140,000 cells of approximately 0.45 hectare. Based on 1 U.S. $ = 38 N.T. $.

4-Band Case

	Time in Seconds		*Cost*	
Operations Performed	*Central Processor*	*Input/Output*	*U.S. $*	*N.T. $*
Format conversion Geometric correction Graymapping	1,300	1,300	$255	$ 9,690
Map classification Display	2,400	400	320	12,160
Totals	3,700	1,700	$575	$21,850

or N.T. $ = 0.35/hectare

2-Band Case

	Time in Seconds		*Cost*	
Operations Performed	*Central Processor*	*Input/Output*	*U.S. $*	*N.T. $*
Format conversion Geometric correction Graymapping	650	650	$125	$ 4,750
Map classification Display	1,000	400	140	5,320
Totals	1,650	1,050	$265	$10,070

or N.T. $ = 0.16/hectare

V. CONCLUSIONS

The results of this study were based upon single date LANDSAT imagery and the availability of limited ground control. The land use/land cover classification scheme could be revised if better ground control data became available and the accuracy of the classification maps correspondingly improved. The testing completed to date has provided a logical, scientific basis for the land use/land cover classification mapping of Taiwan using the LANDSAT MSS imagery. It has covered the complete spectrum of land covers/water types occurring in the study site. The study site was selected as representative of the complete spectrum of land covers and water types of Taiwan and the results should be applicable to the entire island. Additional subdivision of some second level classes, such as the agricultural lands and forested lands, must be investigated in more detail to achieve even more meaningful subcategories of these classes. Offshore seawater classes were found to be more closely related to suspended sediment content than actual water depth but could not be calibrated due to the total lack of ground control. A further investigation should be undertaken of the study of coastal processes by LANDSAT remote sensing.

Three approaches for selection of training sets were tested. The non-supervised method was employed without reference to specific ground control data and classifies the first level classes with a 79% training set accuracy. Ground control data from black and white airphotos extracted by point photointerpretation provided a second method for establishing the training sets. A relatively low training set classification accuracy was obtained when using this sampled data in a supervised approach due to the misregistration of the ground control data and the heterogeneous nature of the training sets selected. Better registration and reliable ground control data at third level classes should improve the accuracy of this approach. The pseudo-supervised approach provided the best training sets and the most accurate training set classification results of 89% for first level classes. However, this approach requires prior information about the natural grouping of land cover types in order to obtain reasonable subdivisions of the second level classes. Based upon these results the best composite approach appears to be:

1. Use unsupervised or cluster analysis to identify and display the natural land cover classes which can be separated in a multispectral sense.
2. Use airphotos to identify the unknown land covers.

3. Select specific training sets to represent these desired land covers and apply the supervised approach to prepare the final classification map.

Statistical cleaning was proposed to increase the training set accuracy. The tests completed in this study have shown that statistical cleaning does not significantly improve the actual training set accuracy. The best way to improve this accuracy was to reselect improved or more representative training sets in an iterative or learning procedure. However, a final evaluation of the value of statistical cleaning remains to be tested by determining its impact upon final map verification accuracy.

Costs and accuracy are the two major considerations in a land use/land cover mapping project. Effort must be made to achieve the highest accuracy at the lowest expense. The quality of training sets selected will directly affect the accuracies of the classification map when a supervised approach is used. Once the training sets have been selected the classification accuracy may be improved by adding spectral bands/ratios. Adding these additional variables correspondingly increases the cost of computing the classification map. The tests made on three different training sets established that four selected MSS bands/ratios provided a comparable accuracy with that obtained by all 10 MSS bands/ratios. The ratios of the MSS bands were shown to contribute little additional accuracy to the training set classifications

performed by stepwise discriminant analysis. Moreover, MSS bands 5 and 7 provide the same overall training set accuracy as the four MSS bands/ratios identified by the stepwise tests. The preliminary verification of the final classification map provided further support for the selection of MSS bands 5 and 7. Thus, substantial savings were achieved by selecting two specific, sensitive spectral bands without any significant loss of final classification accuracy.

The training sets established by the pseudo-supervised approach could be applied to the entire country. The "signature" extension from the northern image, where the training sites occur, to the southern image appears feasible as they were collected only a few minutes apart and are adjacent on the same LANDSAT orbit. However, this supposition should be verified. The land area of Taiwan is equivalent to approximately 60 of the 1:25,000 maps analyzed here. Preparing similar classifications for these 60 maps for the 17 land use/land cover classes using only MSS bands 5 and 7 would cost about $15,000 U.S. ($570,000 N.T.) in computer time (Table 4.4). This mapping approach could be economically completed for the whole island in a short period, yielding timely, up-to-date land use/land cover maps and area statistics.

The final classification map in this study achieved over 89% training set accuracy at the first level of land use/land cover using a single date LANDSAT image. Significant increase in this classification accuracy could be achieved by analyzing LANDSAT imagery

taken on different dates during a given growing season and overlaid to provide a basis for the simultaneous, multispectral, multidate processing already tested by others. Confusions in classes, such as urban lands and crops, can be further reduced by increasing the dimensions of spectral space by the addition of new spectral bands as is planned by NASA for future LANDSAT-type satellites and the thematic mapper satellites. Additional improvements can also be achieved by the input of overlays of cellularized maps, e.g., topography and other ancillary data, into the classification procedure.

Proper display of the final classification map is equally as important as the final map accuracy. A better display of the resulting classification map can encourage wider usage of the approach and product. Computer line printer displays provide a cheap product which is compatible with topographic maps and can portray all the detailed cell-by-cell distribution of each land use/land cover at 1:25,000. Microfilm display of specific theme maps provides a better overview of the spatial distribution of particular land use/land cover classes. Unfortunately, black and white microfilm or line printer displays have insufficient gray levels to effectively visually display more than three to five discrete classes. Display of the final multiclass maps in color on a computer color film generator can overcome many of the display handicaps encountered in this study.

Additional field verification of the three computed classification maps will be undertaken in the near future to obtain map verification accuracy in a more absolute sense. It will also provide more detailed information for further training set selections and the development of an improved land use/land cover hierarchy. The correlation between multispectral clustering and actual occurrence of land use/land cover will also be more accurately established.

REFERENCES CITED

Anderson, J. R. 1971. Land-use Classification Schemes, Photogrammetric Engineering, 37(4):379-388.

Anderson, J. R., E. E. Hardy, and J. T. Roach. 1971. A Land-use Classification System for Use with Remote Sensor Data, U.S. Geological Survey Circular 671, U.S. Geological Survey, Washington, D.C., 16 p.

Anderson, J. R., E. E. Hardy, J. T. Roach, and R. E. Witmer. 1976. A Land Use and Land Cover Classification System for Use with Remote Sensor Data, U.S. Geological Survey Professional Paper 964, U.S. Geological Survey, Washington, D.C., 28 p.

Anuta, P. E. 1973. Geometric Correction of ERTS-1 Digital Multispectral Scanner Data, LARS Information Note 103073, Lab. for Appl. of Remote Sensing, W. Lafayette, Ind., 23 p.

Burley, T. M. 1961. Land-use or Land Utilization? Prof. Geographer, 13(6):18-20.

Chang, T. P. 1974. Application of Remote Sensing to Agriculture and Forestry, Application of Remote Sensing, MRSO Report, No. 140, Mineral Resources and Service Organization, Taipei, Rep. of China, pp. 58-65.

Clawson, Marion, Charles L. Stewart. 1965. Land Use Information. A critical survey of U.S. statistics including possibilities for greater uniformity, The John Hopkins Press for Resources for the Future Inc., Baltimore, Md., 402 p.

Duda, R. O., P. E. Hart. 1973. Pattern Classification and Scene Analysis, John Wiley and Sons, New York, 482 p.

Ells, T. D., L. D. Miller, and J. A. Smith. 1972a. User's Manual for RECOG (pattern RECOGnition programs). Sci. Series No. 3B, Dept. of Watershed Sci., Colo. State Univ., Ft. Collins, Colo., 85 p.

_____. 1972b. Programmer's Manual for RECOG (pattern RECOGnition programs). Sci. Series No. 3C, Dept. of Watershed Sci., Colo. State Univ., Ft. Collins, Colo., 216 p.

Hoffer, R. M., et al. 1974. Natural Resource Mapping in Mountainous Terrain by Computer Analysis of ERTS-1 Satellite Data. LARS Information Note 061575, Lab. for Appl. of Remote Sensing, W. Lafayette, Ind., 124 p.

LANDSAT Data Users Handbook. 1976. Document No. 765D54258, NASA, Goddard Space Flight Center, Greenbelt, MD., 110 p.

Maxwell, E. L. 1974. A Remote Rangeland Analysis System. Report No. 1885-F, sponsored by U.S.G.S., Contract No. 14-08-0001-13561, Dept. of Earth Resources, Colo. State Univ., Ft. Collins, Colo., 110 p.

_____. 1976. Multivariate System Analysis of Multispectral Imagery. Photogrammetric Engineering and Remote Sensing, 42(9):1173-1186.

Miller, L. D. 1974. Lee D. Miller presented a two month short course in Taipei on the subject of remote sensing of natural resources for 32 multidisciplined Taiwan resource managers for various government agencies under sponsorship of the Joint Commission on Rural Reconstruction and other agencies.

Miller, L. D., T. P. Chang, and S. Wang. 1974. A series of presentations on remote sensing were presented in several government agencies by Miller, Chang, and Wang shortly after the completion of the two month short course in Taipei.

Miller, L. D. 1975. Internal research project memorandum by Dr. Lee D. Miller, Dept. of Civil Engineering, Colo. State Univ., Ft. Collins, Colo., 10 p.

Miller, L. D., E. L. Maxwell, and R. Riggs. 1977. The LMS software package was a joint effort of those individuals noted. Final documentation will be issued shortly as a detailed technical report and user's guide.

No Author. 1973. BMD Manual. Univ. of California, Los Angeles, 773 p.

Pan, K. L. 1974. Application of IR Scanning in Taiwan, Application of Remote Sensing. MRSO Report No. 140, Mineral Resources and Service Organization, Taipei, Taiwan, Rep. of China, pp. 50-55.

Pearson, R. L., C. J. Tucker, and L. D. Miller. 1976. Spectral Mapping of Shortgrass Prairie Biomass. Photogrammetric Engineering and Remote Sensing, 42(3):317-323.

Place, J. L. 1973. Change in Land Use in the Phoenix (1:250,000) Quadrangle, Arizona between 1970 and 1972: Successful Use of a Proposed Land Use Classification System. Symposium on Significant Results Obtained from the ERTS-1, NASA, Goddard Space Flight Center, Greenbelt, MD., Vol. I: Technical Presentation Section B, pp. 899-906.

Siegal, B. S. and M. J. Abrams. 1976. Geologic Mapping Using LANDSAT Data. Photogrammetric Engineering and Remote Sensing, 42(3): 325-337.

Smith, J. A., L. D. Miller, and T. Ells. 1972. Pattern Recognition Routines for Graduate Training in the Automatic Analysis of Remote Sensing Imagery-RECOG. Sci. Series No. 3A, Dept. of Watershed Sci., Colo. State Univ., Ft. Collins, Colo., 86 p.

Smith, J. A. 1976. Class notes of Remote Sensing System offered by Dr. James A. Smith, spring semester, 1976, at Colo. State Univ.

Thomson, F. J., J. D. Erickson, R. F. Nalepka, J. D. Weber, and J. G. Braithwaite. 1974. Multispectral Scanner Data Applications Evaluation, NASA JSC-09241, ERIM 102800-41-X, Environmental Research Institute of Michigan, Ann Arbor, Michigan, 357 p.

Tom, C., L. D. Miller. 1976. Spatial Land-Use Inventory-Modeling/Denver Metropolitan Area, unsponsored research presented at Regional Workshop for Remote Sensing and Photogrammetry, Colo. State Univ., Ft. Collins, Colo., Section Two, March 18, 1976, 10 p.

Wang, S. 1974. Structural Trend Revealed by ERTS-1 Imagery in Southern Taiwan. Applications of Remote Sensing, MRSO Report, No. 140, Mineral Resrouces and Service Organization, Taipei, Rep. of China, pp. 56-57.

Wang, S. 1976. ERTS-1 Satellite Imagery and Its Application in Regional Geologic Study of Southwestern Taiwan, Petroleum Geology of Taiwan, Chinese Petrol. Co., Taiwan, Rep. of China, No. 13, pp. 37-57.

Yarger, H. L., J. R. McCauley. 1974. Quantitative Water Quality with LANDSAT and SKYLAB, 3rd ERTS-1 Symposium, Vol. 1, Section B, NASA, Goddard Space Flight Center, Greenbelt, Md., pp. 1637-1651.

APPENDIX A

LANDSAT MAPPING SYSTEM (LMS)

The LANDSAT Mapping System or LMS is a total rewriting of the RECOG or RECOGnition Mapping System (Smith, Miller and Ells, 1972; Ells, Miller and Smith, 1972a and 1972b). RECOG was designed principally for training purposes and this new LMS system is compatible with it. However, the new design is for specific use with LANDSAT imagery for map and composite mapping system (CMS) overlay, low cost, ease in understanding, flexibility, export to other user computers, and high volume production (Miller, Maxwell, and Riggs, 1977).

This system consists of four major steps. The first step is to prepare map overlays in a desired scale by inputting LANDSAT CCTs. The second step is to interleave images from various dates. Multiple ancillary or map data planes can also be overlaid on the image cells in this step. The third step is to compute and optimize the statistical representation of the materials to be mapped. The final step is then to map the distribution of each material sought and display the classification maps as line printer and microfilm rectified and scaled maps.

The computer cost was estimated for one 1:24,000 quadrangle map using a CDC 6400 computer and the charge system of Colorado State University.

STEP 1. IMAGE PREPARATION/MAP OVERLAY.

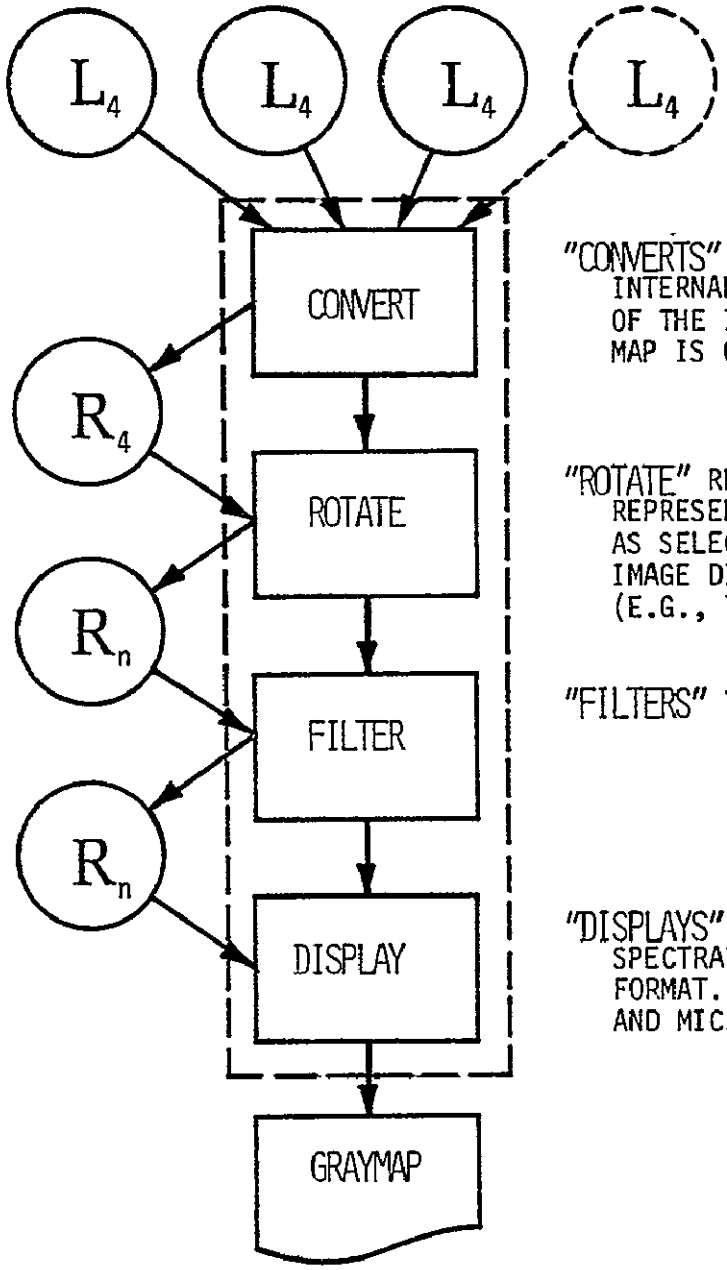

UP TO 4 TAPES, REPRESENTING ~25 MILE E-W SEGMENTS OF A GIVEN LANDSAT IMAGE, MAY BE INPUT SIMULTANEOUSLY.

"CONVERTS" THE LANDSAT FORMAT TAPE(S) INTO THE INTERNAL, SINGLE RECOG TAPE. ONLY THE PORTION OF THE IMAGE NEEDED TO OVERLAY THE SELECTED MAP IS CONVERTED AND POOLED TOGETHER.

"ROTATE" RESAMPLES THE ORIGINAL IMAGE CELLS TO REPRESENT ANY SIZE RECTANGULAR OR SQUARE CELL AS SELECTED BY THE USER. ADJUSTS FOR ORIGINAL IMAGE DISTORTIONS. SCALES IMAGE TO MAP SCALE (E.G., 1:24,000).

"FILTERS" THE IMAGE.

"DISPLAYS" 1, 2, 3 ... OR ALL OF THE INDIVIDUAL SPECTRAL BANDS IN THE ORIGINAL OR MAP OVERLAY FORMAT. DISPLAY OPTIONS INCLUDE LINEPRINTER AND MICROFILM GRAYMAPS.

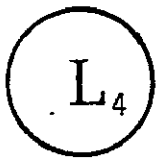

"LANDSAT" COMPUTER COMPATIBLE TAPE (CCT) AS SUPPLIED BY EROS DATA CENTER.

"RECOG" FORMATTED TAPE (OR DISK) FILE - AS STANDARD FORMAT TAPE USED THROUGHOUT THE IMAGE PROCESSING ACTIVITY. (n = 1 to 4)

STEP 2. INTERLEAVES IMAGES FROM VARIOUS DATES.

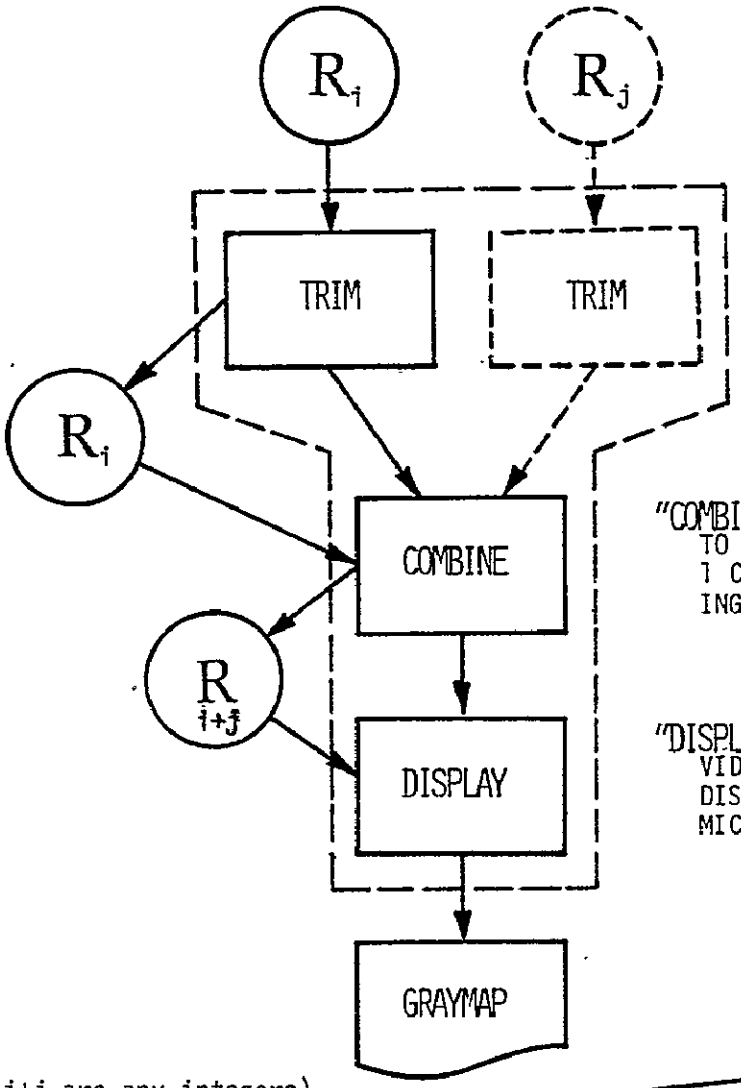

UP TO 10 RECOG FORMATTED TAPES OF A VARYING NUMBER OF SPECTRAL BANDS ARE INPUT.

"TRIMS" EACH RECOG FORMATTED TAPE (OR FILE) TO A SELECTED NUMBER OF LINES AND COLUMNS DESIGNATED BY THE USER, USUALLY THOSE NEEDED TO COVER MAP SELECTED. LINES AND COLUMNS ARE RENUMBERED, BEGINNING AT 1,1.

"COMBINES" RECOG FORMATTED DATA FROM THE 1 TO 10 SEPARATE INPUT TAPES (FILES) INTO 1 COMPOSITE RECOG TAPE (FILE) REPRESENTING A MULTIDATE, MULTISPECTRAL IMAGE.

"DISPLAYS" 1, 2, 3 ... OR ALL OF THE INDIVIDUAL SPECTRAL BANDS IN COMBINED IMAGE. DISPLAY OPTIONS INCLUDE LINEPRINTER AND MICROFILM GRAYMAPS.

(i+j are any integers)

STEP 2. AUXILIARY PROGRAMS.

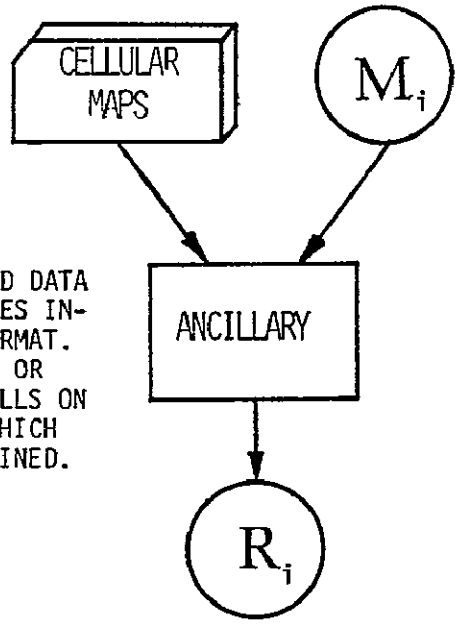

"ANCILLARY" CREATES RECOG FORMATTED DATA FROM CELLULARIZED MAP DATA PLANES INPUT IN CARD OR MAGNETIC TAPE FORMAT. MAP CELLS MUST BE THE SAME SIZE OR SOME INTEGER MULTIPLE OF THE CELLS ON THE RECOG FORMATTED DATA WITH WHICH THE ANCILLARY DATA WILL BE COMBINED.

STEP 3. COMPUTES STATISTICAL "SIGNATURES" OF MATERIALS TO BE MAPPED.

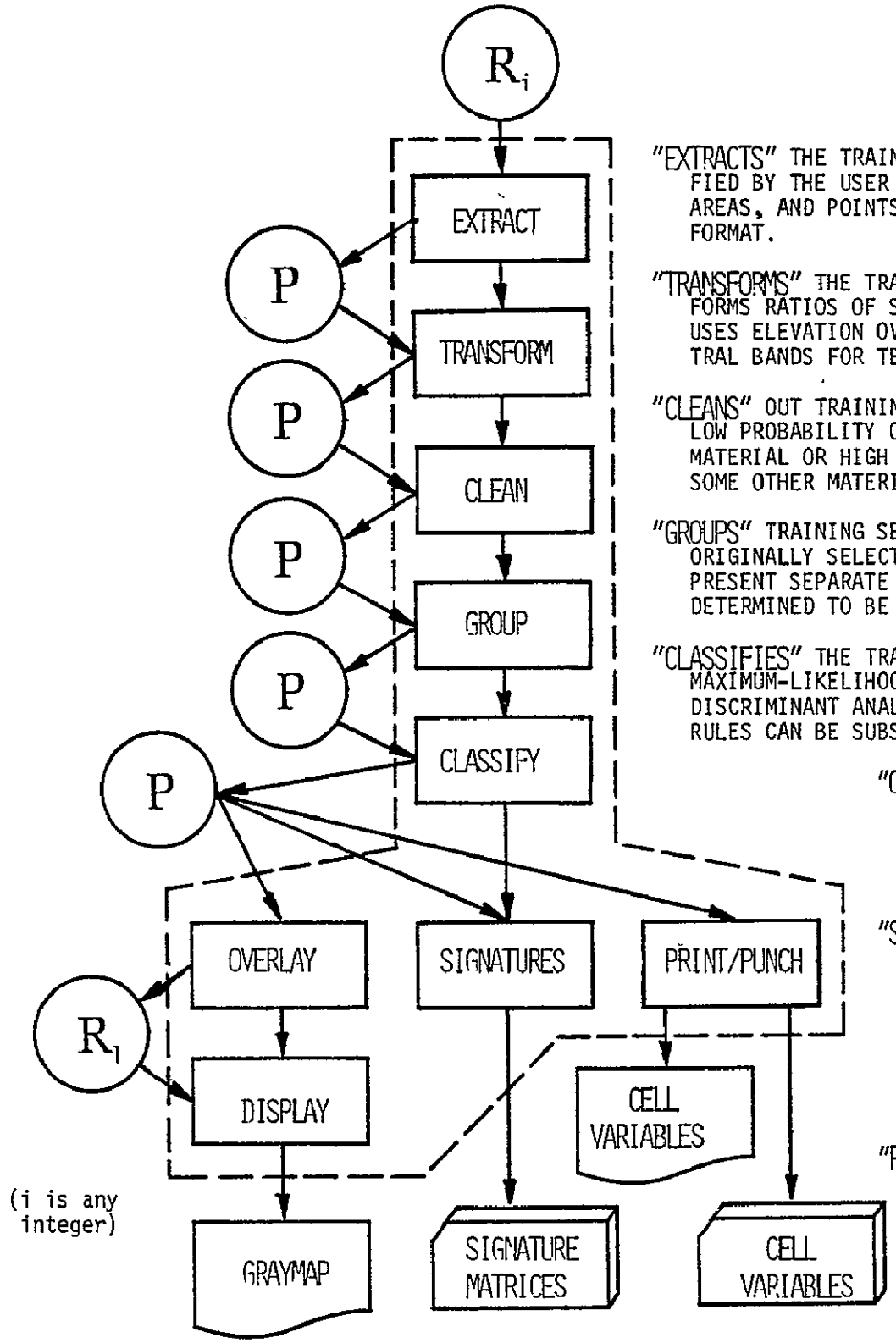

"EXTRACTS" THE TRAINING FIELD DATA IDENTIFIED BY THE USER (RECTANGLES, IRREGULAR AREAS, AND POINTS) FROM THE RECOG IMAGE FORMAT.

"TRANSFORMS" THE TRAINING FIELD DATA. FORMS RATIOS OF SPECIFIED SPECTRAL BANDS, USES ELEVATION OVERLAYS TO ADJUST SPECTRAL BANDS FOR TERRAIN SHADOWING, ETC.

"CLEANS" OUT TRAINING FIELD DATA POINTS WITH LOW PROBABILITY OF BEING THE SELECTED MATERIAL OR HIGH PROBABILITY OF BEING SOME OTHER MATERIAL, ETC.

"GROUPS" TRAINING SETS TOGETHER WHICH WERE ORIGINALLY SELECTED IN EXTRACT TO REPRESENT SEPARATE MATERIALS BUT ARE NOW DETERMINED TO BE STATISTICALLY SIMILAR.

"CLASSIFIES" THE TRAINING FIELDS USING MAXIMUM-LIKELIHOOD APPROACH (STEPWISE DISCRIMINANT ANALYSIS). OTHER DECISION RULES CAN BE SUBSTITUTED HERE.

"OVERLAYS" ANY VARIABLE OR RESULT IN POINT FILE INTO A RECOG FORMAT FOR DISPLAY AND MAP OVERLAY.

"SIGNATURES" COMPUTES STATISTICAL REPRESENTATION OF EACH MATERIAL SPECIFIED BY THE USER FOR USE IN MAPPING THESE MATERIALS ON ANY DATA TAKEN FROM THE SAME ORIGINAL IMAGE.

"PRINTS" OR "PUNCHES" OUT ANY VARIABLE(S) IN THE POINT FILE FOR FURTHER ANALYSIS IN ADDITIONAL PROGRAMS WRITTEN BY THE USER.

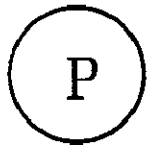

"POINT" BY POINT TAPE (OR DISK) FILE. - AN INTERNAL TAPE, DISK, AND/OR CARD FILE FORMAT WHICH CONTAINS ONLY THE EXTRACTED TRAINING FIELD DATA AND DOES NOT MAINTAIN ITS CORRECT MAP OVERLAY POSITION.

STEP 4. MAPS DISTRIBUTION OF EACH MATERIAL.

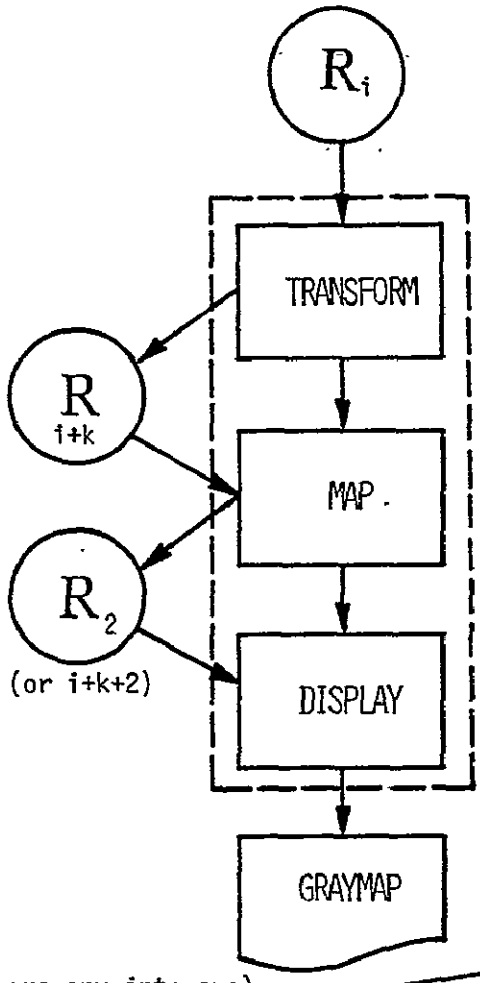

"TRANSFORMS" DATA FOR EACH IMAGE CELL AS TESTED AND SELECTED IN STEP 3.

"MAPS" OUT THE DISTRIBUTION OF EACH SURFACE MATERIAL SPECIFIED BY THE USER.

"DISPLAYS" THE SELECTED IDENTIFICATION OF EACH IMAGE CELL AND/OR PROBABILITY THAT IT IS THE MATERIAL DESIGNATED. DISPLAY OPTIONS INCLUDE LINEPRINTER AND MICROFILM GRAYMAPS AND LINEPRINTER COLOR SYMBOL MAPS.

(i and k are any integers)

STEP 4. AUXILIARY PROGRAM.

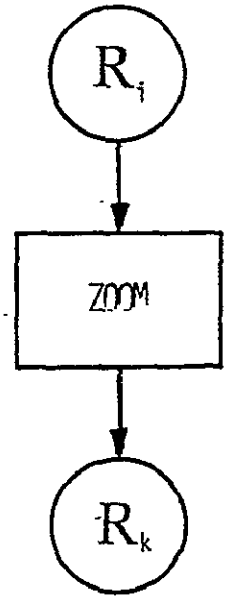

"ZOOMS" OR ENLARGES THE RECOG FORMATTED TAPE (OR FILE) BY ECHOING EACH IMAGE CELL "N" TIMES ON A LINE AND REPEATING EACH LINE "M" TIMES.

LANDSAT MAPPING SYSTEM (LMS)

ITEM	DEVELOPMENT STATUS		COST ESTIMATE*
CONVERT	100%		$5/date
ROTATE	100%		$7/date
FILTER	100%		$6/date
DISPLAY	100%	$1/band/date x 2 bands =	$2/date
STEP 1	100%		$20/date
Assuming 3 dates involved gives $20/date x 3 =			$60
TRIM	100%		$3/date
COMBINE	100%	3 dates combined =	$1
DISPLAY	100%	$1/band/date x 1 band =	$1
ANCILLARY	100%		optional
STEP 2	100%		
Assuming 3 dates gives $3/date x 3 dates + $1 + $1 =			$11
EXTRACT	100%		$10 (approx.)
TRANSFORM	100%		$5 (approx.)
CLEAN	100%	$2/iteration x 3 iterations =	$6 (approx.)
CLASSIFY	100%	$8/iteration x 3 iterations =	$24 (approx.)
SIGNATURES	100%		$2 (approx.)
OVERLAY	90%		optional
GROUP	90%		optional
PRINT/PUNCH	95%		optional
STEP 3	98%		
Based on 2,000 points =			$50 (approx.)
TRANSFORM	0%		$5 (approx.)
MAP	100%**	based on mapping 30 material types	$73 (approx.)
DISPLAY	100%**	black-and-white lineprinter symbol map	$1 (approx.)
ZOOM	0%		optional
STEP 4	75%		
Based on 30 classes mapped =			$79 (approx.)
		STEP TOTAL* =	$200 (approx.)

* Estimated computer costs for 1 of 1:24,000 quad map with:
- ~1 acre cells
- 3 dates (12 spectral bands)
- 2,000 cells defining training fields
- 30 material types
- black-and-white lineprinter display.

** Extensive modification needed to improve efficiency.

APPENDIX B

STEPWISE DISCRIMINANT ANALYSIS

Discriminant analysis consists of finding a transform which minimizes the ratio of the difference between class multivariate means to the class multivariate variances. The algorithm used here and entitled CLASSIFY* (Appendix A) computes a classification function for each of the classes by choosing and inputting the independent variables, the 10 MSS band/ratio values, in a stepwise manner. The variable or band/ratio entered at each step is selected on the basis of its F statistics. As each MSS band/ratio is added a classification function is computed for each land use/land cover class. The equation of the classification function D_{ki} for the k^{th} class for the i^{th} variable or band/ratio is given by

$$D_{ki} = C_{ko} + \sum_{i=1}^{r} e_{ki} \; Z_{1ki}$$

where C_{ko} is a constant term for the k^{th} class, r is the number of input variables (the 10 spectral band and ratios), e_{ki} is the

---

*CLASSIFY is a modified version of BMD07M which is part of the UCLA biomedical statistical package available on most major computers (BMD Manual, 1973). It has not been modified in statistical approach but in input, output, and internal control to enable it to handle much larger data bases in ways not envisioned by the original authors.

discriminant coefficient for the k^{th} group and the i^{th} band/ratio, and Z_{lki} is the measured spectral radiance of the l^{th} cell of the k^{th} class for the i^{th} variable (10 bands/ratios).

The coefficient e_{ki} is computed from $(n-g) \sum_{j=1}^{r} \bar{X}_{kj} a_{ij}$ and the constant term C_{ko} is computed from $-\frac{1}{2} \sum_{i=1}^{r} e_{ki} \bar{X}_{ki}$, where $\bar{X}_{ki}$ is the mean of band/ratio i for class k, and n, number of cells in class k, and g the total number of land use/land cover classes sought in the analyses.

The within and total cross-product matricies are expressed as below:

$$W = \{w_{ij}\}; \quad w_{ij} = \sum_{k=1}^{g} \sum_{n=1}^{n_k} (X_{ikn} - \bar{X}_{ik})(X_{jkn} - \bar{X}_{jk})$$

$$T = \{t_{ij}\}; \quad t_{ij} = \sum_{k=1}^{g} \sum_{n=1}^{n_k} (X_{ikn} - \bar{X}_{i})(X_{jkn} - \bar{X}_{j})$$

where n_k is the number of cells in class k.

i = 1, 2, 3, ...p variables (10 spectral band/ratio radiances)

j = 1, 2, 3, ...p variables (10 spectral band/ratio radiances)

At each step of the procedure the variables (radiances or ratios) are divided into two disjoint sets; those included in the discriminant functions and those not included. Assume for simplicity that the first r variables are included. The within-group matrix of cross products

of deviations (W) and the matrix of cross products of deviations for the total samples (T) are partitioned into

$$W = \begin{bmatrix} W_{11} & W_{12} \\ W_{21} & W_{22} \end{bmatrix} \qquad T = \begin{bmatrix} T_{11} & T_{12} \\ T_{21} & T_{22} \end{bmatrix}$$

where W_{11} and T_{11} are r by r.

The elements a_{ij} are derived from matrix A, and the elements b_{ij} from matrix B:

$$A = \begin{bmatrix} W_{11}^{-1} & & W_{11}^{-1} & W_{12} \\ W_{21} & W_{11}^{-1} & W_{22} & -W_{21} \quad W_{11}^{-1} \quad W_{12} \end{bmatrix} = \{a_{ij}\}$$

$$B = \begin{bmatrix} T_{11}^{-1} & & T_{11}^{-1} & T_{12} \\ T_{21} & T_{11}^{-1} & T_{22} & -T_{21} \quad T_{11}^{-1} \quad T_{12} \end{bmatrix} = \{b_{ij}\}$$

The optimum input variables (spectral bands/ratios) are chosen on the basis of the largest F-statistic, where, for the entry of the j^{th} variable.

$$F_j = \frac{a_{jj} - b_{jj}}{b_{jj}} \cdot \frac{n - r - g + 1}{g - 1}$$

when n is the total number of cells and g is the number of classes. The degrees of freedom are g - 1 and n - r - g + 1. An iterative stepwise technique is used to determine the best linear combination of spectral bands/ratios (Siegel, 1976).

Posterior probability of cell n in group k is computed in stepwise discriminant analysis by the equation shown below (BMD Manual, 1973):

$$P_{kn} = \frac{\exp(D_{kn})}{\sum_{k=1}^{g} \exp(D_{kn})}$$

APPENDIX C

TRAINING SET CLASSIFICATION ACCURACY USING THE "PSEUDO-SUPERVISED" TRAINING DATA

Two iterations of statistical cleaning were applied to the "pseudo-supervised" training sets. The overall and individual class accuracies were interpreted from the 10 band/ratio training set accuracy matrix. 85% overall training set accuracy was achieved before any statistical cleaning was applied. The overall apparent training set accuracy was increased to 99.1% after two iterations of statistical cleaning were applied, while the overall actual training set accuracy was decreased to 83%. The training set accuracy for 17 individual classes is shown on the diagonal of the matrix.

TABLE C-1. A COMPARISON OF THE OPTIMAL FOUR CHANNELS SELECTED FOR THREE SETS OF TRAINING DATA IN ALL LEVELS OF CLEANING AND THEIR RESPECTIVE F VALUES TO ENTER.

Sampling Method	*Before Cleaning*		*1st Cleaning*		*2nd Cleaning*		*3rd Cleaning*	
	Optimal 4	*F to enter*	*Optimal 4*	*F to enter*	*Optimal 4*	*F to enter*	*Optimal 4*	*F to enter*
(1) Unsupervised	7	2862.86	7	3541.67	7/4	3762.05	7/4	3680.59
	5	946.54	4	1422.41	4	1552.12	4	1586.72
	4	316.85	5	468.98	5	512.41	5	507.57
	5/4	382.94	5/4	531.06	5/4	469.79	5/4	464.33
(2) Supervised	6/4	938.25	7/6	1154.84	7/6	1025.73	6	1039.85
	5	215.75	4	485.98	4	629.70	4	782.61
	6	145.34	5	131.91	5	154.66	6/4	392.92
	4	160.58	5/4	124.18	5/4	175.98	5	197.61
(3) Pseudo-supervised	6/4	1457.20	7/4	1890.42	7/4	2127.08	–	–
	5/4	687.32	5/4	940.88	5/4	1044.60	–	–
	6	221.10	7	405.37	7	494.32	–	–
	4	455.94	4	466.57	4	484.66	–	–

TABLE C–2. TRAINING SET CLASSIFICATION ACCURACY USING THE "PSEUDO-SUPERVISED" TRAINING DATA. 17 classes showing the *apparent* increase in training set accuracy *in percent* using 10 channels (4 LANDSAT MSS bands and their 6 ratios). Only the residual training data was classified after the 1st level of statistical cleaning had been applied.

Land Use Class				*No. of Points*	*Urban*		*Agricultural*					*Forested*			*Barren*			*Water*			
Code	*Level I*	*Code*	*Levels II and III*	*in T.S.*	*110*	*120*	*211*	*212*	*221*	*222*	*223*	*311*	*312*	*320*	*410*	*420*	*430*	*510*	*520*	*530*	*540*
100	Urban lands	110	Commercial	90	100	0	0	0	0	0	0	0	0	0	0	0	0	0	0	0	0
		120	Mixed	126	3	90	1	0	0	0	0	0	0	0	6	1	0	0	0	0	0
200	Agricultural lands	211	Grain A	71	0	1	97	0	0	1	0	0	0	0	0	0	0	0	0	0	0
		212	Grain B	96	0	0	0	100	0	0	0	0	0	0	0	0	0	0	0	0	0
		221	Crop A	82	0	0	1	0	94	5	0	0	0	0	0	0	0	0	0	0	0
		222	Crop B	82	0	0	0	0	6	90	0	0	0	0	0	0	0	0	0	0	0
		223	Crop C	59	0	0	0	2	19	0	80	0	0	0	0	0	0	0	0	0	0
300	Forested lands	311	Hardwoods A	131	0	0	0	0	0	0	0	90	10	0	0	0	0	0	0	0	0
		312	Hardwoods B	211	0	0	0	0	3	0	0	2	95	0	0	0	0	0	0	0	0
		320	Conifers	78	0	0	0	0	0	0	0	4	6	90	0	0	0	0	0	0	0
400	Barren lands	410	Gravels	76	0	14	0	0	0	0	0	0	0	0	86	0	0	0	0	0	0
		420	Reclaimed	64	2	0	0	0	0	0	0	0	0	0	0	98	0	0	0	0	0
		430	Tidal flat	91	1	0	0	0	0	0	0	0	0	0	0	0	99	0	0	0	0
500	Water surfaces	510	Shallow seawater	86	0	0	0	0	0	0	0	0	0	0	0	0	0	100	0	0	0
		520	Medium seawater	89	0	0	0	0	0	0	0	0	0	0	0	0	0	0	100	0	0
		530	Deep seawater	89	0	0	0	0	0	0	0	0	0	0	0	0	0	0	0	100	0
		540	Fresh water	79	0	0	0	0	0	0	0	0	0	0	0	0	0	0	0	0	100

Overall accuracy = 94.6% obtained by 1514 correct identifications (diagonal) divided by 1600 residual samples in all training sets.

TABLE C-3. TRAINING SET CLASSIFICATION ACCURACY USING THE "PSEUDO-SUPERVISED" TRAINING DATA. 17 classes showing the *actual* increase in training set accuracy *in percent* using 10 channels (4 LANDSAT MSS bands and their 6 ratios). All the original training data was classified with matrices obtained from the training data which remained after the 1st level of statistical cleaning.

Land Use Class				*No. of Points*	*Urban*		*Agricultural*					*Forested*			*Barren*			*Water*			
Code	*Level I*	*Code*	*Levels II and III*	*in T.S.*	*110*	*120*	*211*	*212*	*221*	*222*	*223*	*311*	*312*	*320*	*410*	*420*	*430*	*510*	*520*	*530*	*540*
100	Urban lands	100	Commercial	100	91	8	0	0	0	0	0	0	0	0	0	1	0	0	0	0	0
		120	Mixed	157	13	72	1	0	0	0	0	0	0	0	12	3	0	0	0	0	0
200	Agricultural lands	211	Grain A	82	0	6	86	0	1	5	0	0	0	0	2	0	0	0	0	0	0
		212	Grain B	96	0	0	0	100	0	0	0	0	0	0	0	0	0	0	0	0	0
		221	Crop A	104	0	0	2	2	75	20	0	0	1	0	0	0	0	0	0	0	0
		222	Crop B	100	0	0	2	0	20	74	0	0	0	4	0	0	0	0	0	0	0
		223	Crop C	75	0	0	0	5	25	0	63	0	7	0	0	0	0	0	0	0	0
300	Forested lands	311	Hardwood A	156	0	0	0	0	4	0	0	76	20	0	0	0	0	0	0	0	0
		312	Hardwood B	246	0	0	0	2	5	0	0	12	81	0	0	0	0	0	0	0	0
		320	Conifers	93	0	0	0	1	3	1	0	8	12	75	0	0	0	0	0	0	0
400	Barren lands	410	Gravels	95	0	30	1	0	0	0	0	0	0	0	69	0	0	0	0	0	0
		420	Reclaimed	70	4	4	0	0	0	0	0	0	0	0	1	90	0	0	0	0	0
		430	Tidal flat	96	6	0	0	0	0	0	0	0	0	0	0	0	94	0	0	0	0
500	Water surfaces	510	Shallow seawater	90	0	0	0	0	0	0	0	0	0	0	0	0	3	97	0	0	0
		520	Medium seawater	90	0	0	0	0	0	0	0	0	0	0	0	0	0	0	99	0	1
		530	Deep seawater	90	0	0	0	0	0	0	0	0	0	0	0	0	0	0	0	99	1
		540	Fresh water	84	0	0	0	0	0	0	0	0	0	0	0	0	0	5	0	0	95

Overall accuracy = 83.3% obtained by 1519 correct identifications (diagonal) divided by 1824 total samples in all training sets.

TABLE C-4. TRAINING SET CLASSIFICATION ACCURACY USING THE "PSEUDO-SUPERVISED" TRAINING DATA. 17 classes showing the *apparent* increase in training set accuracy *in percent* using 10 channels (4 LANDSAT MSS bands and their 6 ratios). Only the residual training data was classified after the 2nd level of statistical cleaning had been applied.

Land Use Class				*No. of Points*	*Urban*		*Agricultural*					*Forested*			*Barren*			*Water*			
Code	*Level I*	*Code*	*Levels II and III*	*in T.S.*	*110*	*120*	*211*	*212*	*221*	*222*	*223*	*311*	*312*	*320*	*410*	*420*	*430*	*510*	*520*	*530*	*540*
100	Urban lands	110	Commercial	86	100	0	0	0	0	0	0	0	0	0	0	0	0	0	0	0	0
		120	Mixed	115	0	99	0	0	0	0	0	0	0	0	1	0	0	0	0	0	0
200	Agricultural lands	211	Grain A	69	0	0	100	0	0	0	0	0	0	0	0	0	0	0	0	0	0
		212	Grain B	96	0	0	0	100	0	0	0	0	0	0	0	0	0	0	0	0	0
		221	Crop A	76	0	0	3	0	97	0	0	0	0	0	0	0	0	0	0	0	0
		222	Crop B	74	0	0	0	0	3	97	0	0	0	0	0	0	0	0	0	0	0
		223	Crop C	48	0	0	2	0	4	0	94	0	0	0	0	0	0	0	0	0	0
300	Forested lands	311	Hardwoods A	118	0	0	0	0	0	0	0	99	1	0	0	0	0	0	0	0	0
		312	Hardwoods B	193	0	0	0	0	0	0	0	0	100	0	0	0	0	0	0	0	0
		320	Conifers	70	0	0	0	0	0	0	0	0	0	100	0	0	0	0	0	0	0
400	Barren lands	410	Gravels	67	0	4	0	0	0	0	0	0	0	0	96	0	0	0	0	0	0
		420	Reclaimed	59	0	0	0	0	0	0	0	0	0	0	0	100	0	0	0	0	0
		430	Tidal flat	84	0	0	0	0	0	0	0	0	0	0	0	0	100	0	0	0	0
500	Water surfaces	510	Shallow seawater	84	0	0	0	0	0	0	0	0	0	0	0	0	0	100	0	0	0
		520	Medium seawater	89	0	0	0	0	0	0	0	0	0	0	0	0	0	0	100	0	0
		530	Deep seawater	85	0	0	0	0	0	0	0	0	0	0	0	0	0	0	0	100	0
		540	Fresh water	79	0	0	0	0	0	0	0	0	0	0	0	0	0	0	0	0	100

Overall accuracy = 99.1% obtained by 1479 correct identifications (diagonal) divided by 1492 total samples in all training sets.

TABLE C-5. TRAINING SET CLASSIFICATION ACCURACY USING THE "PSEUDO-SUPERVISED" TRAINING DATA. 17 classes showing the *actual* increase in training set accuracy *in percent* using 10 channels (4 LANDSAT MSS bands and their 6 ratios). All the original training data was classified with matrices obtained from the training data which remained after the 2nd level of statistical cleaning.

Land Use Class				*No. of Points*	*Urban*		*Agricultural*					*Forested*			*Barren*			*Water*			
Code	*Level I*	*Code*	*Levels II and III*	*in T.S.*	*110*	*120*	*211*	*212*	*221*	*222*	*223*	*311*	*312*	*320*	*410*	*420*	*430*	*510*	*520*	*530*	*540*
100	Urban lands	110	Commercial	100	91	8	0	0	0	0	0	0	0	0	0	1	0	0	0	0	0
		120	Mixed	157	12	73	1	0	0	0	0	0	0	0	13	1	0	0	0	0	0
200	Agricultural lands	211	Grain A	82	0	7	87	0	1	4	0	0	0	0	1	0	0	0	0	0	0
		212	Grain B	96	0	0	0	100	0	0	0	0	0	0	0	0	0	0	0	0	0
		221	Crop A	104	0	0	4	1	74	20	0	0	1	0	0	0	0	0	0	0	0
		222	Crop B	100	0	0	3	0	21	72	0	0	4	0	0	0	0	0	0	0	0
		223	Crop C	75	0	0	1	5	27	0	60	0	7	0	0	0	0	0	0	0	0
300	Forested lands	311	Hardwoods A	156	0	0	0	0	3	0	0	75	21	0	0	0	0	0	0	0	1
		312	Hardwoods B	246	0	0	0	2	5	0	0	11	82	0	0	0	0	0	0	0	0
		320	Conifers	93	0	0	0	3	2	0	0	8	12	75	0	0	0	0	0	0	0
400	Barren lands	410	Gravels	95	0	31	1	0	0	0	0	0	0	0	68	0	0	0	0	0	0
		420	Reclaimed	70	4	4	0	0	0	0	0	0	0	0	0	92	0	0	0	0	0
		430	Tidal flat	96	6	0	0	0	0	0	0	0	0	0	0	0	94	0	0	0	0
500	Water surfaces	510	Shallow seawater	90	0	0	0	0	0	0	0	0	0	0	0	0	4	96	0	0	0
		520	Medium seawater	90	0	0	0	0	0	0	0	0	0	0	0	0	0	0	99	0	1
		530	Deep seawater	90	0	0	0	0	0	0	0	0	0	0	0	0	0	0	0	96	4
		540	Fresh water	84	0	0	0	0	0	0	0	0	0	0	0	0	5	0	0	0	95

Overall accuracy = 83.0% obtained by 1514 correct identifications (diagonal) divided by 1824 total samples in all training sets.

APPENDIX D

ACTUAL INCREASE IN TRAINING SET ACCURACY ACHIEVED AT EACH LEVEL OF STATISTICAL CLEANING

Two iterations of statistical cleaning were applied to the "pseudo-supervised" training sets. Seventeen classes are represented based on classification by the 10 MSS bands/ratios. The training set accuracy was increased as each band/ratio added. The accuracy approaches a limit after three or four bands in urban, agricultural and forested lands. However, barren lands and water classes, such as gravels and medium seawater, fluctuate widely as the first four bands added, then remain stable through 10 bands. Statistical cleaning contributes little to the actual training set accuracy of most classes except mixed urban.

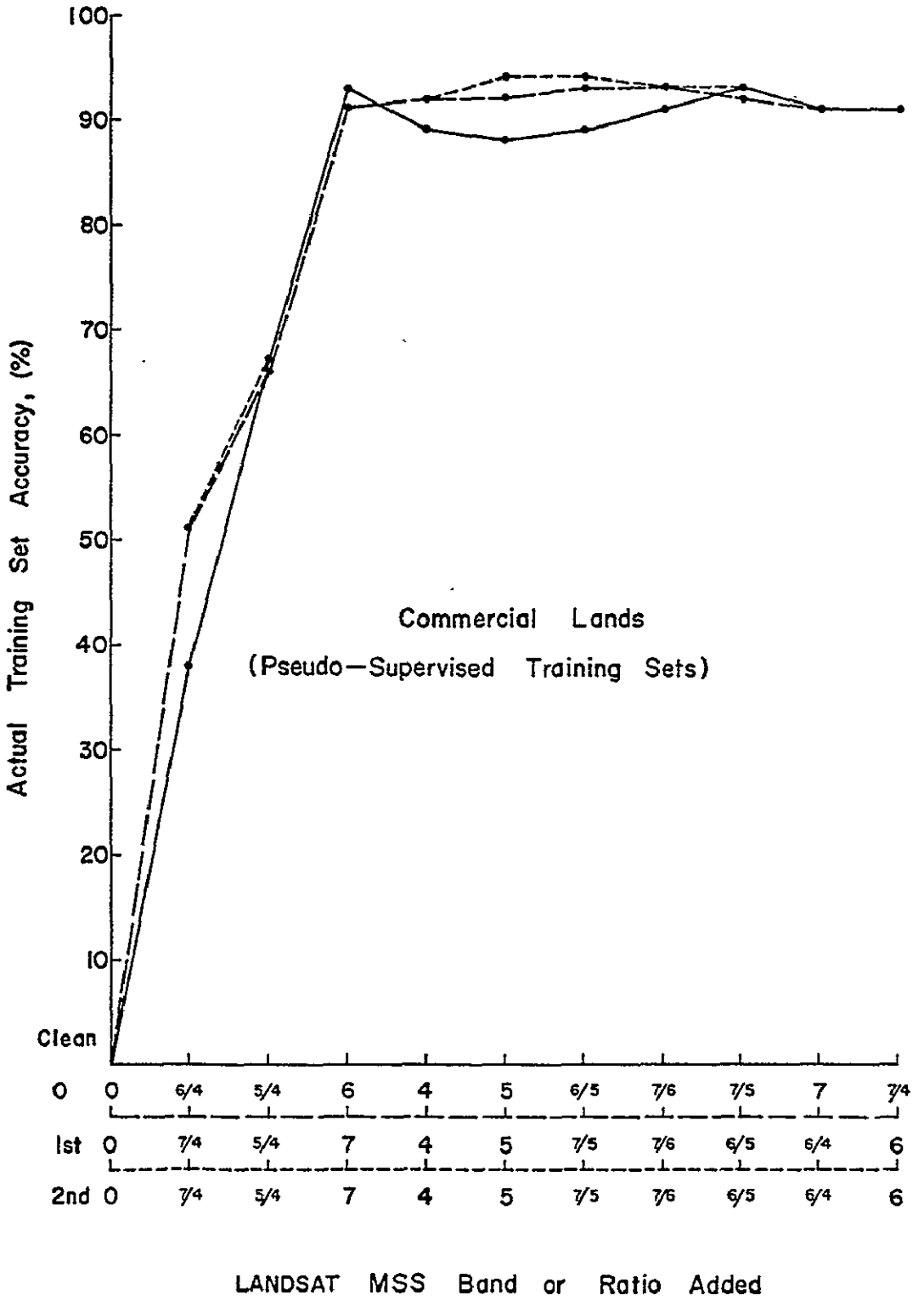
Actual Training Set Accuracy, (%)
100
90
80
70
60
50
40
30
20
10
Clean
Commercial Lands
(Pseudo—Supervised Training Sets)
0 0 6/4 5/4 6 4 5 6/5 7/6 7/5 7 7/4
1st 0 7/4 5/4 7 4 5 7/5 7/6 6/5 6/4 6
2nd 0 7/4 5/4 7 4 5 7/5 7/6 6/5 6/4 6
LANDSAT MSS Band or Ratio Added

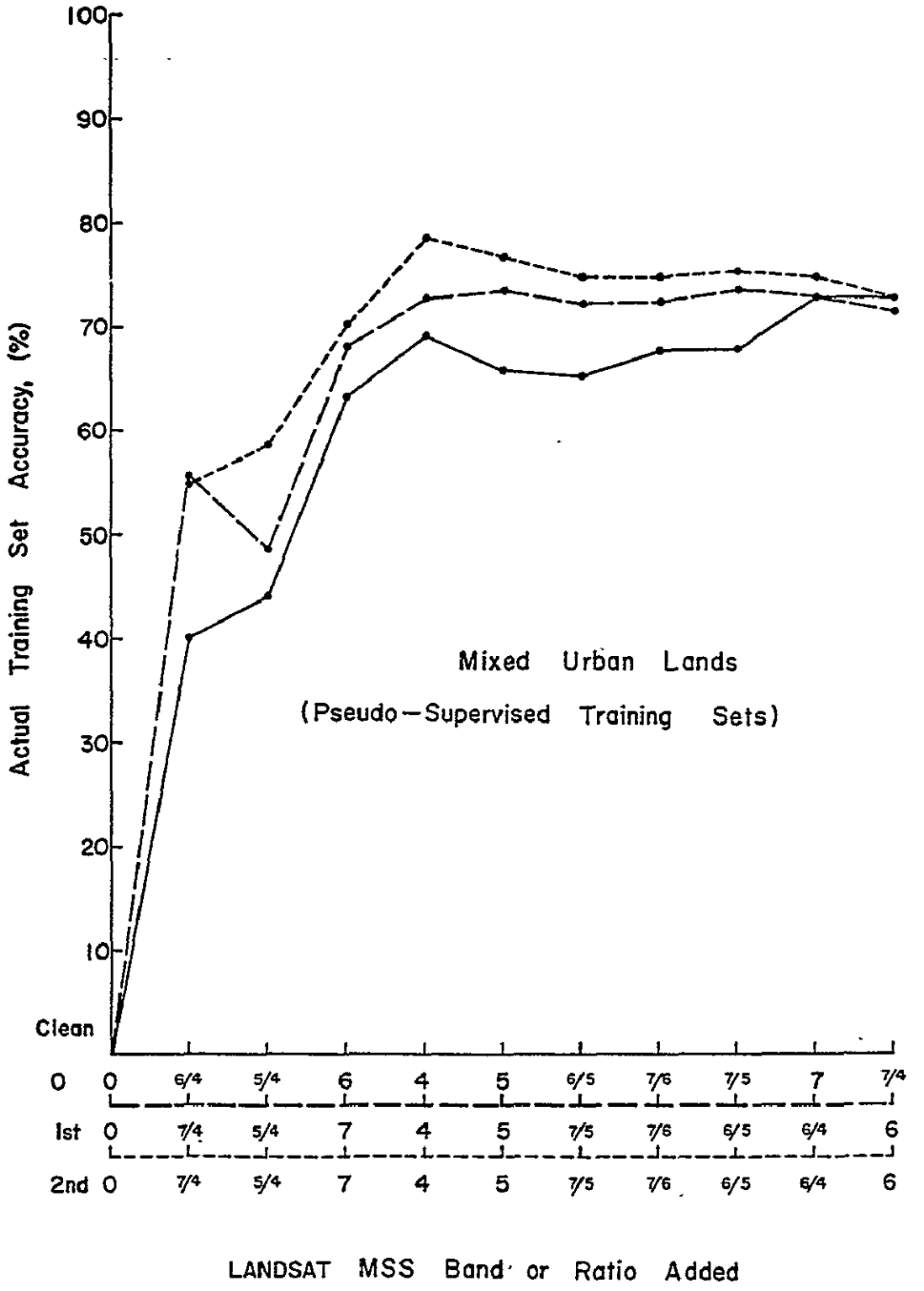
Actual Training Set Accuracy, (%)
100
90
80
70
60
50
40
30
20
10
Clean
Mixed Urban Lands
(Pseudo—Supervised Training Sets)
0 0 6/4 5/4 6 4 5 6/5 7/6 7/5 7 7/4
1st 0 7/4 5/4 7 4 5 7/5 7/6 6/5 6/4 6
2nd 0 7/4 5/4 7 4 5 7/5 7/6 6/5 6/4 6
LANDSAT MSS Band or Ratio Added

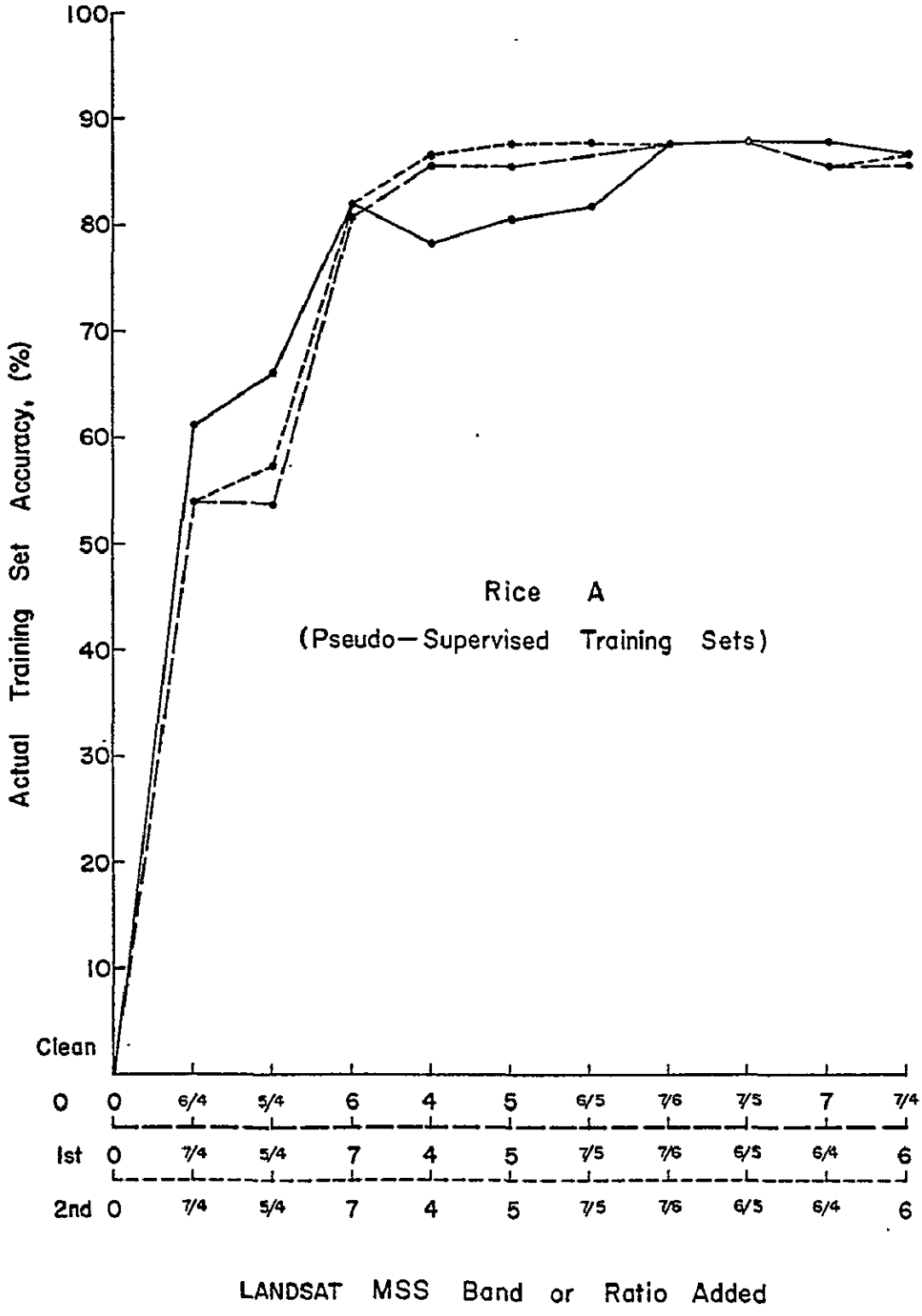
Actual Training Set Accuracy, (%)
100
90
80
70
60
50
40
30
20
10
Clean
Rice A
(Pseudo—Supervised Training Sets)
0 0 6/4 5/4 6 4 5 6/5 7/6 7/5 7 7/4
1st 0 7/4 5/4 7 4 5 7/5 7/6 6/5 6/4 6
2nd 0 7/4 5/4 7 4 5 7/5 7/6 6/5 6/4 6
LANDSAT MSS Band or Ratio Added

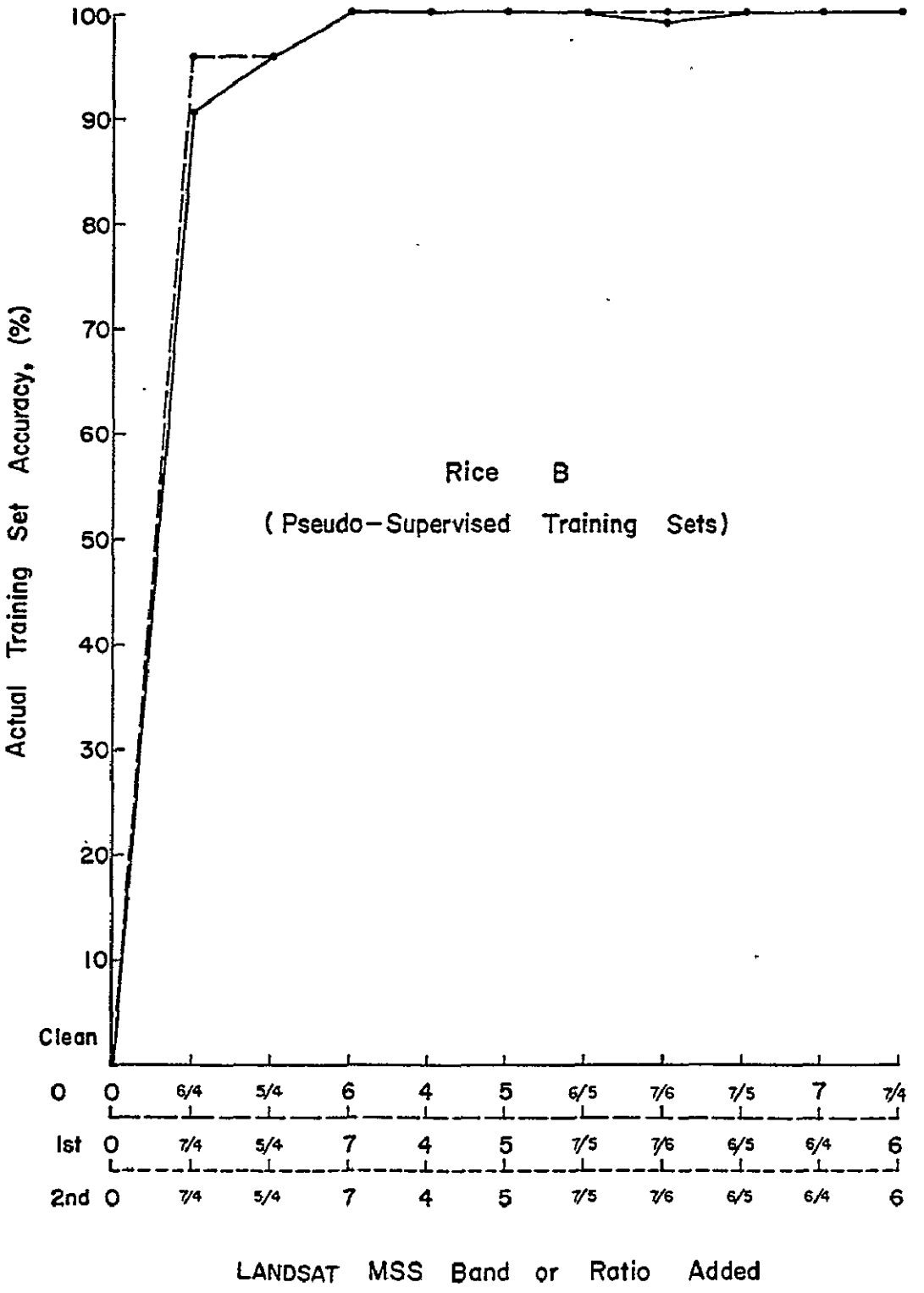
Actual Training Set Accuracy, (%)
100
90
80
70
60
50
40
30
20
10
Clean
Rice B
(Pseudo–Supervised Training Sets)
0 0 6/4 5/4 6 4 5 6/5 7/6 7/5 7 7/4
1st 0 7/4 5/4 7 4 5 7/5 7/6 6/5 6/4 6
2nd 0 7/4 5/4 7 4 5 7/5 7/6 6/5 6/4 6
LANDSAT MSS Band or Ratio Added

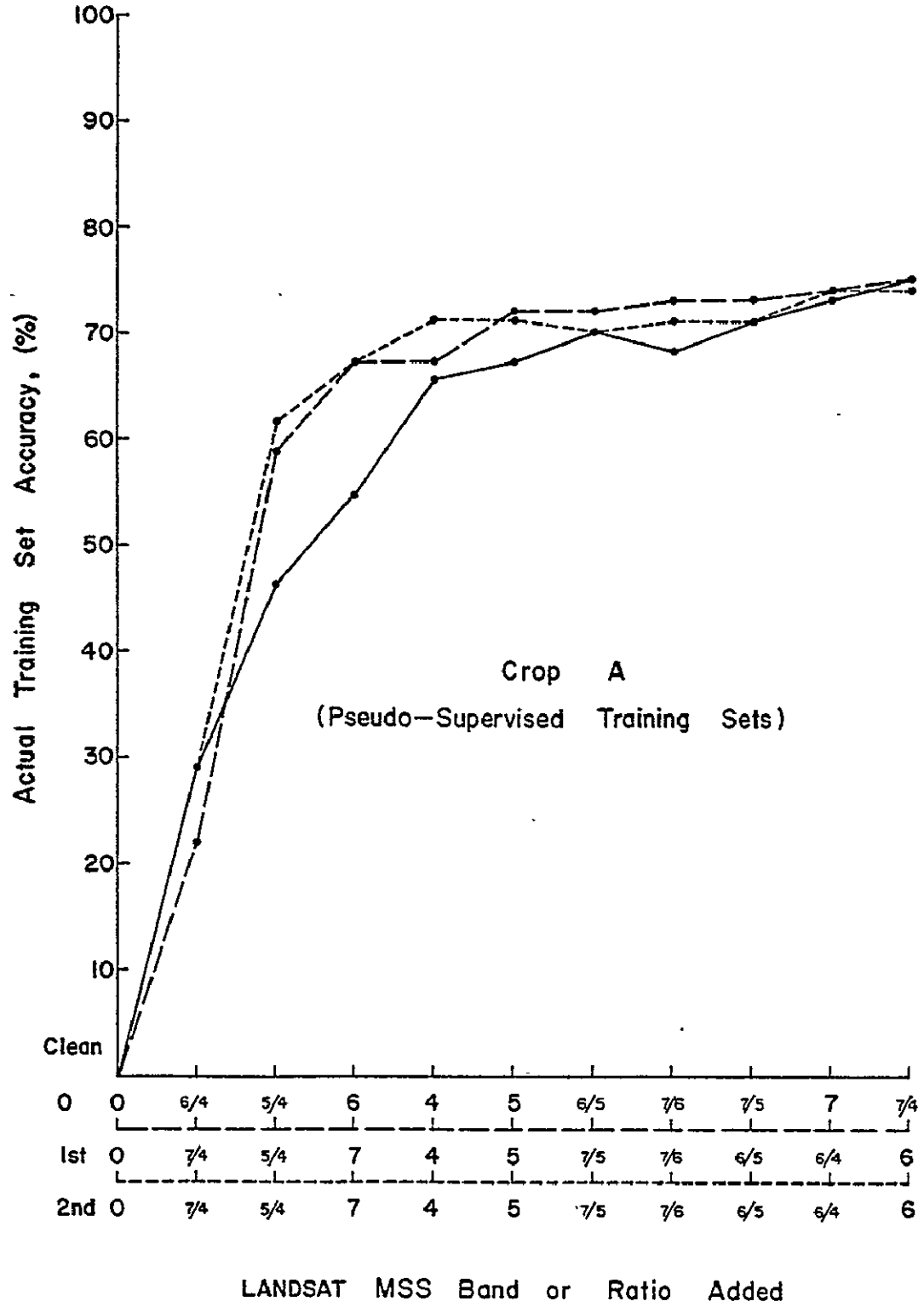
Actual Training Set Accuracy, (%)
100
90
80
70
60
50
40
30
20
10
Clean
Crop A
(Pseudo—Supervised Training Sets)
0 0 6/4 5/4 6 4 5 6/5 7/6 7/5 7 7/4
1st 0 7/4 5/4 7 4 5 7/5 7/6 6/5 6/4 6
2nd 0 7/4 5/4 7 4 5 7/5 7/6 6/5 6/4 6
LANDSAT MSS Band or Ratio Added

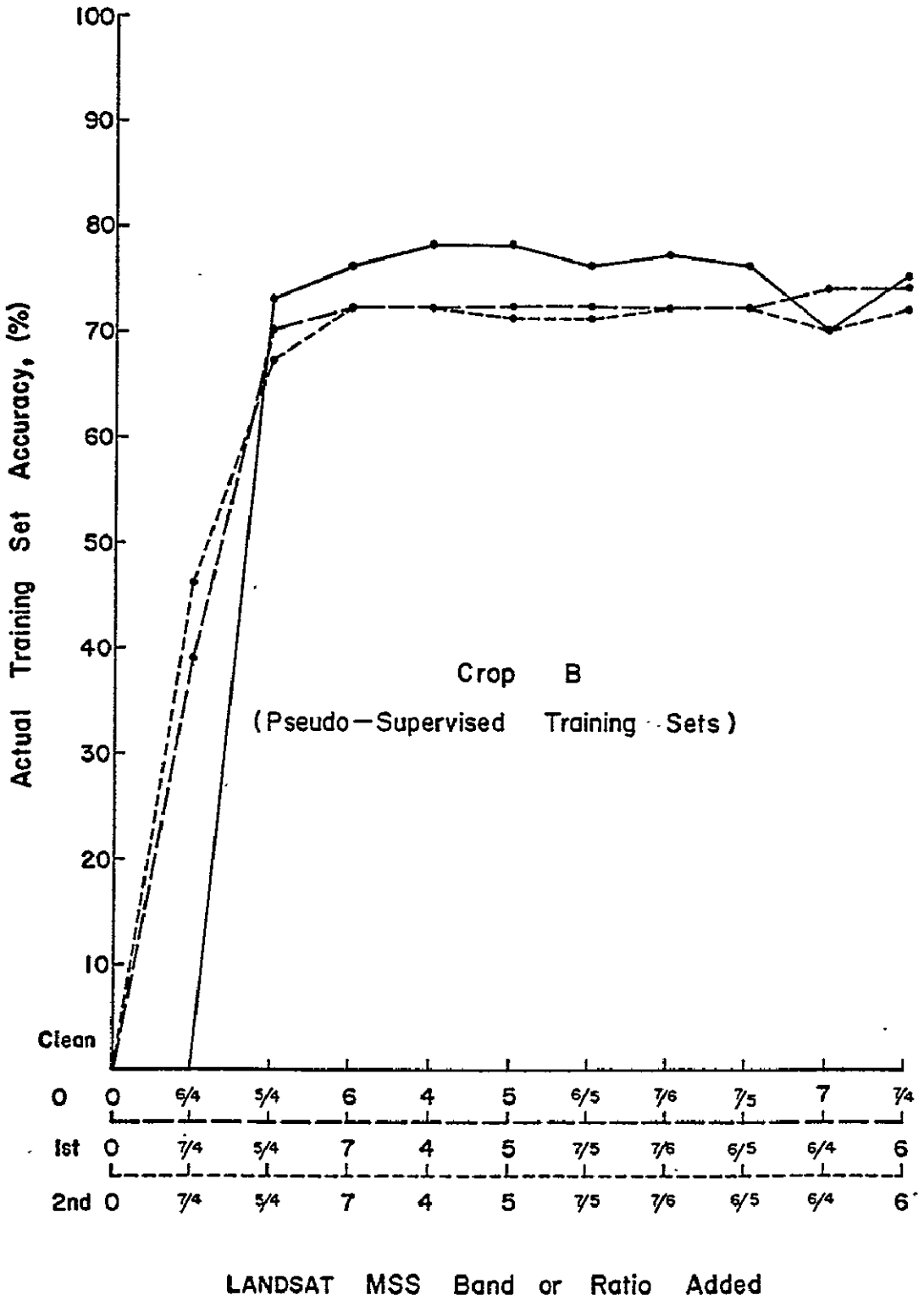
Actual Training Set Accuracy, (%)
100
90
80
70
60
50
40
30
20
10
Clean
Crop B
(Pseudo—Supervised Training Sets)
0 0 6/4 5/4 6 4 5 6/5 7/6 7/5 7 7/4
1st 0 7/4 5/4 7 4 5 7/5 7/6 6/5 6/4 6
2nd 0 7/4 5/4 7 4 5 7/5 7/6 6/5 6/4 6
LANDSAT MSS Band or Ratio Added

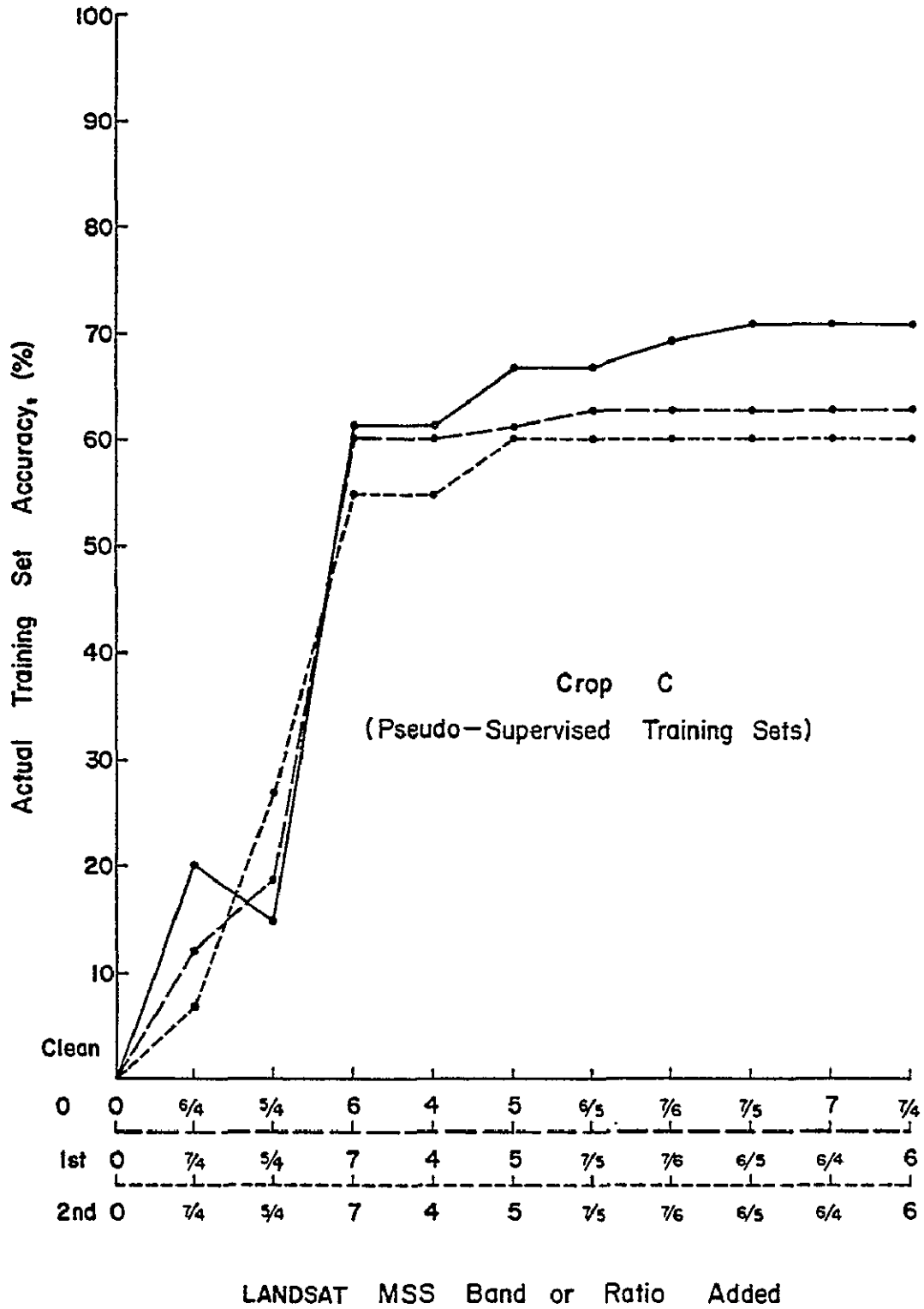
Actual Training Set Accuracy, (%)
100
90
80
70
60
50
40
30
20
10
Clean
Crop C
(Pseudo-Supervised Training Sets)
0 0 6/4 5/4 6 4 5 6/5 7/6 7/5 7 7/4
1st 0 7/4 5/4 7 4 5 7/5 7/6 6/5 6/4 6
2nd 0 7/4 5/4 7 4 5 7/5 7/6 6/5 6/4 6
LANDSAT MSS Band or Ratio Added

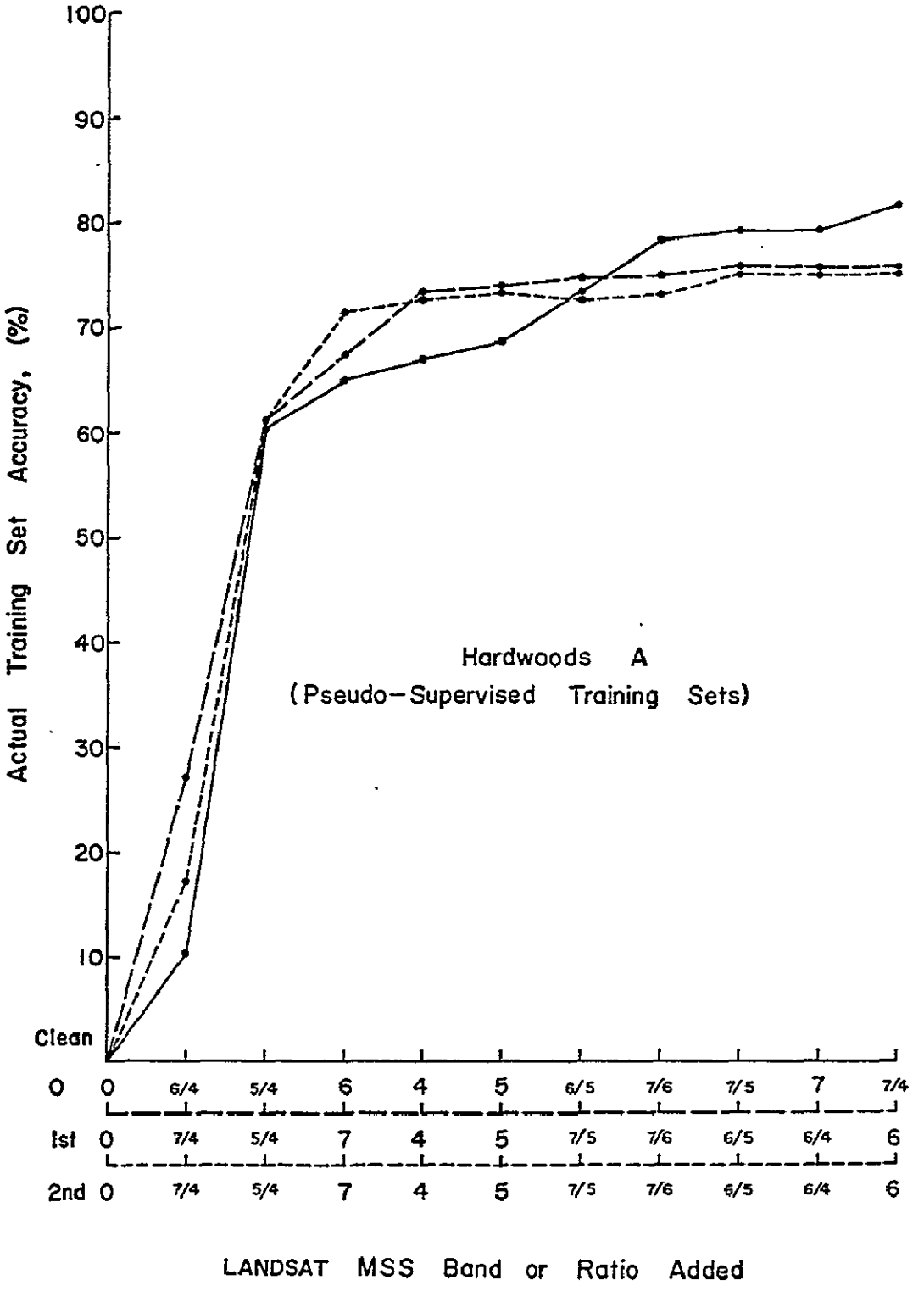
Actual Training Set Accuracy, (%)
100
90
80
70
60
50
40
30
20
10
Clean
Hardwoods A
(Pseudo-Supervised Training Sets)
0 0 6/4 5/4 6 4 5 6/5 7/6 7/5 7 7/4
1st 0 7/4 5/4 7 4 5 7/5 7/6 6/5 6/4 6
2nd 0 7/4 5/4 7 4 5 7/5 7/6 6/5 6/4 6
LANDSAT MSS Band or Ratio Added

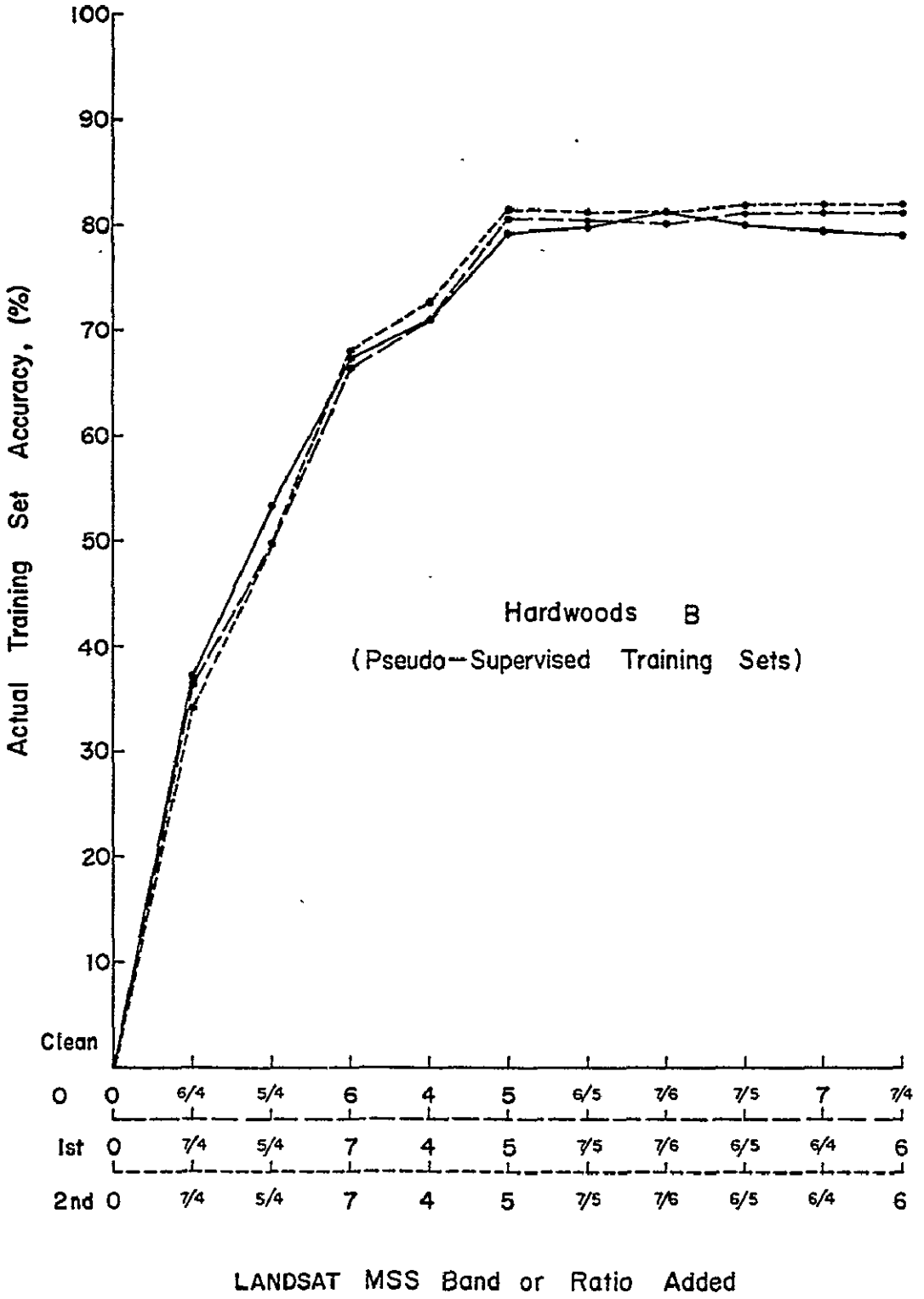
Actual Training Set Accuracy, (%)
100
90
80
70
60
50
40
30
20
10
Clean
Hardwoods B
(Pseudo-Supervised Training Sets)
0 0 6/4 5/4 6 4 5 6/5 7/6 7/5 7 7/4
1st 0 7/4 5/4 7 4 5 7/5 7/6 6/5 6/4 6
2nd 0 7/4 5/4 7 4 5 7/5 7/6 6/5 6/4 6
LANDSAT MSS Band or Ratio Added

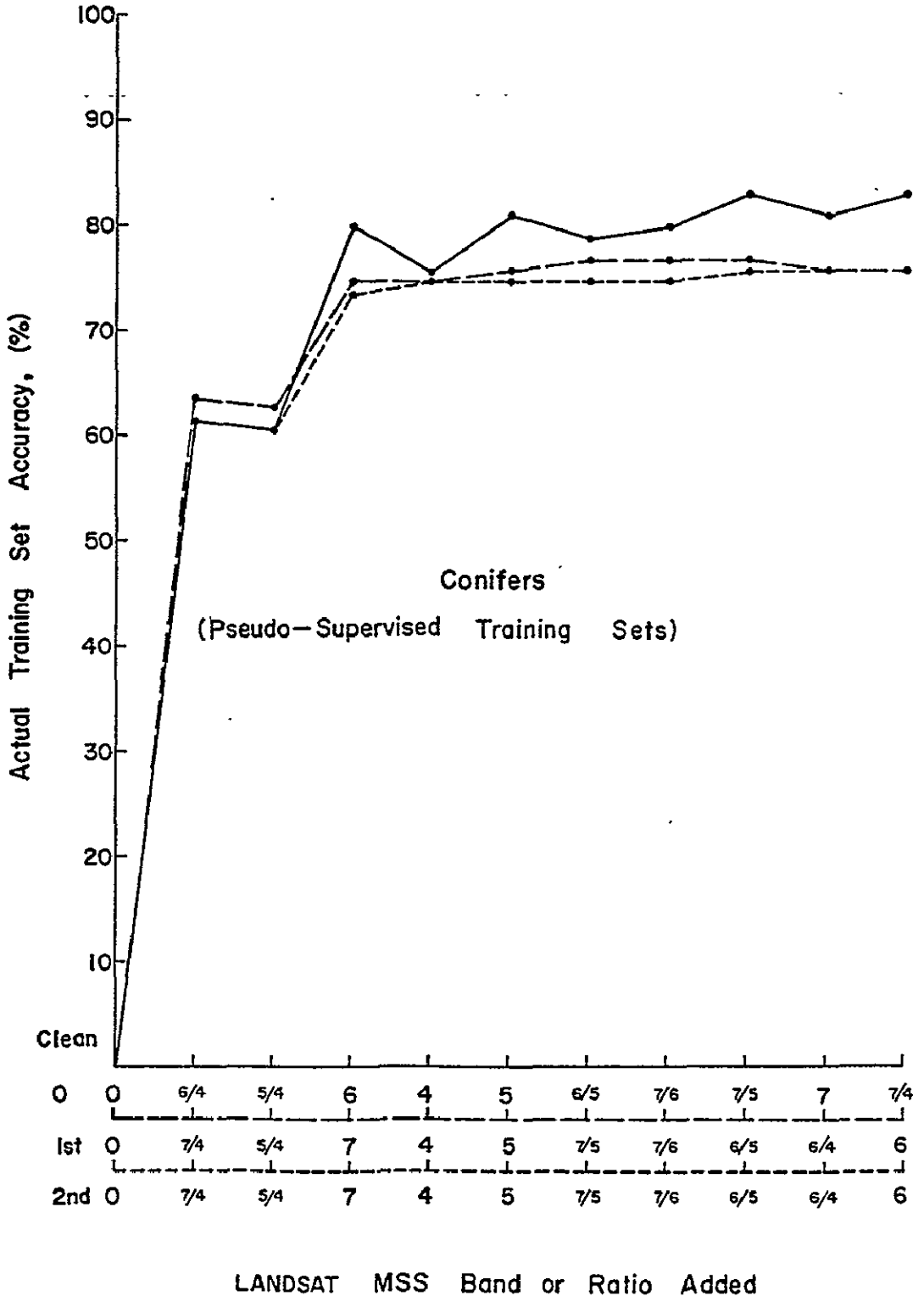
Actual Training Set Accuracy, (%)
100
90
80
70
60
50
40
30
20
10
Clean
Conifers
(Pseudo—Supervised Training Sets)
0 0 6/4 5/4 6 4 5 6/5 7/6 7/5 7 7/4
1st 0 7/4 5/4 7 4 5 7/5 7/6 6/5 6/4 6
2nd 0 7/4 5/4 7 4 5 7/5 7/6 6/5 6/4 6
LANDSAT MSS Band or Ratio Added

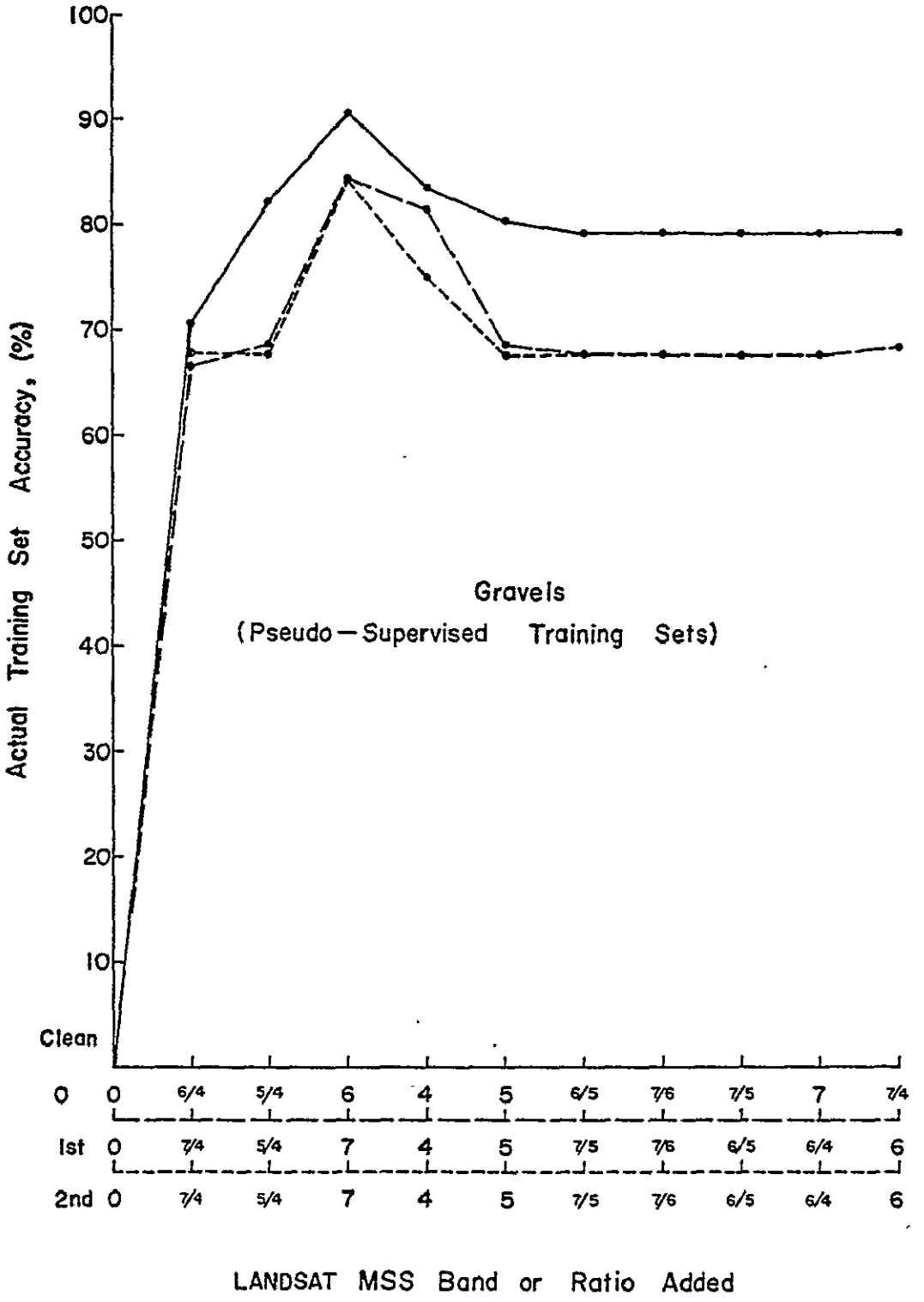
Actual Training Set Accuracy, (%)
100
90
80
70
60
50
40
30
20
10
Clean
Gravels
(Pseudo—Supervised Training Sets)
0 0 6/4 5/4 6 4 5 6/5 7/6 7/5 7 7/4
1st 0 7/4 5/4 7 4 5 7/5 7/6 6/5 6/4 6
2nd 0 7/4 5/4 7 4 5 7/5 7/6 6/5 6/4 6
LANDSAT MSS Band or Ratio Added

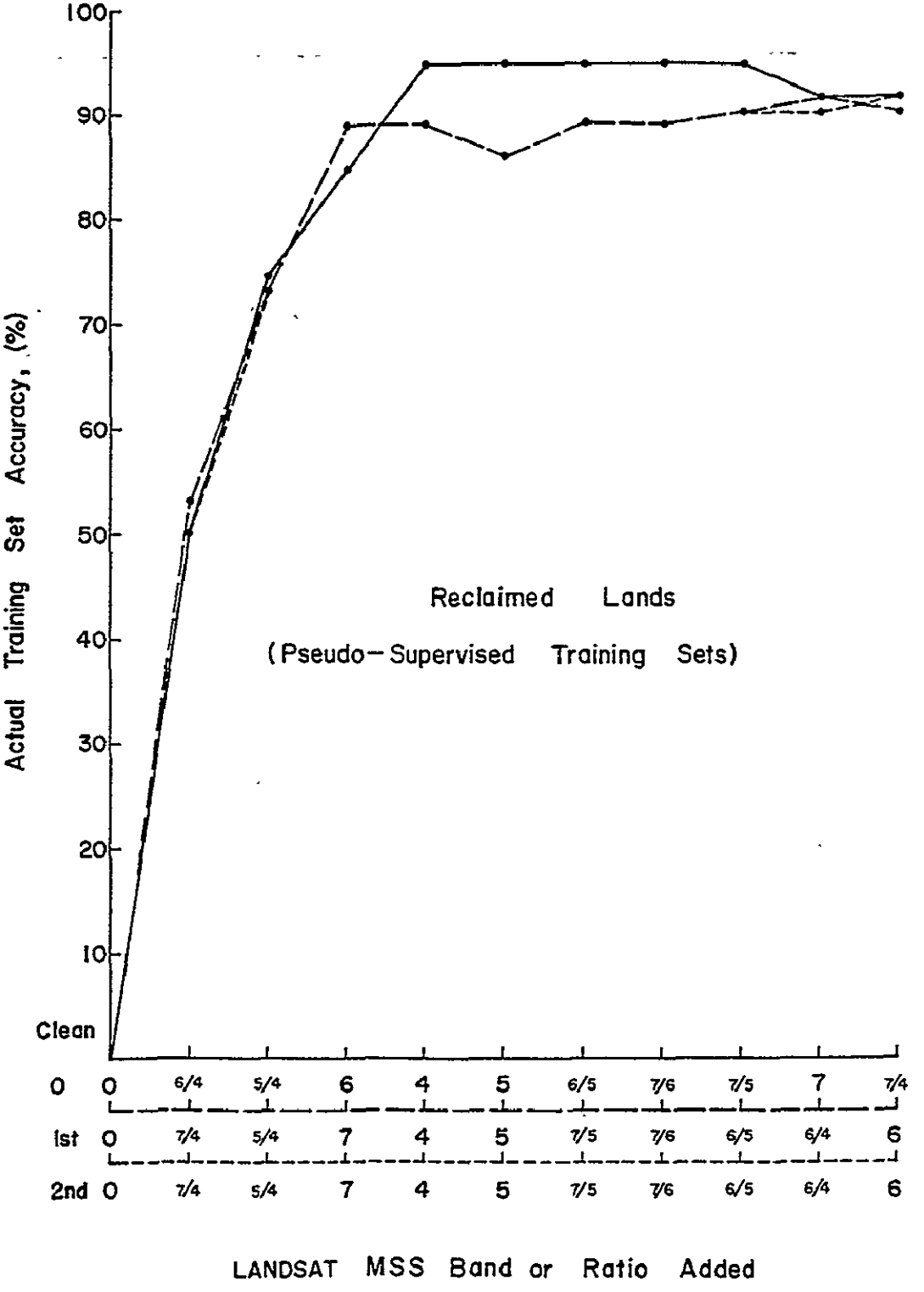
100
90
80
70
60
50
40
30
20
10
Actual Training Set Accuracy, (%)
Reclaimed Lands
(Pseudo-Supervised Training Sets)
Clean
0 0 6/4 5/4 6 4 5 6/5 7/6 7/5 7 7/4
1st 0 7/4 5/4 7 4 5 7/5 7/6 6/5 6/4 6
2nd 0 7/4 5/4 7 4 5 7/5 7/6 6/5 6/4 6
LANDSAT MSS Band or Ratio Added

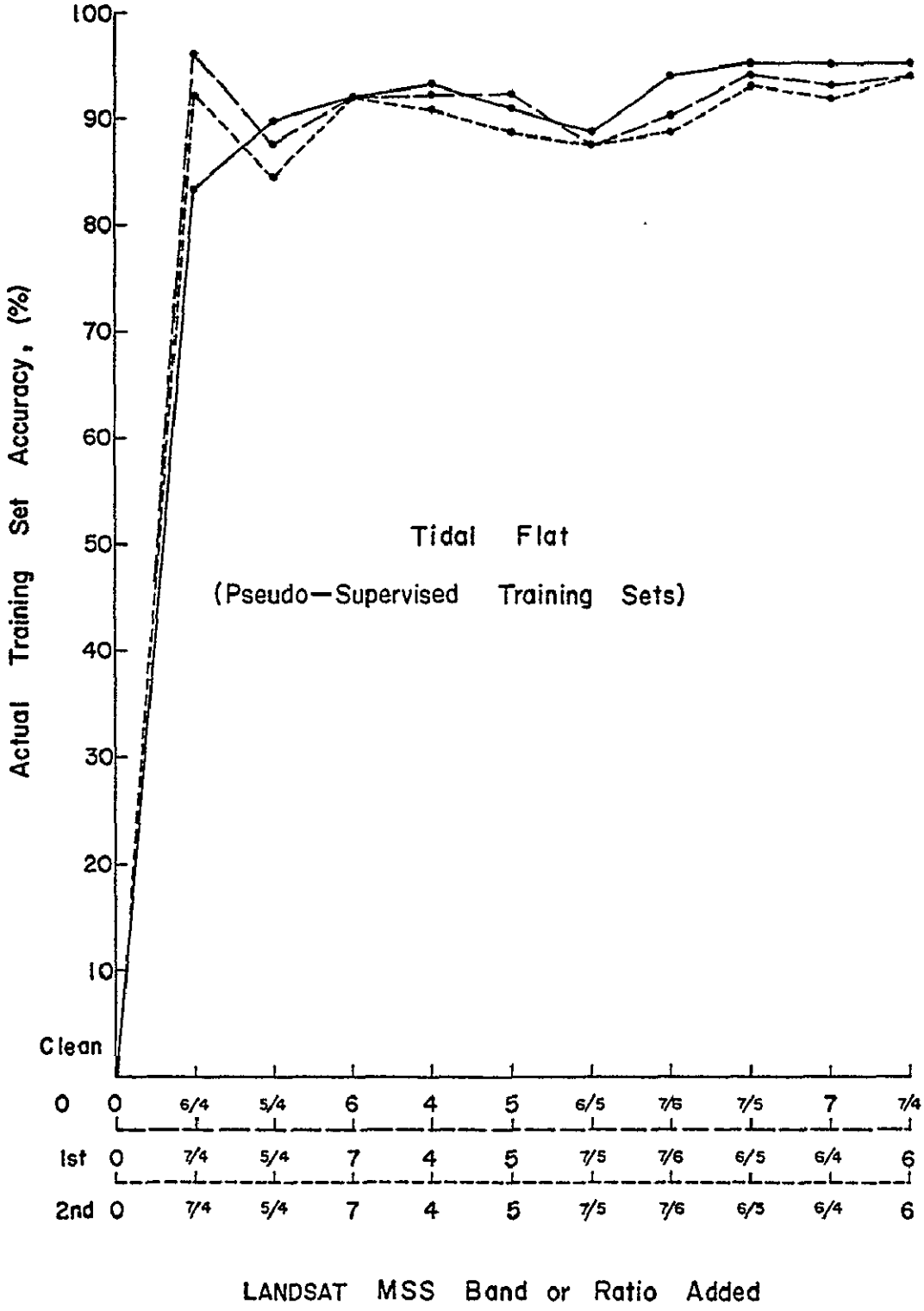
Actual Training Set Accuracy, (%)
100
90
80
70
60
50
40
30
20
10
Clean
Tidal Flat
(Pseudo—Supervised Training Sets)
0 0 6/4 5/4 6 4 5 6/5 7/5 7/5 7 7/4
1st 0 7/4 5/4 7 4 5 7/5 7/6 6/5 6/4 6
2nd 0 7/4 5/4 7 4 5 7/5 7/6 6/5 6/4 6
LANDSAT MSS Band or Ratio Added

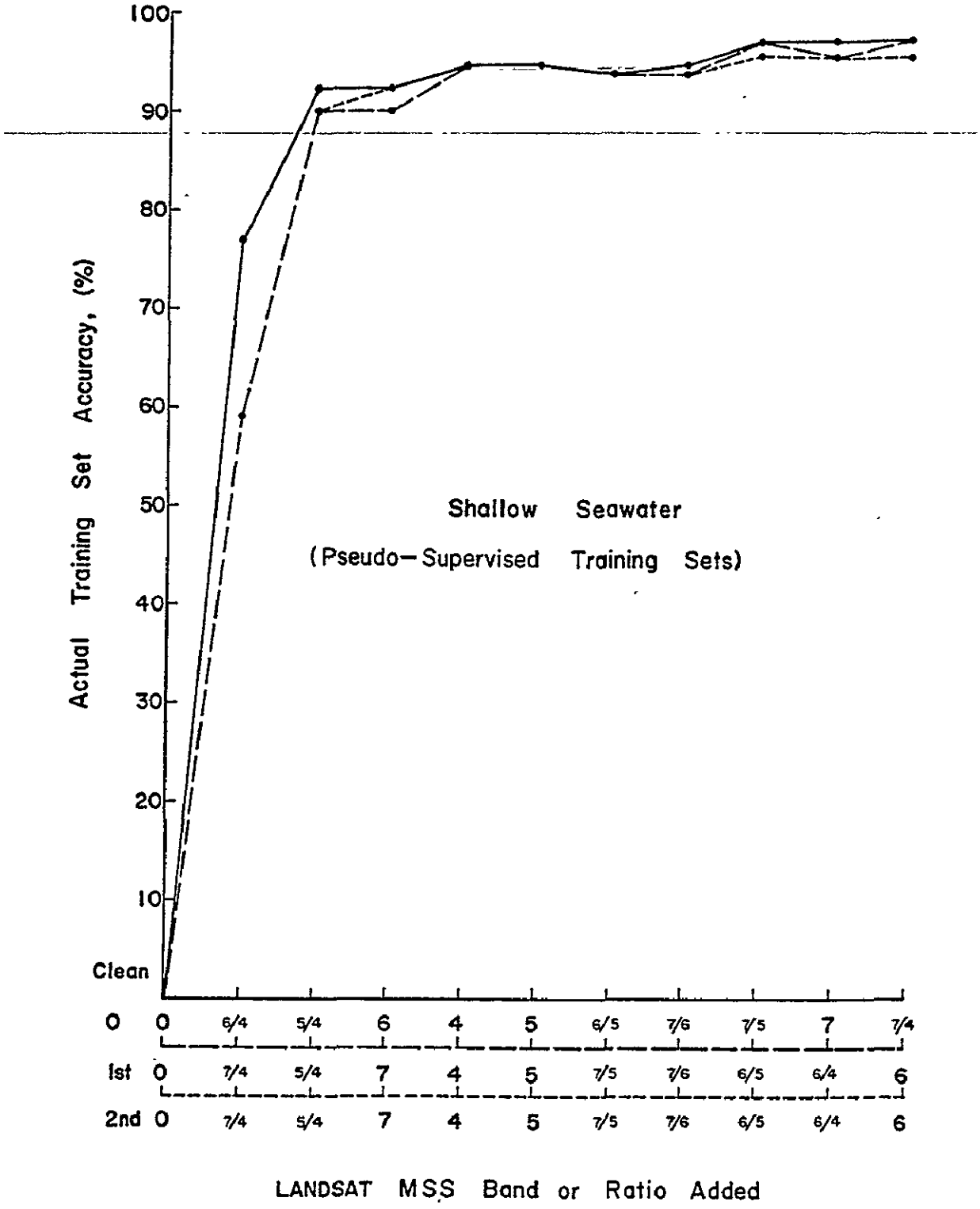
100
90
80
70
60
50
40
30
20
10
Actual Training Set Accuracy, (%)
Shallow Seawater
(Pseudo—Supervised Training Sets)
Clean
0 0 6/4 5/4 6 4 5 6/5 7/6 7/5 7 7/4
1st 0 7/4 5/4 7 4 5 7/5 7/6 6/5 6/4 6
2nd 0 7/4 5/4 7 4 5 7/5 7/6 6/5 6/4 6
LANDSAT MSS Band or Ratio Added

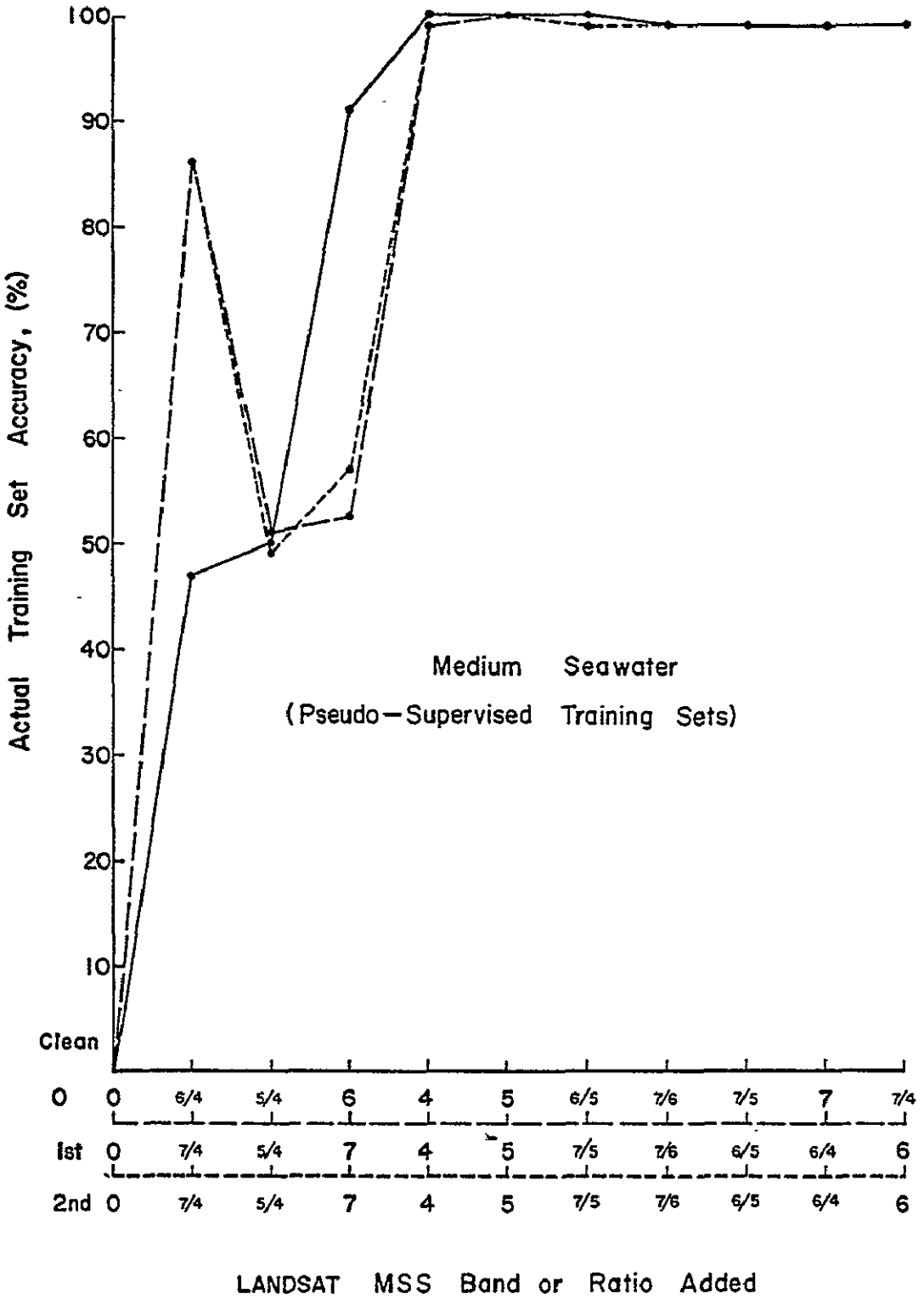
Actual Training Set Accuracy, (%)
100
90
80
70
60
50
40
30
20
10
Clean
Medium Seawater
(Pseudo—Supervised Training Sets)
0 0 6/4 5/4 6 4 5 6/5 7/6 7/5 7 7/4
1st 0 7/4 5/4 7 4 5 7/5 7/6 6/5 6/4 6
2nd 0 7/4 5/4 7 4 5 7/5 7/6 6/5 6/4 6
LANDSAT MSS Band or Ratio Added

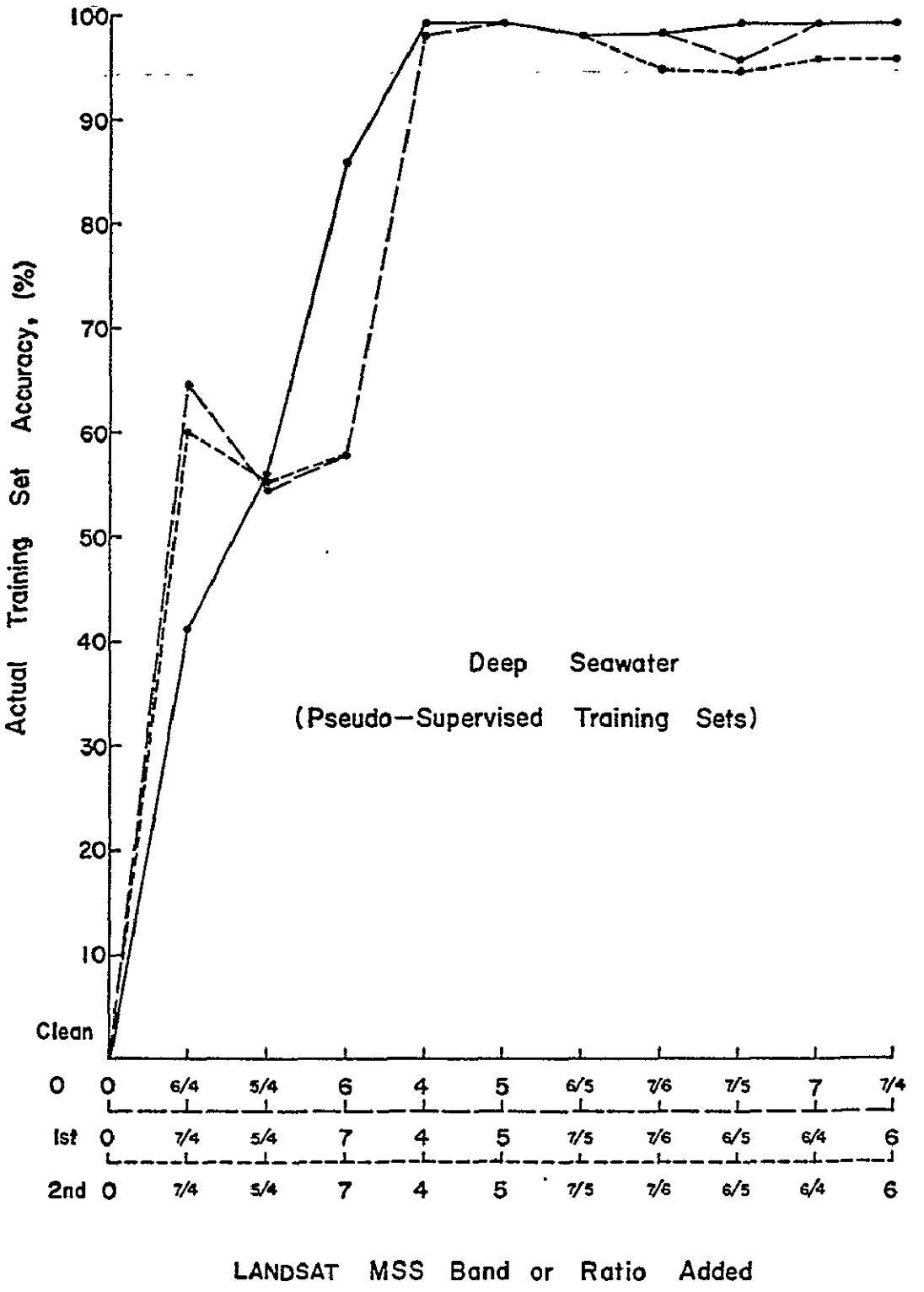
Actual Training Set Accuracy, (%)
100
90
80
70
60
50
40
30
20
10
Clean
Deep Seawater
(Pseudo—Supervised Training Sets)
0 0 6/4 5/4 6 4 5 6/5 7/6 7/5 7 7/4
1st 0 7/4 5/4 7 4 5 7/5 7/6 6/5 6/4 6
2nd 0 7/4 5/4 7 4 5 7/5 7/6 6/5 6/4 6
LANDSAT MSS Band or Ratio Added

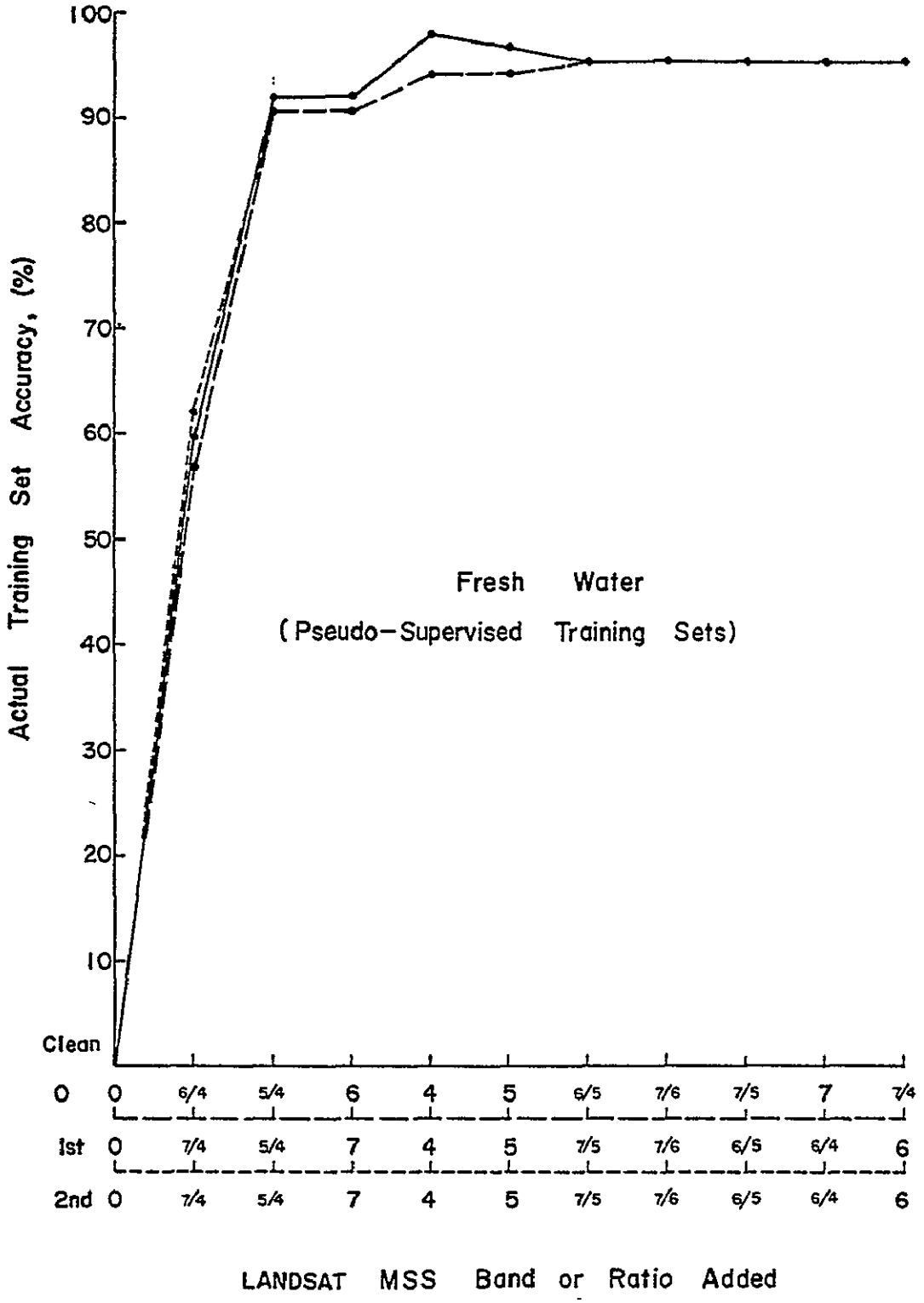
Actual Training Set Accuracy, (%)
100
90
80
70
60
50
40
30
20
10
Clean
Fresh Water
(Pseudo-Supervised Training Sets)
0 0 6/4 5/4 6 4 5 6/5 7/6 7/5 7 7/4
1st 0 7/4 5/4 7 4 5 7/5 7/6 6/5 6/4 6
2nd 0 7/4 5/4 7 4 5 7/5 7/6 6/5 6/4 6
LANDSAT MSS Band or Ratio Added

APPENDIX E

MAXIMUM LIKELIHOOD CLASSIFIER

The maximum likelihood ratioing technique (GLIKE in CSU's RECOG) allows a different covariance matrix for each class. We assume our groups are multivariate normally distributed populations represented by data samples. Each population may be described mathematically by its mean vector, $\underline{\mu}$, and its covariance matrix, $\underline{\Sigma}$ (Suppose we only have three variates, the populations can be shown pictorially in Fig. E-1). The hyper-ellipsoid (i class, defined by $\underline{\mu}_i$ and $\underline{\Sigma}_i$) which each data sample belongs to, is best defined by the Gaussian probability density function, expressed in matrix form as

$$P(\underline{X} \mid C_i) = \frac{1}{(2\pi)^{N/2} \, |\Sigma_i|^{1/2}} [\exp - \tfrac{1}{2}(\underline{X} - \underline{\mu}_i)^T \, \underline{\Sigma}_i^{-1} \, (\underline{X} - \underline{\mu}_i)]$$

where X is the observation vector,

N is the vector dimension size,

$\underline{\mu}_i$ is the mean vector for class i, and

$\underline{\Sigma}_i$ is the covariance matrix for class i.

Defining:

$$d(\underline{X} \mid C_i) = \ln P(\underline{X} \mid C_i)$$

$$= -N/2 \ln 2\pi - 1/2 \ln |\underline{\Sigma}_i| - 1/2 (\underline{X} - \underline{\mu}_i)^T \underline{\Sigma}_i^{-1} (\underline{X} - \underline{\mu}_i)$$

then the decision function is:

if $d(X \mid A) \geq d(X \mid B)$ for all $A \neq B$

$\underline{X}$ is identified as belonging to class A.

In GLIKE, we also can set a minimum acceptance threshold for computed $P(\underline{X} \mid C_i)$ values (Smith, Miller and Ells, 1972).

However, the maximum likelihood ratio approach cannot perform if the covariance matrices are singular because the probability of a data point belonging to a class cannot be computed if $\underline{\Sigma}^{-1}$ is not existed.

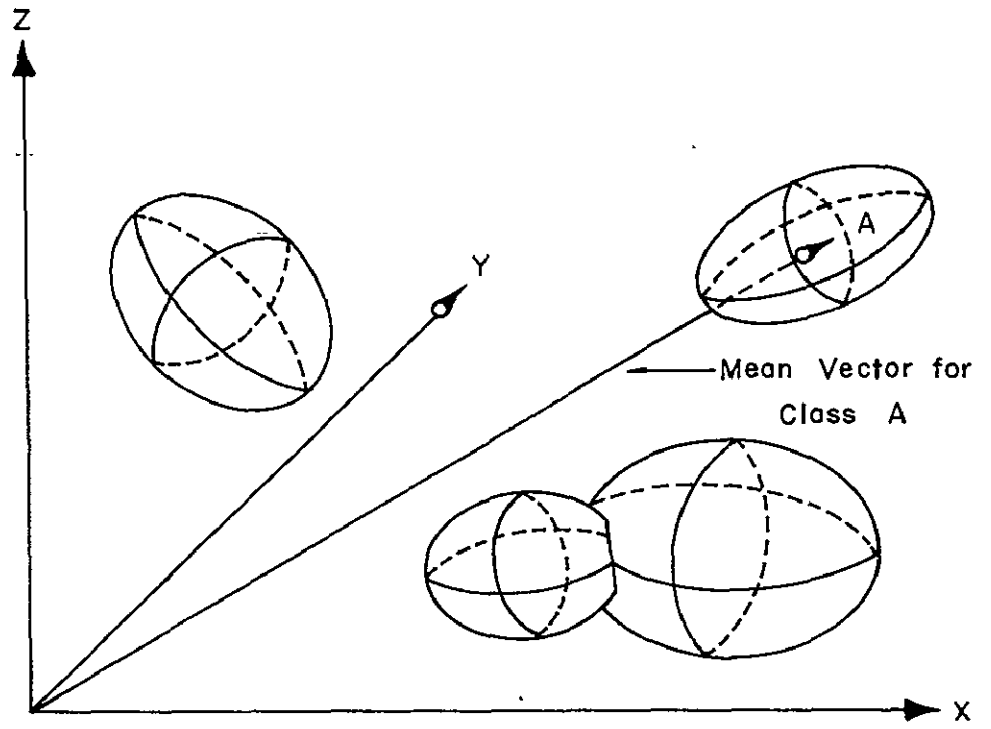

Fig. E-1. ILLUSTRATING DATA GROUPS IN THREE DIMENSIONAL SPACE. Ellipsoids represent the covariance boundaries (from Maxwell, 1974).

The decision to classify a sample point x_j as class A rather than class B is made according to the equation

$$\text{if } \frac{P(x_j|A)}{P(x_j|B)} \geq 1 \text{ for } A \neq B. \quad \text{Decide A.}$$

For simplicity, we can use an exponent test obtained by taking the natural logarithm.